PhD-FSTC-2016-4
The Faculty of Sciences, Technology and Communication

DISSERTATION

Defense held on 28/01/2016 in Luxembourg

to obtain the degree of

DOCTEUR DE L'UNIVERSITÉ DU LUXEMBOURG

EN SCIENCES de L'INGÉNIEUR

by

Anusha MOONSHIRAM
Born on 15 May 1980 in Pamplemousses, Mauritius

PHASED ARRAY ANTENNA WITH DIELECTRIC PHASE SHIFTERS

Dissertation defense committee

Dr.-Ing Michel Marso, dissertation supervisor
Professor, Université du Luxembourg

Dr.-Ing Holger Voos, Chairman
Professor, Université du Luxembourg

Dr.-Ing Jean-Régis Hadji-Minaglou, Vice-Chairman
Professor, Université du Luxembourg

Dr.-Ing Holger Heuermann
Professor, FH Aachen-University of Applied Sciences, IMP-Germany

Dr.-Ing Martin Mikulics
Senior Researcher, Forschungszentrum Jülich GmbH, PGI-9, Jülich, Germany


UNIVERSITÉ DU
LUXEMBOURG

PHASED ARRAY ANTENNA
With
DIELECTRIC PHASE SHIFTERS

Anusha Moonshiram

University of Luxembourg

Faculty of Science, Technology and Communication

This dissertation is submitted for the degree of Doctor of Philosophy

Dissertation Defense Committee: Professor Dr.- Ing Michel Marso,

Professor Dr.- Ing Holger Voos,

Professor Dr.- Ing Jean-Régis Hadji-Minaglou,

Professor Dr.- Ing Holger Heuermann and

Dr.- Ing Martin Mikulics.

Kirchberg, LUXEMBOURG

January 2016

DECLARATION

This dissertation is the result of my own work and includes nothing, which is the outcome of work done in collaboration except where specifically indicated in the text. It has not been previously submitted, in part or whole, to any university of institution for any degree, diploma, or other qualification.

Signed: Anusha Moonshiram

Date: December 15th, 2015

Anusha MOONSHIRAM

Faculty of Science, Technology and Communication

University of Luxembourg

ABSTRACT

This PhD Thesis entitled, “Phased Array antenna with Dielectric Phase Shifters” presents a candidate for a planar, elegant and simple alternative to replace the parabolic antenna on the roof of your house and that of your neighbours. A parabolic antenna is bulky, has an average weight of 25 kg, and it is usually attached with an arm fixture of an average depth of 30 cm. Unlike the parabolic antenna which represents a large unsightly looking necessity on your roof, or balcony of your house, the planar antenna presented here is elegant and discrete. It is cheaply made with simple lightweight dielectric sheets and is mounted directly as a planar surface on the wall of your house oriented towards the satellite Astra 1M and requires no extra mount fixture. The planar antenna is less subjected to environmental conditions such as wind or hail and must not be constantly readjusted to optimize TV reception.

The proposed antenna is made of 32 by 32 elements of a length and a spacing of half wavelength $\lambda/2$ with dielectric phase shifters to orient the main lobe with a 3° beamwidth by 45° in azimuth and from 23° to 43° in elevation. The dielectric phase shifters use a high dielectric constant of ε_r 10.2 on top of an antenna array with a substrate of ε_r 2.2. The difference between the high and the low dielectric value on a coplanar waveguide (CPW) feedline requires a maximum length of 18.7 cm for the 32nd antenna element in order to move the main lobe by a maximum of 45°. The CPW feedline is ideal to minimize mutual coupling among antenna elements. The antenna gain is 32 dBi and the beamwidth is 3°. It occupies a total size of 72.25 cm x 40.96 cm x 6.22 cm.

The antenna presented here is targeted for the reception of satellite television in Europe broadcasting from 10.7 to 12.7 GHz. As it consists of frequency independent antenna elements, it can be resized for any desired frequency range in any part of the world. In short, it is a cheap, light, adaptable and discrete design and especially convenient in regions where unsightly parabolic antennas are prohibited.

ACKNOWLEDGEMENTS

I am grateful to each and every one who supported me during my PhD research project.

I extend my sincere thanks to Professor Dr.-Ing Michel Marso, my project supervisor, who provided me with this opportunity and helped me advance forwards with my graduate studies. Many thanks also to Professor Dr.-Ing Jean-Régis Hadji-Minaglou and Professor Dr.-Ing Holger Voos for their interactive encouragements and for being in my "Comité d'Encadrement de Thèse" (CET). Sincerest thanks go to Professor Dr.-Ing Holger Heuermann and Dr.-Ing Martin Mikulics for being in my PhD jury.

Many thanks to my PhD friends: Anja Degens, Dr. Patricia Benito Martin, Amalya Khurshudyan, Srivathsan Ravi, Dr. Rafiq Ahmad, Christian Lamberti, Pascal Guy Schmalen, Annabella Simon, Simone Drees, Thomas Kopf, Dr. Lars Juul and Dr. Lionel Arend who were great colleagues and provided numerous intelligent conversations during my time at the University of Luxembourg.

A special mention to my Luxembourgish and German classmates and to my language professors: Professor Gaby Schmitz, Dr. Marion Krames, and Salvatrice Steuernagel, and to Virginie Ambroise who enabled me during my language classes at the University of Luxembourg.

Many sincere thanks to the HR staff especially to Katrin Effenberger, the doctoral studies' staff Virginie Mucciante and Véronique Pelt, the IT and support staff: Marco De Cilia, Antonie Zoccolo and Didier Coden, and the catering and cleaning ladies of our university.

Big thanks to my friends Dr. Huei-Li Lin, Mona Advani-Gianchandani and Amèle Salah for being my support friends.

Thank you to my sister Dr. Dooshaye Moonshiram for her attention and support.

My grateful thanks go to my Mother and Father from my natal country, Mauritius Island. My parents were only a phone call away, with their full support during every phase of my work.

Last, but not least, a big thanks and heart-warming love to my small family: my husband, Surena Neshvad, who is working on his PhD, "*Topology and Parameter Estimation in Power Systems through Inverter Based Broadband Simulations*" at the University of Luxembourg with an anticipated completion of mid-2016, and to our two sons, the joys of our life, Adrian, 5 and Darius, 2.5, who are continually giving us a deep life lesson on strength, love, tolerance, humility and patience. This PhD degree is only possible because of your understanding.

Thank you.

Anusha Moonshiram

Kirchberg, Luxembourg, December 2015

DEDICATION

To my Mother: my deepest love and sincerest devotion go to you.

Thank you.

CONTENTS

DECLARATION **1**

ABSTRACT **2**

ACKNOWLEDGEMENTS **3**

DEDICATION **5**

CONTENTS **6**

LIST OF TABLES **10**

LIST OF FIGURES **11**

1. INTRODUCTION **15**

1.1 This PhD Thesis 15
1.2 The Thesis Flowchart 16
1.3 Thesis Summary: Chapter by Chapter 18
1.4 Dissertation Statement 19

2. DEFINITIONS & INFORMATION **20**

2.1 Definitions of the Thesis Specifications 20
2.2 Definitions of 3B's: Bandwidth, Beamwidth and Beam Gain 20
2.3 Definition of the Azimuth and Elevation planes 21
2.4 Polarization of the Antenna element 22
2.5 Cross-Polarization 22
2.6 The Metal and Substrates used in the Thesis 23
2.7 The Efficiency of the Antenna 23
2.8 Spacing out the Antenna Elements in the Array: Mutual Coupling 24
2.9 Spacing out the Antenna Elements in the Array: Grating Lobes 25
2.10 Chapter Conclusion 27

3. BACKGROUND **28**

3.1 The Big Butterfly Antenna Theory 28
3.2 Chapter Conclusion 30

4. MICROSTRIP ANTENNA 31

4.1 The Microstrip or Patch Antenna 31
4.2 Chapter Conclusion 35

5. CST MICROWAVE STUDIO 36

5.1 CST 3D Simulation Software 36
5.2 Which Solver to use? 36
5.3 Antenna Magus 38
5.4 Chapter Conclusion 38

6. USING CST TO SIMULATE THE PATCH ANTENNA 39

6.1 The Patch Antenna Design 39
6.2 Chapter Conclusion 41

7. BANDWIDTH ENHANCEMENT 43

7.1 Bandwidth Improvement of the Patch Antenna 43
7.2 H-shaped Patch Antenna 45
7.3 Design Methodology of the H-shaped Patch Antenna 48
7.4 S-parameters results of the H-shaped Patch Antenna 56
7.5 Superstrate Effect of the H-shaped Patch Antenna 58
7.6 Chapter Conclusion 59

8. THE BUTTERFLY ANTENNA 61

8.1 Back to the Roots 61
8.2 Old is Gold 61
8.3 The Gem of Antenna Elements: The Slotted Butterfly Antenna 64
8.4 Chapter Conclusion 69

9. FREQUENCY INDEPENDENT ANTENNAS 70

9.1 The Butterfly Antenna is a Frequency Independent Antenna. 70
9.2 The Design of the Butterfly Antenna 72
9.3 The Results of the Frequency Independent Antennas 75
9.4 Chapter Conclusion 80

10. THE ANTENNA ARRAY 81

10.1 The Antenna Array 81
10.2 The History of the Antenna Array 83
10.3 The Antenna World: A Matter of Size 85
10.4 The Origins of Phase Shifters in an Array 86

11. ARRAY FEED 89

11.1 The Antenna Feed 89

12. THE DIELECTRIC PHASE SHIFTERS 97

12.1 The Dielectric Phase Shifters 97

12.2 Design of the Dielectric Phase Shifters 99
12.3 The Group Delay 100
12.3 Dielectric Phase Shifters Measurement Boards 104
12.4 The Scaled Slotted Butterfly Antenna Element 105
12.5 The Antireflection Coating of the Phase Shifters 108

13. PHASED ARRAY ANTENNA WITH DIELECTRIC PHASE SHIFTERS 111

13.1 The Phased Array Antenna with Dielectric Phase Shifters 111
13.2 Chapter Conclusion 123

14. FUTURE WORK 124

15. CONCLUSION 125

16. BIBLIOGRAPHY 127

17. PUBLICATIONS & PATENTS 135

17.1 Publications during PhD 135
17.2 Publications from 2005 to 2007 136
17.3 Publications from Bachelor Degree & Master Degree 136
17.4 Patents 137

LIST OF TABLES

Table 1 The pros and cons of the patch antenna element 33

Table 2 The characteristics for the solver choice. 37

Table 3 The dimensions from Figure 16-19 55

Table 4 The antenna naming convention 73

Table 5 The European countries along with their Elevation Angle [97] 123

LIST OF FIGURES

Figure 1 The Thesis Flowchart 17

Figure 2 The 3D radiation patterns of Figure 11 and 12 respectively 22

Figure 3 The mutual impedance of two side-by-side λ/2 diploes where Spacing is expressed in terms of λ 25

Figure 4 The formation of grating lobes formation with λ 26

Figure 5 The built-up from one antenna element to the array with phase shifters. 27

Figure 6 The first biconical antenna in 1898 by Lodge 29

Figure 7 The infinite biconical antenna, the 3D version of the planar butterfly antenna 30

Figure 8 The microstripline antenna from Deschamps' patent 32

Figure 9 The patch antenna on Rogers with ε_r 2.2 33

Figure 10 The fringing fields of the patch antenna on Rogers of ε_r 2.2 34

Figure 11 A corporate fed patch antenna element 40

Figure 12 The inside fed patch antenna element 41

Figure 13 The stacked patch antenna element 44

Figure 14 The design of a coupled line with a phase shifter with different substrates 48

Figure 15 The optimization steps and S_{11} (dB) of the H-shaped patch element 51

Figure 16 The parasitic elements added on top and below the centrally located asymmetrical rectangular patches 53

Figure 17 The inter-optimized H-shaped parasitic elements 53

Figure 18 The strongly optimized H-shaped parasitic elements 53

Figure 19 Zoomed-in of Figure 18 to show the inter gap dimensions 54

Figure 20 The slots in the substrate layer under the metal layer 54

Figure 21 The antenna element design of 25.6 mm x 25.6 mm x 2.56 mm 55

Figure 22 The four layer design of the H-shaped patch element 56

Figure 23 The port set up at the end of the centrally located coplanar $S^{+}S^{-}$ feedline 56

Figure 24 The S_{11} (dB) vs. frequency/ GHz and gain for the optimized antenna element showing a bandwidth of 34%. 58

Figure 25 The gain in dBi of the antenna element with and without superstrate 59

Figure 26 The butterfly antenna element 63

Figure 27 The slotted butterfly antenna element 66

Figure 28 The stacked slotted bow–tie antenna element with a superstrate and four metal rectangles placed on top of the corners of the slotted butterfly 69

Figure 29 The butterfly with a flare angle of 60° and straight ends (antenna straight-60). ... 74

Figure 30 The butterfly with a flare angle of 60° and round ends (antenna round-60)..... 74

Figure 31 The S_{11} (dB) of the four butterfly antennas from 5 to 60 GHz 75

Figure 32 The VSWR of the four butterfly antennas from 5 to 60 GHz..... 76

Figure 33 The impedance of 189Ω of the antenna from 5 to 60 GHz..... 76

Figure 34 The E-fields (left) and the H-fields (right) at the port of the antenna 77

Figure 35 The directivity plots in the φ= 0° plane (azimuth)..... 78

Figure 36 The directivity plots in the φ= 90° plane (elevation) 78

Figure 37 The 3D radiation patterns of the four butterfly antennas at 11.7 GHz 79

Figure 38 An array with circular polarization from linearly polarized rectangular patches [81]. 82

Figure 39 The first switchable phased array with a three element system [83] 83

Figure 40 The early warning Mammut Radar [85] 84

Figure 41 The World largest phased array antenna in Alaska/Canada [86]..... 84

Figure 42 The world largest single aperture antenna [87]..... 85

Figure 43 The radiation from a parabolic antenna [89] 86

Figure 44 The serial fed with the patch antenna [91] 90

Figure 45 The serial feed with the slotted stacked butterfly antenna 90

Figure 46 The S_{11} (dB) versus frequency/GHz for serial feed 91

Figure 47 The patch array fed in the middle 91

Figure 48 The S_{11} (dB) versus frequency /GHz for mid fed patch array 92

Figure 49 The butterfly antenna fed in the middle 93

Figure 50 The S_{11} (dB) versus frequency /GHz for the mid fed butterfly array 93

Figure 51 The butterfly antenna with the zoomed-in views 94

Figure 52 The S_{11} (dB) versus frequency/GHz with PEC metal 95

Figure 53 The S_{11} (dB) versus frequency/GHz with Copper metal 95

Figure 54 The main lobe movement in the azimuth and the elevation planes 99

Figure 55 The single-ended phase shifter 101

Figure 56 The group delay for the single-ended transmission line 101

Figure 57 The CPW phase shifter 102

Figure 58 The group delay of the CPW transmission line 103

Figure 59 The built and measured boards with dimensions 2.5 cm by 2.5cm and phase shifters (*rightmost*) 104

Figure 60 The resized and optimized slotted butterfly antenna element 105

Figure 61 shows the S_{11} (dB) for the optimized slotted butterfly antenna element 106

Figure 62 The 3D far-field patterns of the optimized slotted butterfly antenna element 106

Figure 63 The directivity in the $\varphi = 0°$ plane (azimuth) at 11.7 GHz 107

Figure 64 The directivity in the $\varphi = 90°$ plane (elevation) at 11.7 GHz 107

Figure 65 The design of the antireflection coating on the CPW with phase shifter 108

Figure 66 The zoom-in transmission line from Figure 65 109

Figure 67 The S_{11} (dB) versus frequency/GHz, with and without the antireflection coating, for the transmission line that includes the phase shifter 110

Figure 68 The 32 antenna elements added next to each other..... 112

Figure 69 The 32 x 1 array with the feed network 112

Figure 70 A zoomed-in of the feed network connection with the 2 vias transitions..... 113

Figure 71 The 4 layers of the 32 x 1 array with the feed network 114

Figure 72 The S_{11} (dB) of 32 x 1 array without phase shifters..... 114

Figure 73 The S_{11} (dB) of 32 x 1 array with phase shifters..... 115

Figure 74 The 32 x 1 array stacked 32 times on top of each other to form a 32 x 32 array. 116

Figure 75 The far-field at 11.7 GHz in the φ= 90° plane without phase shifters..... 117

Figure 76 The far-field at 11.7 GHz of 32 x 1 array with phase shifters 118

Figure 77 The 32 x 1 array plot in the φ= 90° plane with phase shifters 119

Figure 78 The 32 x 32 antenna array at 11.7 GHz without phase shifters 119

Figure 79 The far-field at 11.7 GHz of 32 x 32 array with phase shifters 120

Figure 80 The 32 x 32 array plot in the φ= 0° plane with phase shifters 121

1. INTRODUCTION

1.1 This PhD Thesis

This PhD thesis investigates a phased array antenna with dielectric phase shifters.

It reveals an array of 32 x 32 antenna elements with phase shifters made of a substrate of high dielectric constant placed on top of the feedlines of the antenna elements. That way, the phase velocity of the feedlines is changed and the main lobe of the array moves to cover the angular direction for satellite TV broadcasts

The dielectric phase shifters uses a high dielectric constant of ε_r 10.2 on top of an antenna array built with a substrate of ε_r 2.2. The difference between the high and the low dielectric value on a CPW feedline requires a maximum length of 18.7 cm for the 32^{nd} antenna element in order to move the main lobe by 45°. The antenna is communicating with the SES ASTRA 1 M satellite on the geo orbit so it must have a gain of approximately 30 dBi.

In order to design a phased array antenna with dielectric phase shifters, the antenna element making up the antenna array must first be designed. Then this antenna element is replicated N times in the x and y direction in order to occupy the surface area to satisfy the 3° beamwidth of the main lobe. Here N = 32. The step by step movement required to progress toward the design of the phased array antenna with dielectric phase shifters is shown in the next section: The Thesis Flowchart.

1.2 The Thesis Flowchart

The thesis flowchart, shown in Figure 1, covers the requirements of the thesis, that is, the flow of constraints that must be followed for the reception of optimal results.

The phased array antenna with dielectric phase shifters means that an array of antenna elements must be constructed with identical properties. Since the phased array antenna is designed to replace the parabolic antenna on top of the roof of your house and that of your neighbours, it has the same properties as the parabolic antenna. This means that it must cover the bandwidth from 10.7 GHz to 12.7 GHz and must have a gain of approximately 30 dBi. The main lobe must have a beamwidth of 3° and the main lobe must move up to 45° with the help of the dielectric phase shifters.

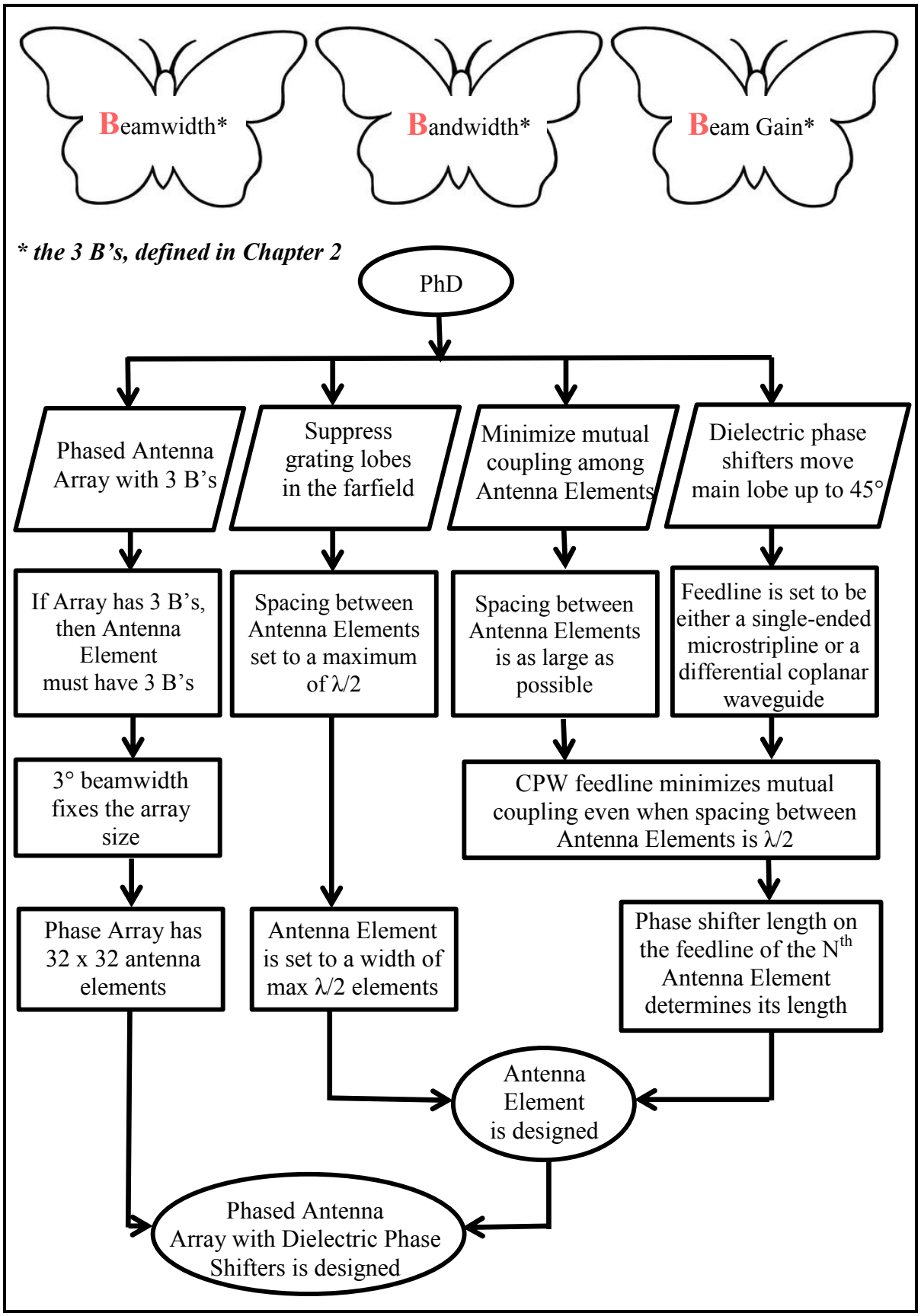

Figure 1 The Thesis Flowchart

1.3 Thesis Summary: Chapter by Chapter

The present manuscript is divided in several sections where each chapter progresses step by step to gradually reveal the phased array antenna with the dielectric phase shifters.

Chapter 1 introduces the thesis requirements and the dissertation statement. It also summarises the PhD thesis in a concise flowchart with the design objectives and constraints. It also contains the chapter descriptions *(presently described)* in a summarized format. Chapter 2 defines the thesis specifications, and other technical terms used in this work. It also describes the metal and substrates used throughout the thesis as well as the spacing requirements between the antenna element to avoid grating lobes and to minimize mutual coupling in the array configuration. Chapter 3, also known as the history chapter, dives into the ancestry of antennas and the interesting work of numerous scientists who have dedicated their career on this topic. The fourth chapter jumps right into the methodology and results of the PhD work. The design of the simplest antenna element, the microstrip antenna, which possesses fine qualities, is implemented. The designs are achieved with the 3D software revealed in Chapter 5. Further along, the microstrip antenna is detailed in Chapter 6 and its bandwidth enhancements using research work, well documented in the literature by our fellow scientists, are presented in Chapter 7. Subsequently, a novel H-shaped antenna, which is an enhancement of the patch antenna element, is revealed. Unfortunately it has a major caveat of being way too large to fit in an antenna array. The size of the antenna element is crucial in an array environment and thus a butterfly antenna is examined as an alternative antenna element in Chapter 8. The puzzle resolves itself with the use of the slotted version of the butterfly antenna. The slotted version of the butterfly antenna originates from the butterfly antenna, also known as a frequency independent antenna as shown in Chapter 9. A quick history is given in Chapter 10 on the antenna array and phase shifters. The array feed is considered in Chapter 11. The slotted butterfly antenna element to be used in an array version is refined in Chapter 12 where both its width and length are revealed following the phase shifters' length that is required to move the array's main lobe up to 45° as requested by the thesis specifications. The mystery is untangled and the optimized feed network is attached to the array of antenna elements as achieved in Chapter 13. The PhD target is reached. Future suggestions are recommended in Chapter 14 and the project is concluded in Chapter 15. Chapter 16 lists the references from the thesis chapters while the final Chapter 17 proudly

reveals the long list of publications that were successfully published along with the two patents obtained from not such a distant past.

1.4 Dissertation Statement

This thesis covers an interesting and original way of orienting the main lobe of an array antenna by using simple dielectric phase shifters on top of the feedline of the antenna array.

It is a simple idea that is quite complex to achieve where the change in dielectric constants from high to low is used to vary the phase velocity of the beam signal in order to shift the direction of the main lobe of a phased array antenna.

The delicate and complicated task of designing a phase array antenna with dielectric phase shifters arises due to the lossy problems linked with the mutual coupling between the antenna elements, or linked with grating lobes in the far-field when the ideal antenna spacing is not utilized, or with the difficulty of building an array with a large feed network. On top of all, since the studied system is simulated, the effects of feedline interference and mutual coupling of the elements are exacerbated in a large array requiring long computer processing times to accurately replicate the reality of antenna design.

Nevertheless, a simple design has been successfully implemented, to lead to an elegant phased antenna array comprising a main lobe with a 3° beamwidth that replicates the performance of the parabolic antenna. The dielectric phase shifters to move the main lobe of an antenna array reach the same performance as a parabolic antenna with a 3° beamwidth and a gain of approximately 30 dBi. The gain requirement is set to 30 dBi because the satellite, Astra 1M with which the antenna array is supposed to communicate is on the geo level.

Now to phase shift the array, the phase shifter must be designed so that it moves each element and allows it to cover the desired angular elevation and azimuth angles. Why is this an advantage? The phased array allows the array to operate as a large antenna with many designs and size advantages. For example, with planar sheets of dielectric structures, despite a finally simplistic architecture and a small size, the performance of a large parabolic antenna can be replicated. The iterative and progressive design elaboration coming naturally together with its related constraints, are presented in the following chapters.

2. DEFINITIONS & INFORMATION

2.1 Definitions of the Thesis Specifications

The thesis flowchart from the introductory chapter summarised the thesis specifications that must be followed in order to reach our project goal. These are defined in this chapter. The choice of metal and substrates used throughout the thesis for the antenna elements, the antenna array and the dielectric phase shifters are given. The efficiency of the antenna element is also discussed. Finally, the spacing constraints of the antenna elements in an array configuration to minimize mutual coupling and to avoid grating lobes are summarized.

This chapter thus provides the background of the terms that must be taken into consideration as the antenna elements, array and dielectric phase shifters are conceived and designed.

2.2 Definitions of 3B's: Bandwidth, Beamwidth and Beam Gain

The bandwidth of an antenna is defined as the range of frequencies over which the antenna can properly radiate or receive energy. The antenna bandwidth is commonly defined as the frequency range where the return loss S_{11} is less than -10 dB, that is, 90% of the antenna power is used for radiation.

The Bandwidth is also defined in Equation 1.

$$Bandwidth = \frac{f_{upper} - f_{lower}}{f_{center}} * 100\% \quad \text{Eq. 1}$$

where f_{upper} is the upper operational frequency i.e. 14.2 GHz in the studied case and f_{lower} is the lower operation frequency, here, 10.1 GHz and f_{center} is the center frequency where $f_{center} = (f_{upper} - f_{lower})/2$. Here f_{center} is 12.1 GHz.

The Beamwidth is measured in degrees between the half power points (3 dB) of the major lobe of the antenna. The Beamwidth can be expressed in terms of elevation (vertical plane or the φ = 90° plane) and azimuth (horizontal plane or the φ = 0° plane).

The Beam Gain of an antenna is defined as its directivity multiplied by its electrical efficiency where the directivity is the ratio of the radiation intensity in a given direction to the radiation intensity that would be obtained if the power accepted by the antenna was radiated isotropically or equally in all direction

2.3 Definition of the Azimuth and Elevation planes

The azimuth and elevation planes are defined in Figure 2 where the left plot shows the 3D radiation patterns from the patch antenna from Figure 11 while the right plot shows the 3D radiation patterns from Figure 12. The azimuth plane is defined as the φ = 0° plane or the horizontal or the xy plane while the elevation plane is also known as the φ = 90° plane or the vertical or the yz plane.

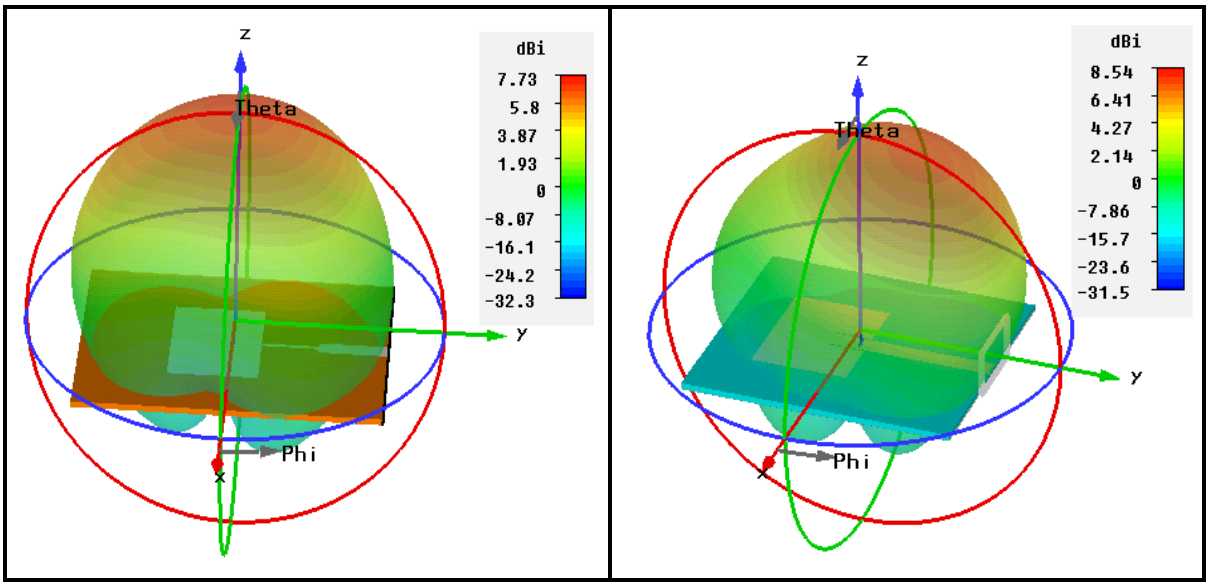

Figure 2 The 3D radiation patterns of Figure 11 and 12 respectively

2.4 Polarization of the Antenna element

An antenna element can radiate in different polarizations. Thus it can be elliptically, circularly or linearly polarized. In our case, we need linear polarized since the satellite with which the antenna elements interact is also linearly polarized. Linear polarization means that the antenna can radiate in two perpendicularly polarized signals completely independent of each other. Thus the electric fields that are radiated from both signals are always 90° to each other and as well to the direction of propagation.

2.5 Cross-Polarization

One important topic to take into consideration after polarization section is the cross-polarization. Cross Polarization is defined in [1]. Any concern to an eventual cross polarization does not matter since the design of the antenna element is planar and the polarization is linear. The radiation pattern of a planar antenna element is in two directions, both oriented perpendicular to the surface of the antenna element. The same antenna element can be used for vertical and horizontal polarization. Or it can be used for one polarization only and the other polarization can be either absorbed or reflected with the help of a wideband reflector.

2.6 The Metal and Substrates used in the Thesis

Throughout the project metal is design as a perfect electric conductor (PEC). The PEC simulates faster with the 3D electromagnetic software as compared when a 1 oz. Copper is used as it requires less mesh cells. A comparison between the performance of a PEC or Copper is made in Chapter 11 to show that there is no performance difference when either the PEC or Copper is used as metal. For the substrate, usually a dielectric with a low permittivity close to 1 would enable the element to radiate the most [2]. Rogers of ε_r 2.2 (Rogers RT5880) is used as the dielectric substrate because a low dielectric substrate close to air or close to 1 will allow a higher radiation pattern as compared to much higher permittivity value [2,3]. RT/Duroid 5880 is a glass microfiber reinforced PTFE composite where the glass reinforcing microfibers are randomly oriented to maximize the benefits of fiber reinforcement. The dielectric constant of the RT/Duroid 5880 laminate is uniform from panel to panel and is constant over a wide frequency range. Its low dissipation factor extends the usefulness to the Ku-band and above. Moreover, Roger's laminates are easily cut, sheared and machines to shape. They are resistant to all solvents and reagents, hot or cold, normally used in etching printed circuits or in plating edges and holes. These characteristics are useful as the substrate needs to allow the antenna element to perform under environmental conditions where temperature or humidity can vary [4]. The Rogers substrate is commonly obtained, reliable, popular and intensively used in the literature along with the substrate Rogers RT6010 of ε_r 10.2 [5] which is used to design the phase shifters. RT6010 has an ε_r that is high enough to be used as a phase shifter and is commonly available and must not specially be made. Moreover, the two substrates used in this project are maintained to be Rogers to maintain uniform humidity, temperature influences when the phased array is placed outdoors.

2.7 The Efficiency of the Antenna

The efficiency of the antenna must be addressed. An antenna radiates and receives microwave signals. It is a reciprocal device such that the same antenna element can receive or transmit the signal. The role of the antenna is to act as the interface between a free space wave and a guided wave. While a transmission line must have zero to scarce radiation, an antenna element is designed to radiate the maximum possible. The radiation of an antenna is created by discontinuities causing the propagation of electric and magnetic fields. Any wireless

system cannot exist without an antenna that enables the signal to be transmitted to free space and vice versa.

An antenna element or antenna array will have a certain bandwidth. An antenna's efficiency can be expressed in terms of its bandwidth and it can also be related to the VSWR: - the Voltage Standing Wave Ratio.

Further to the definition given above in this chapter, the bandwidth is also defined as the frequency range over which the antenna has a VSWR less than 2 which translates to an S_{11} of less than -10 dB or an efficiency of 89% or permitting a power reflection of 11%.

Just like in transmission line theory, the antenna element can be visualized as a one port device with S_{11}, the return loss or by Γ the reflection coefficient.

The VSWR and the return loss S_{11} are related to Γ as

$$\text{VSWR} = \frac{1 + |\Gamma|}{1 - |\Gamma|} \quad \text{Eq. 2}$$

$$S_{11}(\text{dB}) = -20\log|\Gamma| \quad \text{Eq. 3}$$

As Γ is the reflection coefficient, the best VSWR is obtained when Γ= 0 or VSWR = 1 or when S_{11} is infinitely low. However if 89% efficiency is acceptable, then a VSWR of less than -2 or a return loss less than -10 dB is considered as an acceptable standard.

2.8 Spacing out the Antenna Elements in the Array: Mutual Coupling

Mutual coupling is the electromagnetic interactions between the antenna elements in an array where the current developed in each antenna element of an array depends in their own excitation and also on the contributions from adjacent antenna elements. Mutual coupling between antenna elements affects the antenna parameters like impedance, reflection coefficients and hence the antenna array performance in terms of radiation characteristics and bandwidth are affected [6]. The mutual coupling must be minimized in order to allow the

optimum performance of the antenna array. Mutual coupling is inversely proportional to the spacing between the different antenna elements in an array [7].

Thus, the larger the spacing between the antenna elements, then the lower is the mutual impedance and hence the lower is the mutual coupling as shown in Figure 3 [7]. In Figure 3, the mutual impedance is plotted against the spacing where Spacing is expressed in terms of λ where one spacing = one λ.

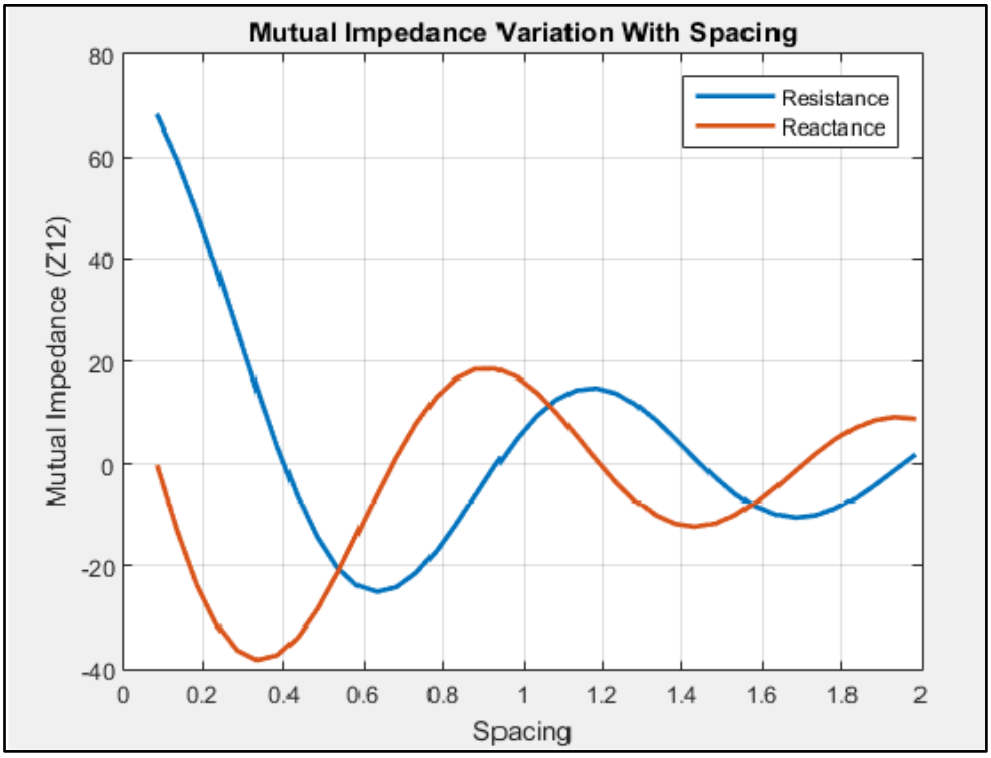

Figure 3 The mutual impedance of two side-by-side λ/2 diploes where Spacing is expressed in terms of λ

2.9 Spacing out the Antenna Elements in the Array: Grating Lobes

Grating lobes are the unwanted beams of radiations of an antenna array. They occur in uniformly spaced arrays when the antenna element separation is too large [8]. Figure 4 from [9] shows the plot of grating lobes when the spacing *d*, as described in Figure 5, is changed. Thus we can see that a spacing of λ/2 represents a better antenna spacing as compared to λ in order to avoid grating lobes.

This is described in further details in Figure 5. *d* is the mid to mid spacing between the antenna elements and typically set to λ/2 to prevent antenna interference and grating lobes.

Here, if $d = \lambda/2$, then the length of the width of the antenna elements must be a maximum of λ/2. When the frequency range is 10.7 GHz, zo 12.7 GHz, and the mid frequency is 11.7 GHz, then λ= 2.56 cm or λ/2 = 1.28cm.

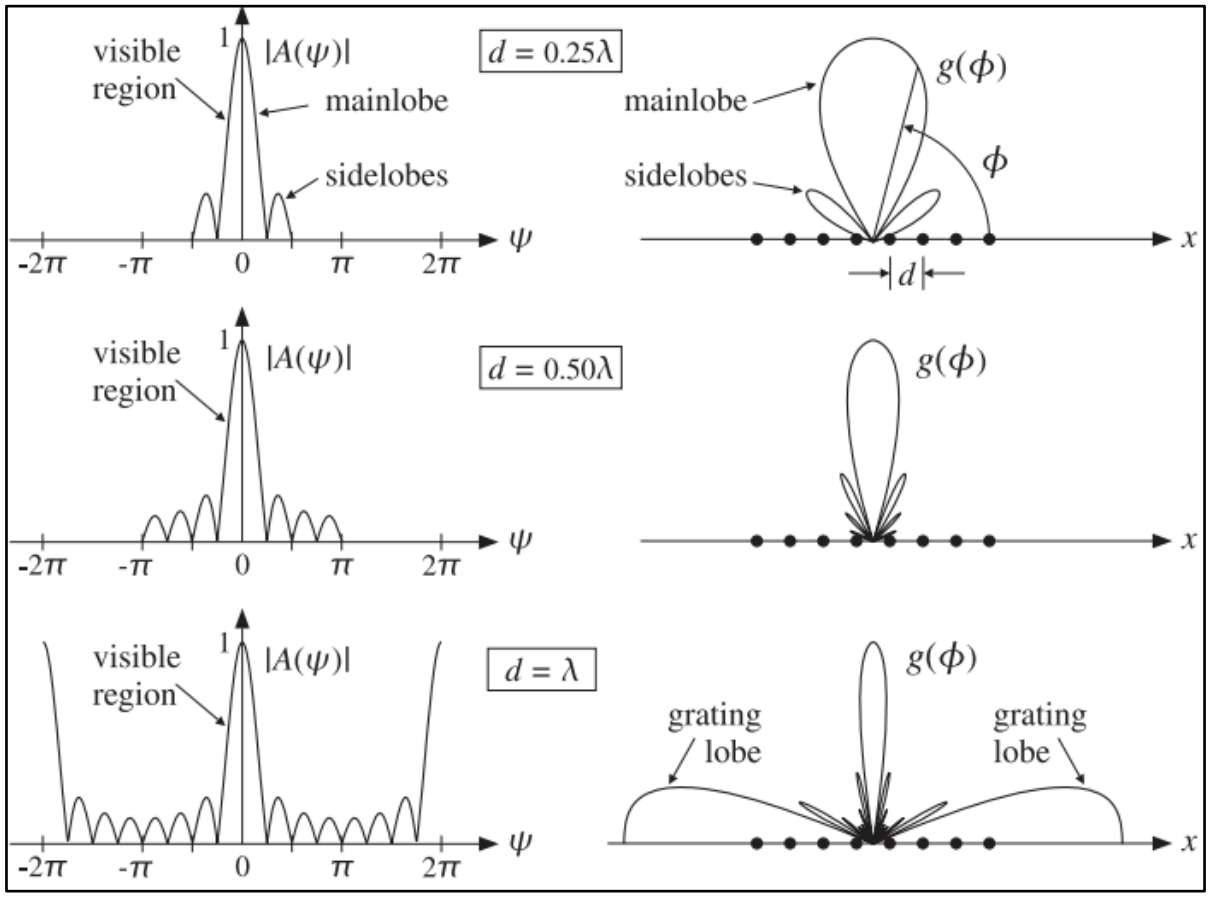

Figure 4 The formation of grating lobes formation with λ

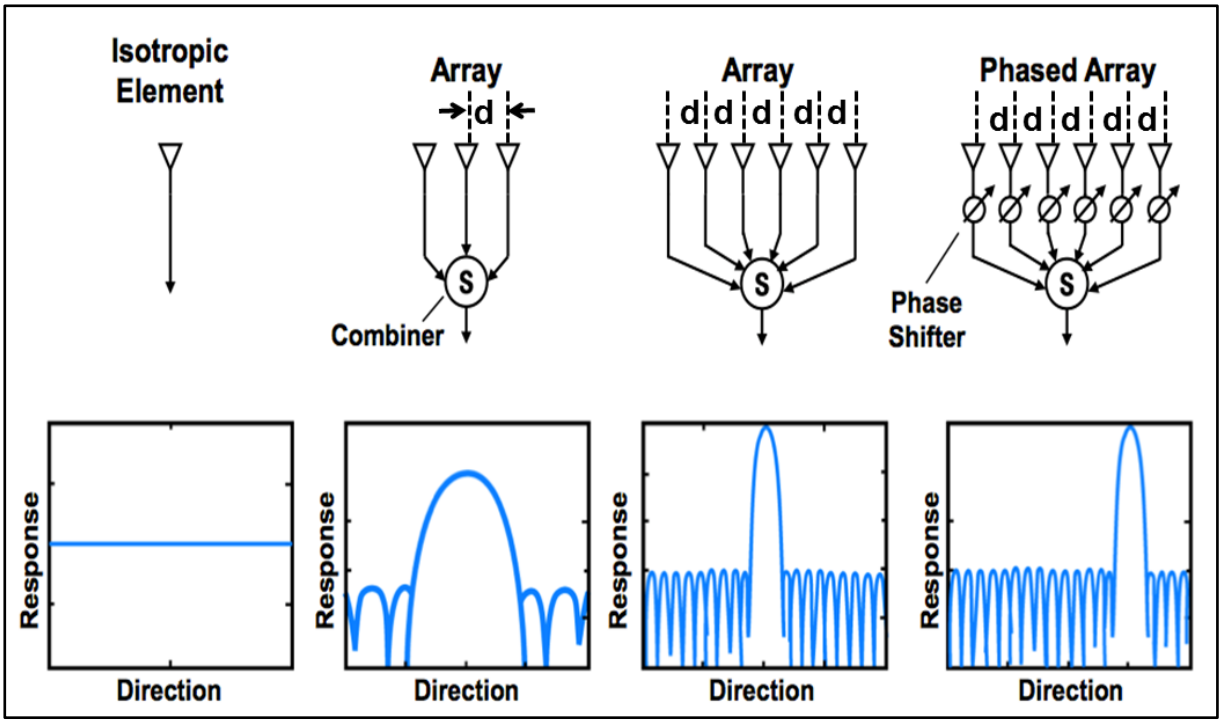

Figure 5 The built-up from one antenna element to the array with phase shifters.

This section is concluded by stressing on the important of λ/2 spacing to avoid grating lobes.

2.10 Chapter Conclusion

Now that the important specifications of the thesis have been defined and some information has been provided to serve as a project foundation, one can move on to the background of antennas, and that of antenna elements, and to study the antenna elements that will answer the thesis.

3. BACKGROUND

3.1 The Big Butterfly Antenna Theory

Professor Ian Stewart published in 2013 "In pursuit of the unknown, 17 Equations that changed the world" [10] and he rightfully showed how all the everyday advances, that we take for granted, started with an equation statement. Maxwell's Equations certainly figure in these 17 equations. In fact, at the end of the last millennium, in 2000, Maxwell was elected as the third greatest physicist of the millennium right after Newton and Einstein [11]. In 1873, after James Clerk Maxwell published his four famous linear partial differential equations that summarize the classical properties of the electromagnetic fields [12], Sir Oliver Lodge began his work on the generation and detection of electromagnetic waves. Lodge published his work in 1888 while recognizing Heinrich Rudolf Hertz's research work [13]. On June 1, 1894, Sir Oliver Lodge was the first to mention Hertzian waves to further acknowledge Hertz's proof of the existence of electromagnetic waves during a memorial lecture on Hertz who unfortunately died at the age of 36 [14]. Lodge patented his work in 1898 on syntonic tuning which means the same frequency can be used to receive and send [15]. Amos Dolbear a physics Professor at Tufts University, in Medford, Massachusetts (*my alma mater*) wrote a US patent in 1886 where he was able to send wireless signals over a distance of 0.5 miles, relying not on electromagnetic radiation but on phones grounded by metal rods into the ground [16]. Both patents were purchased by Guglielmo Marconi who first sent wireless signals over a distance of 1.5 miles in 1895 [17]. The broadcasting range of Marconi's transmitter was extended to more than 15 km by Ferdinand Braun. In 1899, Braun would apply for the patent, *Wireless*

electro transmission of signals over surfaces, when he successfully produced a sparkles antenna circuit [18]. Deeper details on the origins of wireless communications can be explored in the 2010 book from Sungook Hong, "From Marconi's black box to the Audion" [19].

Marconi and Braun went on to win the Nobel Prize in 1909 in recognition of their contributions to the development of wireless telegraphy. Sir Lodge continued his research to invent the biconical antenna in 1894, same patent as syntonic tuning [15]. At that time he was focusing more on a narrow-band frequency domain radio but this same patent also became the first ultra-wideband antenna. Figure 6 depicts the first biconical antenna initiated by Lodge.

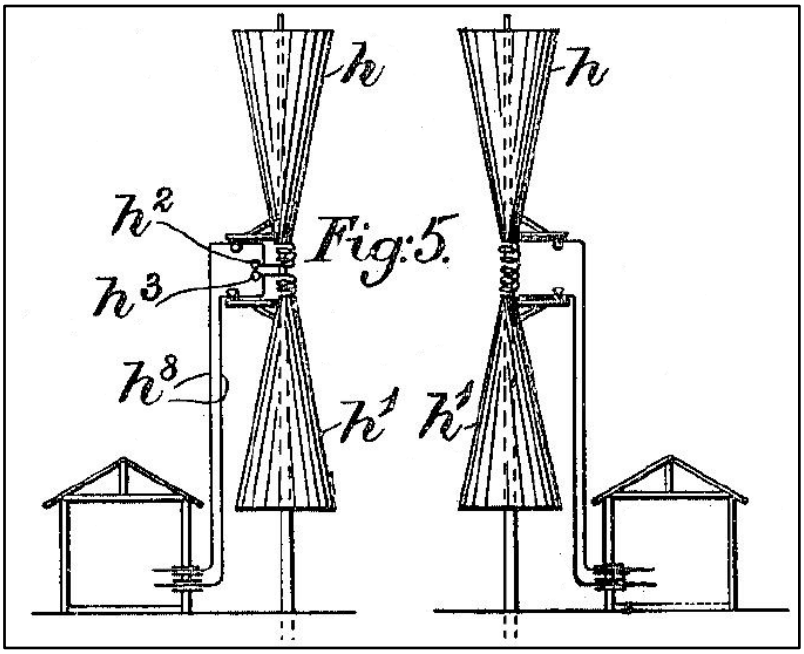

Figure 6 The first biconical antenna in 1898 by Lodge

The infinite biconical antenna [20] is an infinite transmission line where the input impedance of the antenna is given by Equation 4 where α is the angle between the inner arms also known as the flare angle of the biconical antenna as shown in Figure 7.

$$Z_{in} = 120 \ln\left[\cot\left(\frac{\alpha}{4}\right)\right] \quad \text{Eq. 4}$$

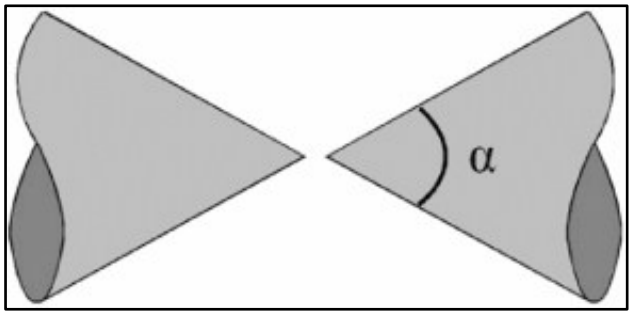

Figure 7 The infinite biconical antenna, the 3D version of the planar butterfly antenna

The bandwidth is typically about 120 to 150% and it is linearly polarized with a maximum gain of 4 dB per antenna element. The butterfly or the bow-tie antenna is a planar version of the finite biconical antenna and can be printed on a substrate. H. Brown and M.Woodward examined the effect of the flare angle α for a butterfly antenna [21], while Jean-Marc Laheurte showed [22] that the butterfly antenna comes from the dipole antenna which is basically a wire antenna. The antenna is made up of 2 aligned metal arms fed at the center point. Laheurte explains how the ends of the arms are open circuits which resonant at their extremities. The butterfly antenna can also be produced using slots in a metal plate or on a substrate [23], which results in an unsymmetrical. In this way, its feed can be ensured by the use of a coaxial cable without the use of a balun. However, the input impedance of such an antenna typically remains around 80Ω.

3.2 Chapter Conclusion

We have seen in this short chapter how the butterfly antenna dates back from the first patent of Lodge and it is further explored in the next chapter. Historically, the butterfly antenna is the Father of the simplest antenna described in more details in the next chapter: the microstrip or patch antenna.

4. MICROSTRIP ANTENNA

4.1 The Microstrip or Patch Antenna

The microstrip antenna is a very popular antenna element. As from November 2015, it is found in the research papers of 13% of all antenna papers from IEEE website. *(The word "antenna" returns 193 500 results, while the word microstrip antenna returns 25 000 results from www.ieee.org)* [24].

It arises from George Deschamps, who wanted to obtain a high resolution X-band antenna with a beamwidth < 1°. His design was half of a planar round-ended butterfly antenna fed with microstripline as shown in Figure 8 [25]. One particularity of this array is the use of circular bends in the feedline, which Deschamps claimed, to reduce radiation loss and mismatch. This feedline pattern was not further explored as, while it must certainly be possible with four elements, it becomes much more challenging with larger number of antenna elements or, in the studied case here, 32 antenna elements. It is also not a convenient way to maintain a uniform feedline to enable a smooth and steady change in direction of the main lobe with the dielectric phase shifters presented in this thesis. Furthermore, such circular bends will occupy quite a lot of real estate as the radii of the bend depends on the strip width, as explained in Deschamps' patent, which becomes larger the more the number of elements in the array increases.

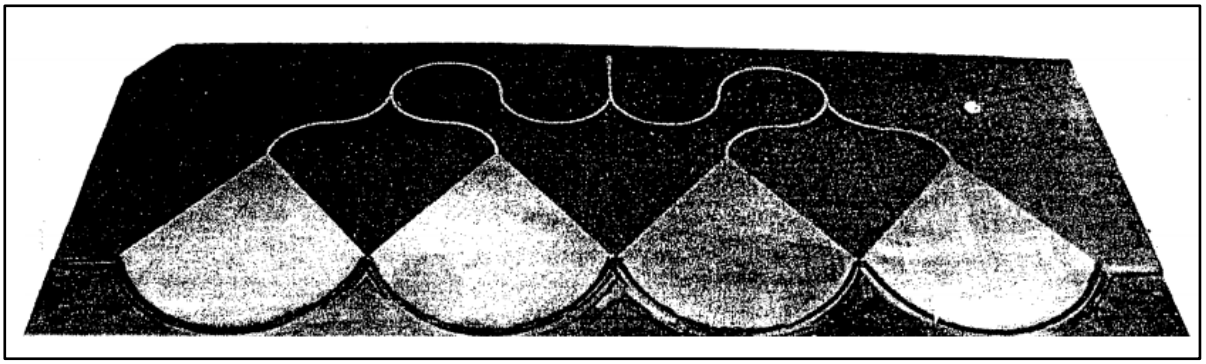

Figure 8 The microstripline antenna from Deschamps' patent

Howard and Munson further simplified Deschamps' microstrip antenna to present the simplest and most popular form of the microstrip antenna [26]. With Howard and Munson's simplification, a microstrip or patch antenna is now simply a metal layer of any shape on top of a substrate and terminated with a ground plane at the back. It is considered as the simplest antenna element as it is just a radiator on top of a dielectric backed by a ground plane. The microstrip or patch antenna can be cheaply manufactured just the way printed circuit boards are made. In fact, the feedline and matching networks can be fabricated simultaneously with the antenna element. It thus features a robust antenna element antenna element with a light weight, a small volume and a thin profile configuration. Linear polarizations are possible with a simple feed.

In fact, its main recognized weak point is its bandwidth. The patch antenna is a resonant structure with a high Q-factor and this translates into a narrow bandwidth.

The bandwidth, BW, which can be expected from a patch antenna, is given by Equation 5.

$$\mathrm{BW} \propto \frac{3.77(\varepsilon_r - 1)W}{\varepsilon_r^2 L \lambda_0} \quad \text{Eq. 5}$$

Equation 5, defined by Jackson and Alexopoulos [27], gives the approximate bandwidth of the patch antenna where λ_0 is the center frequency, ε_r is the dielectric constant of the substrate and L and W are respectively the length and width of the patch antenna.

Table 1 summarises the advantages and disadvantages of the microstrip or patch antenna.

Advantages	**Disadvantages**
Light weight	Narrow bandwidth
Low volume	Large loss in the feed structure of arrays
Thin profile configurations	
Low fabrication cost	
Readily amenable to mass production	
Feedlines and matching networks can be fabricated simultaneously with the antenna structure	

Table 1 The pros and cons of the patch antenna element

One of the most common types of microstrip antenna is the rectangular patch. Figure 9 shows a typical rectangular patch antenna with width W and length L over a grounded dielectric substrate with dielectric constant ε_r. Ideally, the ground plane on the underside of the substrate is of infinite extent. Normally, the thickness of the dielectric substrate, h, is designed to be $\leq 0.02\lambda$, where λ is the wavelength in the dielectric.

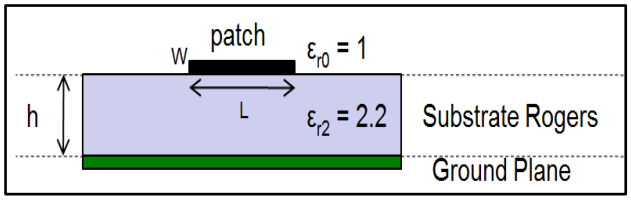

Figure 9 The patch antenna on Rogers with ε_r 2.2

Equation 6 shows the equation for the length of the patch,

$$L = \frac{c}{f_r\sqrt{\varepsilon_r}} \quad \text{Eq. 6}$$

and Equation 7 is for the width of the patch,

$$W = \frac{c}{f_r}\sqrt{\frac{2}{\varepsilon_r + 1}} \quad \text{Eq. 7}$$

where c is the speed of light and f_r is the resonance frequency while ε_r is the dielectric constant of the patch's substrate.

When the patch is excited by a feed, a charge distribution is established on the underside of the patch metallization and the ground plane. The repulsive force between the positive charges on the patch pushes some charges towards the edge, resulting in a large charge density, the source of fringing field and radiation. Radiation from the microstrip patch antenna occurs from the fringing fields between the patch and the ground layer as shown in Figure 10.

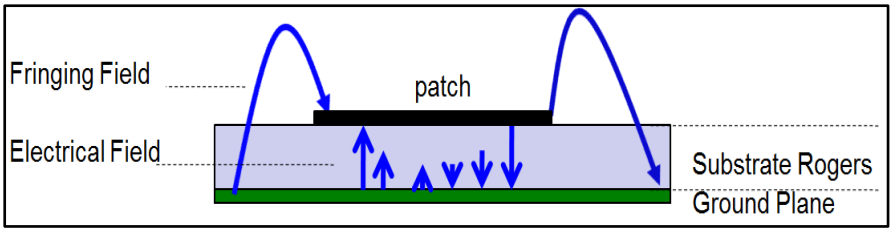

Figure 10 The fringing fields of the patch antenna on Rogers of ε_r 2.2

These fringing fields mean that the electrical length of the patch antenna element is larger than its actual length L and a ΔL must be added to account for this extra length extension. The definition of ΔL is given in Equation 8. Here are also shown the equations for the effective dielectric constant, $\varepsilon_{effective}$ and for the characteristic impedance Z_o. In the Equations 8-10 the variable W is the width of the patch while h is the height of the substrate while ε_r is its dielectric constant.

$$\Delta L = 0.412h\left(\frac{\varepsilon_{effective} + 0.3}{\varepsilon_{effective} - 0.258}\right)\left(\frac{\frac{W}{h} + 0.264}{\frac{W}{h} + 0.8}\right) \quad \text{Eq. 8}$$

$$\varepsilon_{effective} = \frac{\varepsilon_r + 1}{2} + \frac{\varepsilon_r - 1}{2}\left(1 + \frac{12h}{W}\right)^{-0.5} \quad \text{Eq. 9}$$

$$Z_0 = \frac{120\pi h}{W\sqrt{\varepsilon_{effective}}} \quad \text{Eq. 10}$$

For a given center fundamental frequency of the individual patch antenna element, the substrate height *h* may not exceed 5% of the wavelength in the medium.

With the addition of *ΔL* on each side of the patch antenna, the total length of the patch becomes *L + ΔL*. This length can also be expressed in a concise equation with respect to the resonance wavelength λ_0 as shown in Equation 11. From the latter, the resonance frequency, f_r, is obtained as shown in Equation 12.

$$(L + 2\Delta L) = \frac{\lambda_0}{2\sqrt{\varepsilon_{effective}}} \quad \text{Eq. 11}$$

$$f_r = \frac{c}{2\sqrt{\varepsilon_{effective}}(L + 2\Delta L)} \quad \text{Eq. 12}$$

4.2 Chapter Conclusion

While all these equations are interesting to know in order to obtain a rule of thumb or a first approximation of the resonant frequency, and the approximate bandwidth that can be obtained with the patch, a 3D electromagnetic simulation software is essential to replicate accurately the performance of the antenna design, as described in the next chapter.

5. CST MICROWAVE STUDIO

5.1 CST 3D Simulation Software

CST, Computer Simulation Technology, is a 3D simulation tool for electromagnetic design and analysis. It is user friendly and allows the optimization of devices in practically limited applications as claimed by the software guarantees. For this work, CST is ideal to design and optimize the antenna element and array over the desired frequency range from 10.7 to 12.7 GHz. It also allows the simulation of the feed network along the antenna structure. The software has two main solvers that can be used for antenna design and simulation: the time domain solver also known as the transient solver or the frequency domain solver.

5.2 Which Solver to use?

Time Domain or Frequency domain?

CST microwave is a software focused on 3D electromagnetic simulation [28].

It has two main solvers, the frequency domain solver and the time domain solver. The choice of the solver depends on the application. Table 2 summarises the choice criteria to select the correct solver.

Characteristics	**Solver choice**
Bandwidth	The time domain solver is preferred for a large continuous bandwidth while the frequency domain is more for a narrowband application or for a single frequency.
Resonances	The frequency domain solver is more suitable when the project has strong resonances.
Project Size	The time domain solver is more suitable when the total design size > 20 to 30 λ while the frequency domain is preferred when the project is < λ.

Table 2 The characteristics for the solver choice.

In all the cases presented here, the time domain solver is the ideal choice. The transient or time domain solver utilizes the fast and memory efficient finite integration technique. It calculates the S-parameters by applying Fourier transform to time signals. It allows the calculation of the far-field gain as well as beam directions for a broadband range of frequencies. In order to allow faster computation time, the GPU is supported and hardware acceleration is possible. The time domain solver uses hexahedral meshing.

The frequency domain solver, on the other hand, uses a tetrahedral or hexahedral meshing. It also allows the calculation of S-parameters as well as the calculation of the far-field gain and the beam directions. However, neither the GPU nor the hardware acceleration can be used.

5.3 Antenna Magus

The software Antenna Magus complements CST. It has a huge database of extensive antenna designs which can be integrated in the design workflow and can be used to extract simple designs of antenna elements [29].

In fact several antenna elements can easily be explored depending on size, resonance frequency, required bandwidth or gain and the most useful designs can be used and exported to CST. Then, the antenna element can further be refined and optimized with CST and the results can be examined and analysed.

5.4 Chapter Conclusion

The conclusion of this chapter is that antenna design will start with a rule of thumb from approximations and equations, and such software as Antenna Magus can be used to guess the best choice of antenna element that fulfils the specifications that can answer our thesis requirements. These designs can further be refined and examined and optimized in CST before building it into an array. This is explored in more details in the upcoming chapter where CST is used to simulate the investigated antenna elements.

6. USING CST TO SIMULATE THE PATCH ANTENNA

6.1 The Patch Antenna Design

CST Microwave Studio, complemented by Antenna Magus, is used to design and simulate the patch antenna. The time domain solver is used as decided in the last chapter. The patch antenna can be built with a corporate feedline as shown in Figure 11. The length of the patch may be changed to shift the resonance of the center fundamental frequency of the individual patch antenna element.

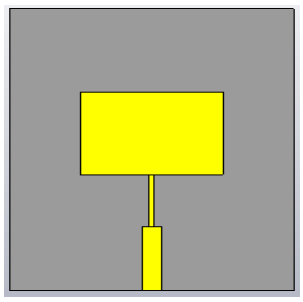

(a) Corporate fed patch

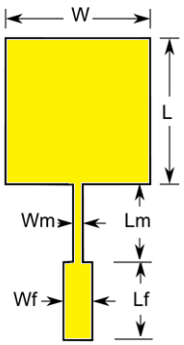

(b) Top view

(c) Side view

L : 8.06 mm	Lf: 6.22 mm
W : 10.7 mm	Wf: 1.05 mm
Lm : 5.06 mm	H: 0.508 mm
Wm : 0.410 mm	ε_r: 2.2

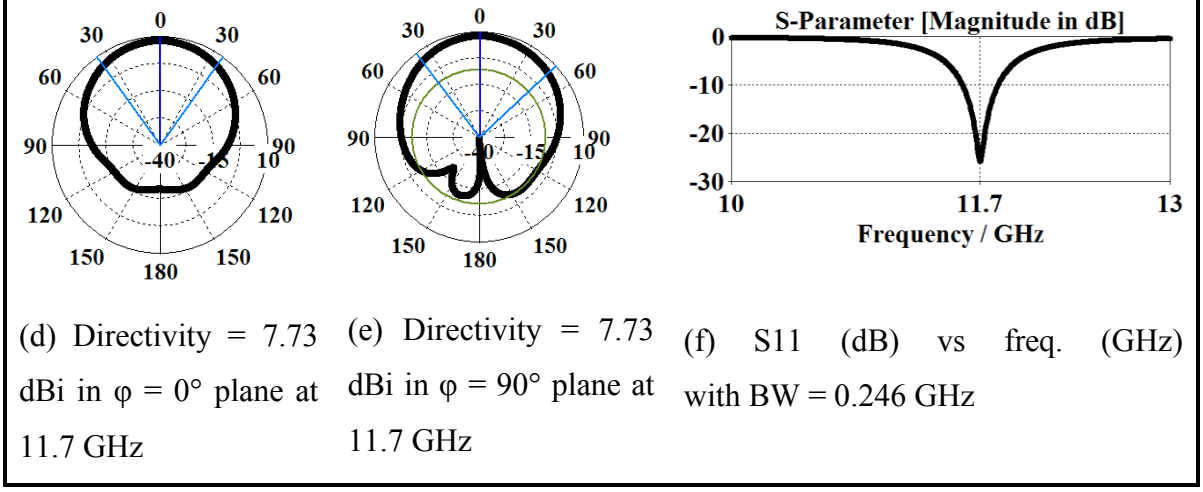

(d) Directivity = 7.73 dBi in φ = 0° plane at 11.7 GHz

(e) Directivity = 7.73 dBi in φ = 90° plane at 11.7 GHz

(f) S11 (dB) vs freq. (GHz) with BW = 0.246 GHz

Figure 11 A corporate fed patch antenna element

(metal layer = yellow, substrate layer = grey)

The metal is simulated as a perfect electric conductor (PEC). A comparison between PEC and normal Copper is shown in Chapter x to show that there is no difference when the metal used in the simulation is set to PEC or normal copper. Here, for a square patch antenna, the input impedance is around 300Ω. By increasing the width of the patch antenna, the impedance can be reduced. Here in Figure 8, the bandwidth (BW) is very narrow at only 0.246 GHz while the far-field radiation patterns are appreciable with a directivity of 7.73 dBi in both the φ = 0° plane and in the φ = 90° plane. If a uniform feedline is required, an inside feedline is utilized to lower the impedance from 300Ω to 50Ω. The uniformity of the feedline is important to enable a simple phase shifter calculation later on during the design of the phased array antenna with dielectric phase shifters. The far-field patterns of the patch antenna element with insert feed are similar to those of the patch with a corporate feed at 7.53 dBi when φ = 0°. This is also known as the horizontal or azimuth or xy plane, and it is 8.55 dBi when φ = 90°. This is also known as the vertical or elevation or yz plane. The bandwidth (BW) is a narrow 0.247 GHz as shown in Figure 12.

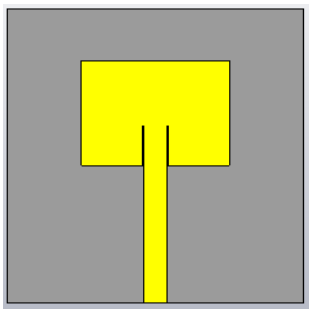

(a) Insert fed patch

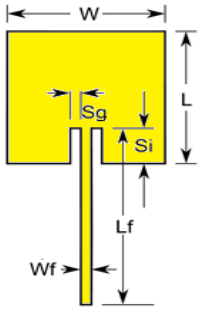

(b) Top view

(c) Side view

L : 8.32 mm	Lf : 14.1 mm
W : 10.5 mm	Wf : 1.63 mm
Sg : 0.133 mm	H : 0.508mm
Si : 3.13 mm	ε_r: 2.2

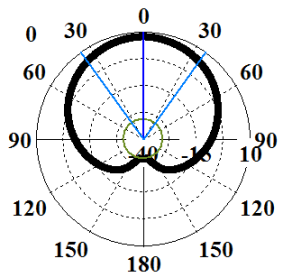

(d) Directivity = 7.52 dBi in φ = 0° plane at 11.7 GHz

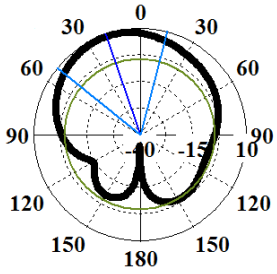

(e) Directivity = 8.55 dBi in φ = 90° plane at 11.7 GHz

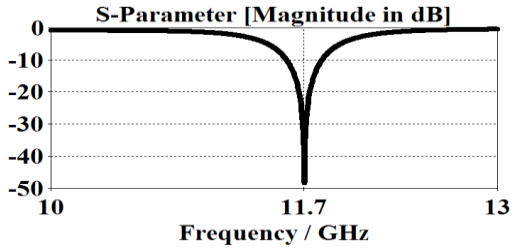

(f) S11 (dB) vs freq. (GHz) with BW=0.247 GHz

Figure 12 The inside fed patch antenna element

(metal layer = yellow, substrate layer = grey)

The patch antenna is ideal but it has such a narrow bandwidth that it cannot be used for the phased array as it does not cover the desired bandwidth of 2 GHz.

6.2 Chapter Conclusion

To conclude this chapter, it can be mentioned that the main disadvantage of the patch antenna is that it unfortunately has a very narrow bandwidth and does not satisfy the 2 GHz bandwidth

requirement of the specifications. Bandwidth enhancement methods must be investigated to fill this gap as revealed in the next chapter.

7. BANDWIDTH ENHANCEMENT

7.1 Bandwidth Improvement of the Patch Antenna

An antenna element is any part of an antenna that is actively used for the reception or transmission of signals. The most common and popular antenna element is the patch antenna element. It has become a very popular antenna element due to its low profile, simplicity, lightweight, ease of fabrication using the same technology as printed circuits and its ease of integration with feed networks [30]. However, the main disadvantage of the patch antenna is its narrow bandwidth usually limited to about 5% of the center frequency [31]. Much effort is being made to develop techniques to enhance its bandwidth and its gain by working in layers [32], modifying its shape [33, 34], adding parasitic elements [35], changing its feedline from single ended corporate feed to single ended insert feed [36] or from single ended microstripline to coplanar or coplanar waveguide [37], increasing the thickness of the dielectric substrate [38], or by adding slots [39].

Stacking the patches is the first simplest change that can be made to enhance the bandwidth and enable an impedance matching. The next antenna element shown in Figure 13 is the stacked patch antenna. In fact, the easiest way to enable an impedance match without changing the shape of an antenna is to use its stacked version. The stacked version allows for a larger radiating surface area and works as an integrated antenna element assuming the correct optimized spacing is used on the top stacked layer. The stacked version of the patch

antenna also reduces the impedance variation of the patch across frequency and thus allows an impedance matching across a broad frequency band. The stacked patch antenna can thus be used to act as a wideband antenna or if one desires, as a dual frequency antenna. As shown in Figure 13, the stacked patch shows an amelioration with a 1.245 GHz bandwidth and a directivity of 12.8 dBi in both the $\varphi = 0°$ plane and in the $\varphi = 90°$ plane.

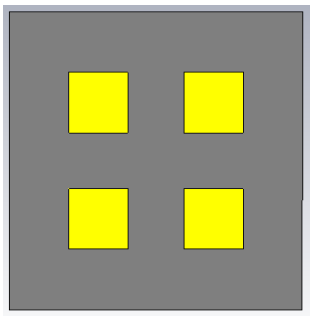

(a) Stacked patch

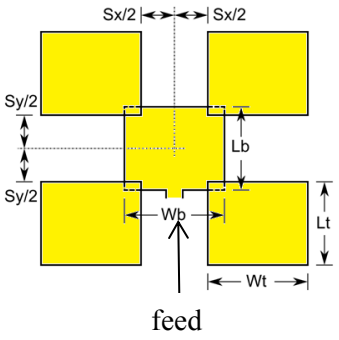

(b) Top view

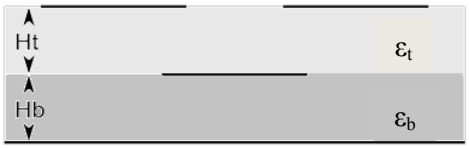

(c) Side view

Lb : 7.84 mm Sx/2 : 3.45 mm
Wb : 7.23 mm Sy/2 : 3.58 mm
Lt : 8.66mm Ht= Hb:0.508mm
Wt : 8.66 mm $\varepsilon_t = \varepsilon_b$: 2.2

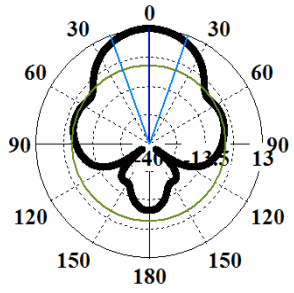

(d) Directivity = 12.8 dBi in $\varphi = 0°$ plane at 11.7 GHz

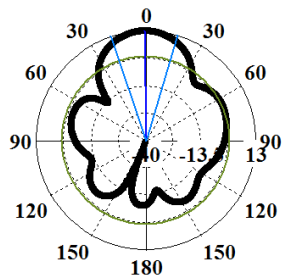

(e) Directivity = 12.8 dBi in $\varphi = 90°$ plane at 11.7 GHz

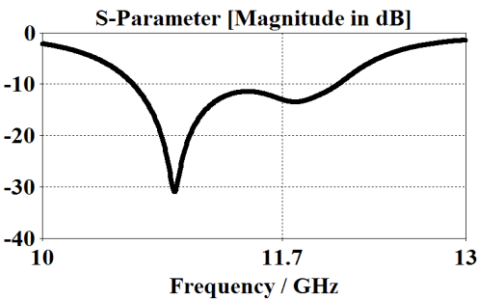

(f) S11 (dB) vs freq. (GHz) with BW = 1.453 GHz

Figure 13 The stacked patch antenna element

(metal layer = yellow, substrate layer = grey)

The stacked patch antenna provides a large bandwidth and a large radiation pattern in the far-field but it is not easy to achieve miniaturization and it occupies a large real estate. This is not suitable in the further development of an array version as the inter element spacing will be too

large [40] and thus, the grating lobes of the side lobes will overwhelm the antenna main lobe in the far-field as an array is built up with a stacked patch antenna.

In fact here the bandwidth of 2 GHz has not been achieved. Concerning the beamwidth, ideally, with the one element it must have a large opening angle or beamwidth, and then it can be built in the array.

The patch must be modified using other techniques, different from the stacking option, in order to increase its bandwidth.

7.2 H-shaped Patch Antenna

In order to enhance the patch antenna, an H-shaped patch antenna is designed with a large bandwidth and a large beamwidth. In fact, this section reveals a patch antenna with a large bandwidth of 34% and a high gain of 8 dBi in the frequency range from 10.1 GHz to 14.2 GHz. The H-shaped patch antenna is a four layer design comprising of a superstrate dielectric layer of ε_r 10.2 on top of a metal layer with six small simply designed parasitic H-shaped elements, which are optimized using CST Microwave Studio. The six H-shaped parasitic elements are centrally located on the metal layer. On the same layer, the antenna is fed through a coupled feedline in order to reduce the mutual coupling. The antenna is thus a perfect candidate to preserve its wideband feature in an antenna array. Right underneath the metal layer is the substrate dielectric layer of ε_r 2.2 with two strategically placed slots underneath the metal layer in order to decrease the back radiation of the H-shaped parasitic elements. The whole design is terminated with a final metal layer to act as a conductor backed antenna to push most radiations out. The final antenna occupies a volume of 25 mm x 25 mm x 2.56 mm. The design has a high gain of 8 dBi in both the $\varphi = 0°$ plane and the $\varphi = 90°$ plane with a large beamwidth of 77° in the $\varphi = 0°$ plane and 83° in the $\varphi = 90°$ plane in the far-field, as published in the journal and the conference paper in [41, 42].

The H-shaped antenna was first introduced by V. Palanisamy and R. Garg in 1985 as an alternative to the rectangular patch antenna to permit improvements over a simple patch antenna element [43]. The H-shaped patch only showed a 1% bandwidth but a large beamwidth of 112° in the $\varphi = 0°$ plane and 88° in the $\varphi = 90°$ plane. Further work was done by Thakur where an H-shaped fractal patch was introduced and fractal geometry and slots were applied in order to obtain an H-shaped antenna with a maximum bandwidth of 9% and a

gain of 6.05 dBi at 2.7 GHz [44]. Kushwaha, Srivastava and Saint showed a high gain wideband H-shaped slot-loaded microstrip patch antenna fed with coaxial cable and the authors showed a 19% bandwidth at 2.42 GHz with no mention of the antenna gain [45]. Islam, Shakib and Misran showed a broadband inverted E-H shaped microstrip patch antenna with L-probe feed technique for wireless system with a 30% bandwidth, a maximum gain of 9.37 dBi and beamwidth of 64° in the $\varphi = 0°$ plane and 51° in the $\varphi = 90°$ plane at 2.07 GHz [46]. Kumara showed a concaved H-shaped patch antenna with improved bandwidth of 70% between 2 to 6 GHz but with no mention of the gain or beamwidth of the concave antenna [47]. Tarange showed a 46% bandwidth at 2GHz using a capacitive scheme consisting of a radiation patch and a feed strip where the design of the antenna incorporates the capacitive feed strip which is fed by a coaxial probe. A slot is used in the radiating patch along the radiating edge to improve the bandwidth using a thick substrate of height 1.56 mm and an air gap of 5.4 mm on Rogers 3003 of ε_r 3. However the gain is not mentioned [48].

This section presents a patch antenna where a high bandwidth and a high gain with a bonus of a large beamwidth obtained in both the $\varphi = 0°$ plane and the $\varphi = 90°$ plane with a simple design tweak of resizing the H-shaped antenna element and lots of structural optimization using CST Microwave Studio 2015. The design is a four-layer one with a superstrate Rogers RT6010 of ε_r 10.2 as the top layer added on top of a metal layer. The shape of the patch element is modified by adding six H-shaped parasitic elements fed by coplanar lines in the center of this metal layer. The coplanar lines end in an open-ended coupled stub tuning the design in order to enhance bandwidth. The thickness of the dielectric substrate of Rogers RT5880 of ε_r 2.2 underneath the metal layer is increased and slots are strategically added on this substrate layer in order to be situated under the H-shaped parasitic elements. The whole element designed has the dimensions of 25.6 mm x 25.6 mm x 2.56 mm.

Rogers's substrate and superstrate used in the H-shaped patch element in this paper are a glass microfiber reinforced PTFE composite where the glass reinforcing microfibers are randomly oriented to maximize the benefits of fiber reinforcement. The dielectric constant is uniform from panel to panel and is constant over a wide frequency range. Its low dissipation factor extends the usefulness to the Ku-band and above. Moreover, Roger's laminates are easily cut, sheared and shaped. They are resistant to all solvents and reagents, hot or cold, normally used in etched printed circuits or in plating edges and holes. These characteristics are useful as the substrate and superstrate allow the antenna element to perform under environmental conditions where temperature or humidity can vary. Here the superstrate layer is built on

Rogers RT6010 with ε_r 10.2, the same substrate is used for the phase shifters used in the antenna array [9].

To the common knowledge, the H-shaped antennas documented in the literature are limited to frequencies below 10 GHz. This is because it requires very careful design optimizations to obtain a large bandwidth and an appreciable gain at frequencies greater than 10 GHz with an H-shaped element.

This simple H-shaped four-layer antenna element works in the 10.1 to 14.2 GHz and it is ideal for satellite broadcast television frequencies. The design is terminated with coupled line in order to reduce the mutual coupling and is thus an optimum candidate to be integrated in a large antenna array. The antenna element is optimized to obtain a high bandwidth of 34% and a high gain of 8 dBi in both the $\varphi = 0°$ plane and the $\varphi = 90°$ plane with a large beamwidth of 77° in the $\varphi = 0°$ plane and 83° in the $\varphi = 90°$ plane in the far-field. The importance of the superstrate top layer with substrate of dielectric ε_r 10.2 is enforced by showing the comparison between the design with and without the top layer and the resulting gain in both the $\varphi = 0°$ plane and the $\varphi = 90°$ plane. The addition of a dielectric slab of ε_r 10.2 on top of the metal layer allows for a constant gain amelioration of about 2 dBi along the whole frequency range from 10.1 GHz to 14.2 GHz. This is because the backlobe radiations of the microstrip antenna are decreased with the introduction of the top dielectric superstrate while causing an increase in the front lobe radiations and thus permitting higher gain as explained through closed form expression by Zhong, Liu and Qasim [49] shown in Figure 14. The equations governing the design methodology using the superstrate and increased substrate height or different substrate materials are shown in Equations 13 to 18. However a high dielectric constant substrate also introduces surface waves. These surface waves created by a high dielectric superstrate can be eliminated as described by Alexopoulos and Jackson [50] with the proper choice of dielectric constant and superstrate thickness resulting in the enhancement of the antenna gain in both the $\varphi = 0°$ plane and the $\varphi = 90°$ plane.

7.3 Design Methodology of the H-shaped Patch Antenna

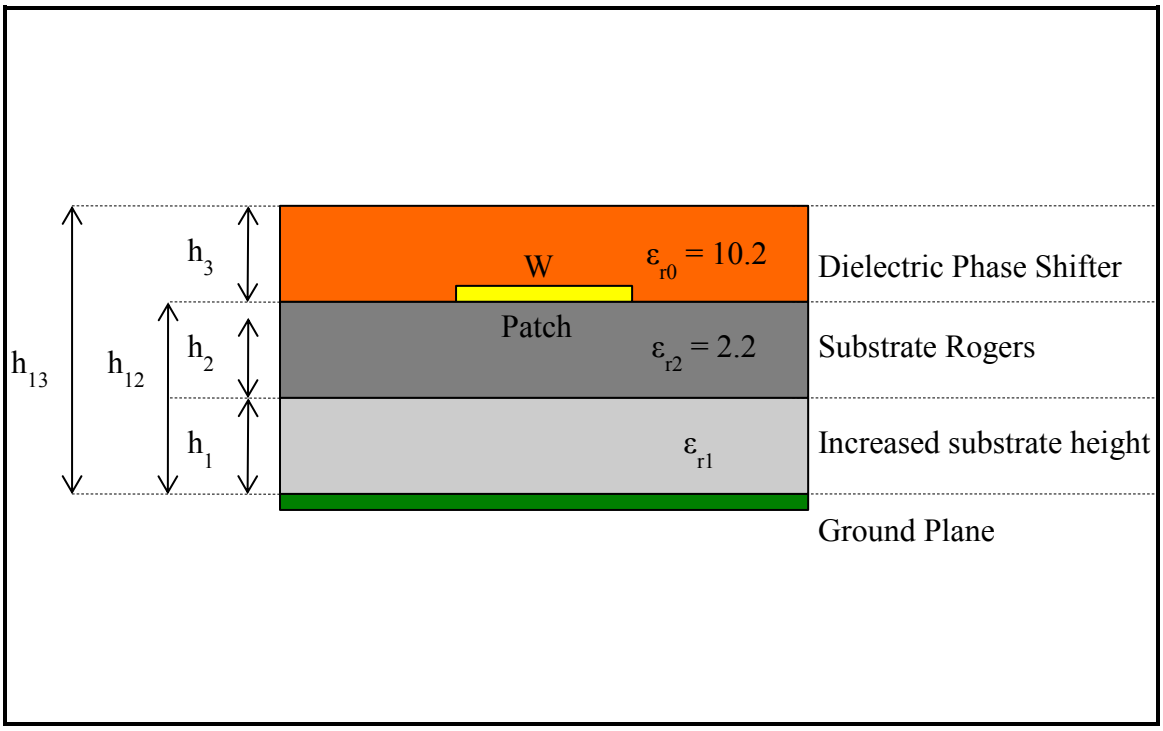

Figure 14 The design of a coupled line with a phase shifter with different substrates

The Equations 13 to 18 to bring an approximation to the design of a transmission line with a superstrate material and built on top of two different substrates.

Here $\varepsilon_{effective}$ is the effective dielectric constant of all the substrates involved where ε_{r1} and ε_{r2} the dielectric constant of the dielectric substrate as shown in Figure 12 above. The variables a_1, a_2 and a_3 are calculated in Equations 14-16. h_1, h_2, and h_3, h_{12}, h_{13} are the heights shown in Figure 14 as well. W_e and V_e are also variables calculated in Equations 17-18 while W is the width of the patch antenna.

$$\varepsilon_{effective} = \varepsilon_{r1}\varepsilon_{r2}\frac{(a_1a_2)^2}{(\varepsilon_{r1}a_2\varepsilon_{r2}a_1)} + \varepsilon_{r3}\frac{(1-a_1-a_2)^2}{\varepsilon_{r3}(1-a_1-a_2-a_3)+a_3} \quad \text{Eq. 13}$$

$$a_1 = \frac{h_1}{2h_{12}}\left\{\left\{1+\frac{\pi}{4}-\frac{h_{12}}{W_e}\ln\left[2\frac{W_e}{h_1}\sin\left(\frac{\pi h_1}{2h_{12}}\right)+\cos\left(\frac{\pi h_1}{2h_{12}}\right)\right]\right\}\right. \quad \text{Eq. 14}$$

$$a_{2=}\ 1 -\ a_1\ -\ \frac{h_{12}}{W_e}\ \ln\left(\frac{\pi W_e}{h_{12}} - 1\right) \quad \text{Eq. 15}$$

$$a_{3=}\ 1 -\ a_1 - a_2\ -\ \frac{h_{12} - v_e}{2W_e}\ \ln\left(\frac{2W_e}{2h_{13} - h_{12} + v_e}\ \cos\left(\frac{\pi v_e}{2h_{12}}\right) + \sin\left(\frac{\pi v_e}{2h_{12}}\right)\right) \quad \text{Eq. 16}$$

$$W_{e=}\ W + \frac{2h_{12}}{\pi}\ \ln\left(17.08\left(\frac{W}{2h_{12}} + 0.92\right)\right) \quad \text{Eq. 17}$$

$$V_{e=}\ \frac{2h_{12}}{\pi}\ \tan^{-1}\left(\frac{2\pi}{\pi W_e - 4h_{12}}(h_{13} - h_{12})\right) \quad \text{Eq. 18}$$

The width of the antenna can increase the fringing fields as well as the radiation. The fringing field can also be increased by using a low ε_r closest to 1 and by increasing the substrate thickness [51]. Rogers substrate with ε_r 2.2, tan δ=0.0009 (@10 GHz is a stable, low loss and low cost material with an excellent chemical resistance at high temperature. When the substrate height *h* of the patch antenna is increased, the design becomes mechanically stronger and the radiating power increases, and the bandwidth increases while the conduction loss decreases. However, the weight of the patch antenna increases as well as the dielectric and surface wave losses. Also, the substrate height h cannot be increased indefinitely as the patch antenna stops radiating when $h > 0.11\ \lambda$ where λ is the wavelength. Moreover, as the height increases, surface waves are introduced and these are not desirable as they extract power from the total power available for direct radiations. The surface waves degrade the antenna radiation pattern when it travels through bends and surface discontinuities such as dielectric to dielectric or dielectric to ground transition.

Microstrip patch antenna can be fed by different ways such as microstrip feed, probe feed, aperture coupled and proximity coupled feedline. Using a coupled feedline ensures a decrease in mutual couplings in the antenna element and this is an important consideration when the element is used in an array, as mutual couplings are the main culprit for breaking down a large array of patch antenna elements.

The use of the slots in the substrate layer of ε_r 2.2 allows for a smaller slot size for efficient electromagnetic energy coupling and thus a reduction in the back radiation of the slot. The larger bandwidth is because the coupling slot is placed at the patch center and has a better electromagnetic energy coupling resulting in a good impedance matching over a wider frequency range.

The design of the H-shaped metal layer is shown in Figure 15 where all layers have square dimensions of λ by λ or 25.6 mm x 25.6 mm when the center frequency is 11.7 GHz.

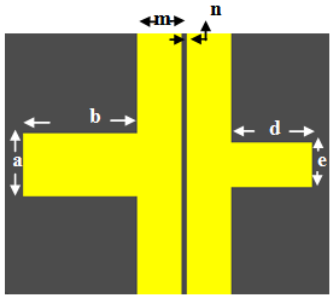

Fig. 15_{a1}) shows the centered asymmetrical rectangular patches on each side of the coupled feedline to create two resonance frequencies closely spaced in order to appear as one resonance frequency.

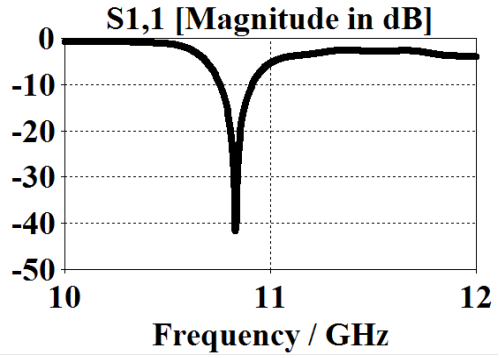

Fig. 15_{a2}) shows S_{11} (dB) versus frequency/ GHz for the closed spaced asymmetrically rectangular patches shown in Fig. 15_{a1})

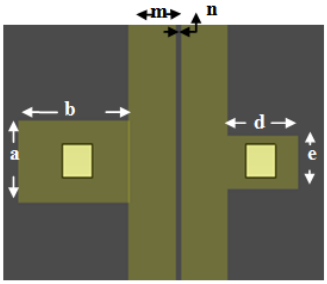

Fig. 15_{b1}) shows the two slots in the substrate right underneath the centered asymmetrical rectangular patches

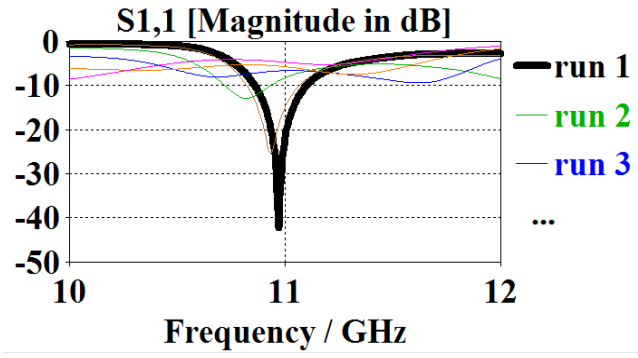

Fig. 15_{b2}) plots S_{11} (dB) versus frequency/ GHz for the two slots in the substrate right underneath the two asymmetrical rectangular patches from Fig. 15_{b1}). Run 1 to Run N shows the optimization runs as the variables are optimized.

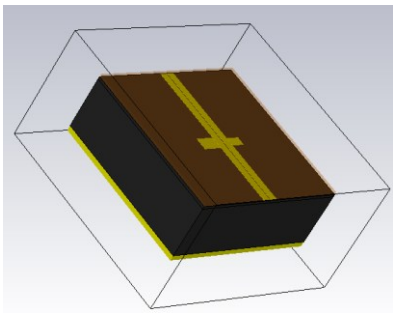

Fig. 15_{c1}) shows the optimization step of the substrate height to 1.23 mm

a) Foampad of ε_r 1 added under Rogers of ε_r 2.2 with results shown in Fig. 15_{c2})

OR

b) Substrate height is increased with same substrate Rogers ε_r 2.2 with results shown in Fig. 15_{c3})

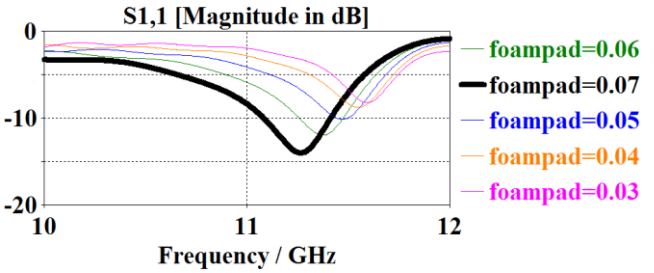

Fig. 15_{c2}) shows S_{11} (dB) versus frequency/ GHz for optimisation of the substrate height using an added substrate of foampad with ε_r 1, underneath the substrate Rogers ε_r 2.2 shown in Fig. 15_{c1})

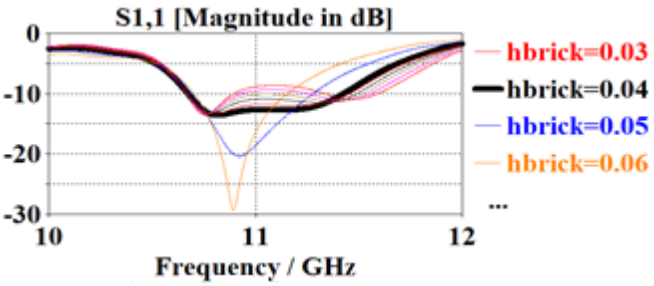

Fig. 15_{c3}) shows S_{11} (dB) versus frequency/ GHz for optimisation of the substrate height using a thicker substrate height of the substrate Rogers ε_r 2.2 shown in Fig. 15_{c1})

Figure 15 The optimization steps and S_{11} (dB) of the H-shaped patch element

First two centered asymmetrical rectangular patches on each side of the coupled feedline are designed to create two closely spaced resonance frequencies as shown in Fig. 15_{a1}). The patches are centered in the middle of the square antenna element of dimensions λ by λ or 25.6 mm x 25.6 mm when the center frequency is 11.7 GHz to cause the maximum of radiations and the coupled feedline extends on each side to create symmetry. On one side, it is used as a coupled feedline and on the other side it is an open circuit spaced λ/2 away from the center of the antenna element. This symmetry with an open circuit on one side cancels out the refection of the unmatched patch load on the transmission line by adding an equal and opposite

reflection from the open circuit stub [52]. Then two slots are added on the substrate layer right underneath the two asymmetrical rectangular patches as shown in Fig. 15_{b1}). The equation shown in Equation 19 to calculate the size of the slot under the patch is given by [53] where λ_0, W and h are the resonant wavelength, width and height of the patch respectively.

$$\frac{\lambda_{slot}}{\lambda_0} = 1.05 - 0.04\varepsilon_r + 1.411 * 10^{-2}(\varepsilon_r - 1.421)$$

$$* \ln\left(\frac{W}{h} - 2.012(1 - 0.146\varepsilon_r)\right) + 0.111(1 - 0.366\varepsilon_r)\sqrt{\frac{W}{\lambda_0}}$$

$$+ 0.139\left(1 + 0.52\varepsilon_r \ln(14.7 - \varepsilon_r)\right)\left(\frac{h}{\lambda_0}\right)\ln\left(\frac{h}{\lambda_0}\right) \quad \text{Eq. 19}$$

Next, the substrate height is increased in order to lower the Q-factor and increase the bandwidth of the antenna element. An optimization of the ideal substrate height is performed and the substrate height is set to 1.23 mm as shown in Fig. 15_{c1}). This optimization is performed using a) a combination of 2 substrates of Rogers ε_r 2.2 and Foampad of ε_r 1 or b) by simply increasing the height of the substrate Rogers ε_r 2.2. Through optimizations from CST Microwave Studio 2015, the metal layer is modified into six parasitic patches as shown in Figure 16. Further optimization of the six parasitic patches converts them into six parasitic H-shaped elements centrally located and fed through coupled lines. This is shown in Figure 17 and Figure 18. This loading effect produced by the parasitic patches also helps to enhance the bandwidth. Thus, by carefully optimizing the distance between the resonance frequencies of each patch, a large bandwidth increase can be obtained.

A zoomed-in of the design from Figure 18 is shown in Figure 19 where the detail of the two slots on the substrate layer right under the middle H-shaped elements is shown in Figure 20. In Figure 20, the slots are in the substrate layer and do not extend to the metal layer. All the design dimensions are shown in Table 3. The square antenna elements are always λ by λ or 25.6 mm by 25.6 mm.

The final design is shown in Figure 21 with the four layers each separately shown in Figure 22. The feedline is thus a coupled line ended in a coupled open circuit stub, which acts as a tuning stub and contributes to an enhanced bandwidth.

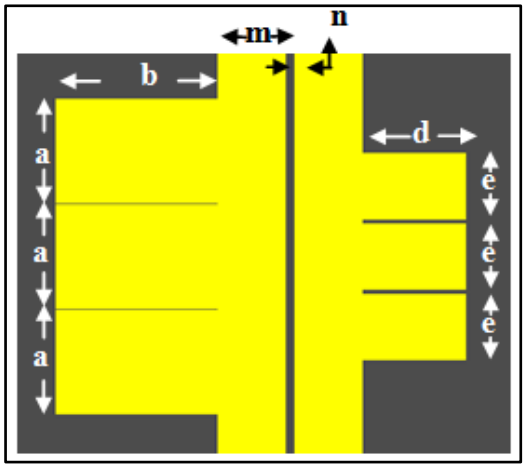

Figure 16 The parasitic elements added on top and below the centrally located asymmetrical rectangular patches

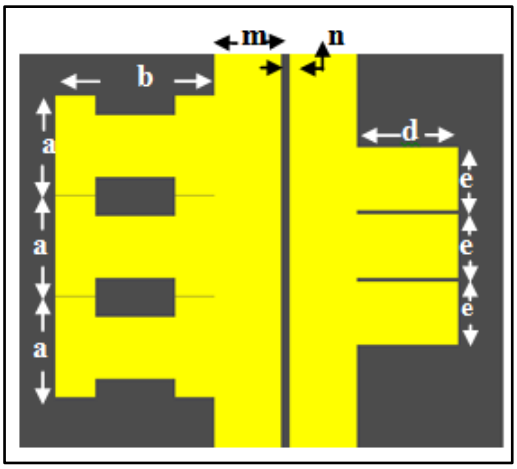

Figure 17 The inter-optimized H-shaped parasitic elements

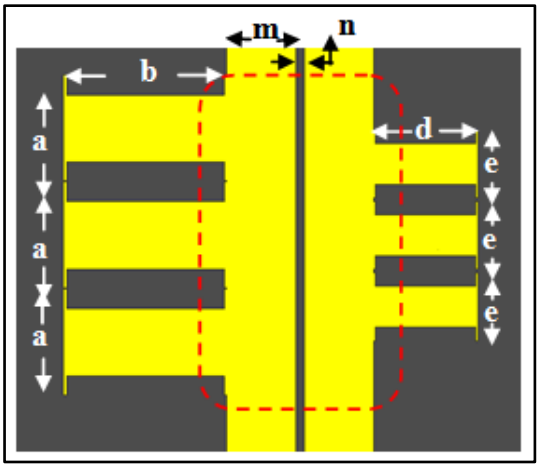

Figure 18 The strongly optimized H-shaped parasitic elements

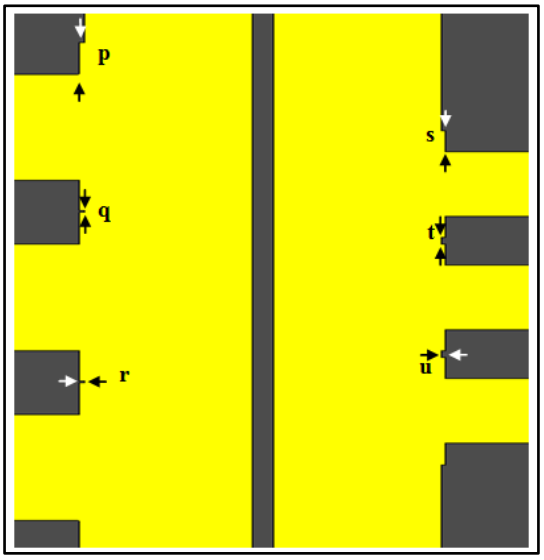

Figure 19 Zoomed-in of Figure 18 to show the inter gap dimensions

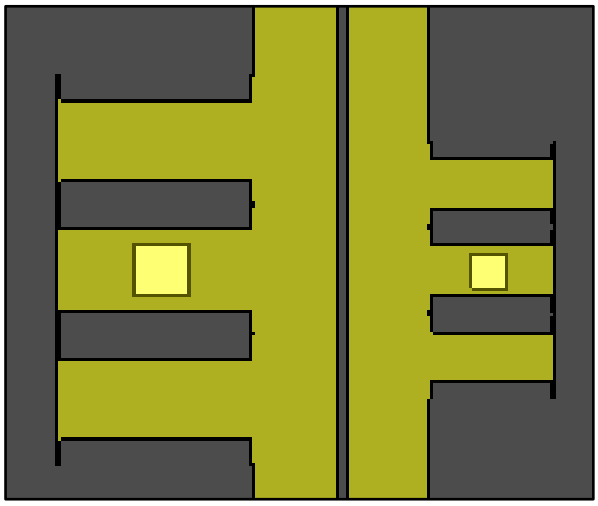

Figure 20 The slots in the substrate layer under the metal layer

(the slots do not extend to the metal layer)
with the left slot of square dimensions 0.8 mm x 0.8 mm
and the right slot of square dimensions 0.5 mm x 0.5 mm.

Label	Dimensions/mm
a	1.91
b	2.89
d	1.84
e	1.21
m	1.21

n	0.15
p	0.36
q	0.02
r	0.06
s	0.24
t	0.07
u	0.04

Table 3 The dimensions from Figure 16-19

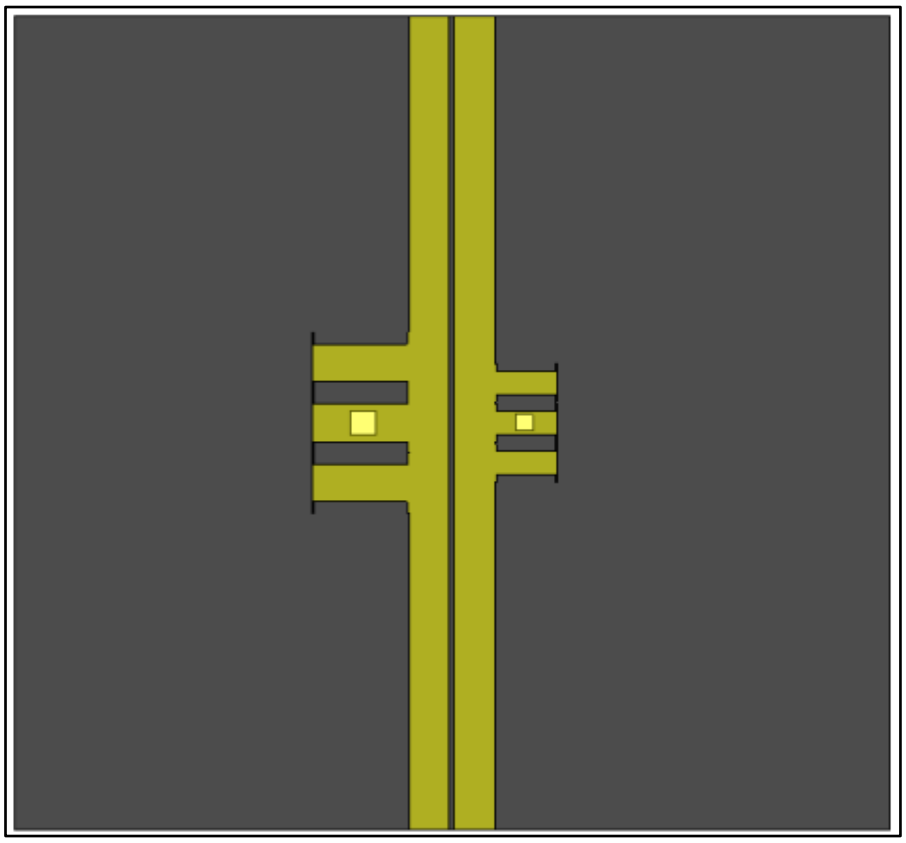

Figure 21 The antenna element design of 25.6 mm x 25.6 mm x 2.56 mm

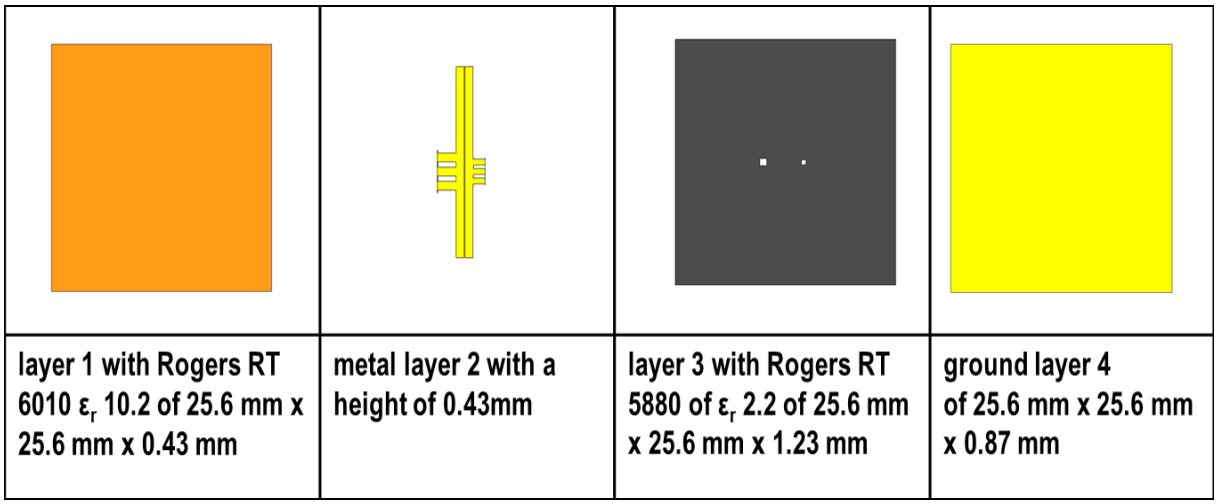

Figure 22 The four layer design of the H-shaped patch element

7.4 S-parameters results of the H-shaped Patch Antenna

The port set-up of the studied antenna element is shown in Figure 23 where the coupled feedline ends in S^+ and S^-.

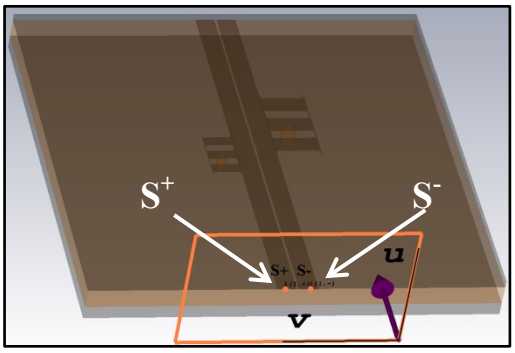

Figure 23 The port set up at the end of the centrally located coplanar S^+S^- feedline

Figure 15 shows the return loss S_{11} (dB) plotted vs. frequency in GHz. Each S-parameter plot shows the results of the design flow. Thus, Fig. 15_{a2}) shows the results from Fig. 15_{a1}) where an asymmetrical rectangular patch is designed to increase the resonance bandwidth by closely spacing two resonance frequencies together. Fig. 15_{b2}) shows the optimization runs for the two slots in the substrate layer right underneath the two asymmetrical rectangular patches while Fig. 15_{c2}) and Fig 15_{c3}) shows the optimization of the substrate height. In this step,

firstly a) Foampad with ε_r 1 was added under Rogers ε_r 2.2. We know that a dielectric constant closest to ε_r 1 gives the best results for maximum radiation across a largest bandwidth as described in Chapter 2. An increased substrate height of Rogers ε_r 2.2 gave a better answer instead of using a combinations of Rogers and Foampad, because a discontinuity in the two dielectric substrates was less prone to give a large bandwidth as compared to when the substrate height of Rogers ε_r 2.2 was simply increased to a much higher value. This was an interesting observation to conclude that simpler is better, in the case of substrate height. The final results leading to the final antenna design is 34% as shown in Figure 24. The radiation patterns are also shown in Figure 24. The 3D radiation patterns show a high gain of 8 dBi and the wide beamwidth of the antenna element can be seen in the $\varphi = 0°$ plane and in the $\varphi = 90°$ plane.

Although this antenna element is intended to cover the thesis specifications of a bandwidth of 2 GHz covering the frequencies from 10.7 GHz to 12.7 GHz with a center frequency of 11.7 GHz, the center frequency here is in fact 12.1 GHz. The center frequency is shifted as explained in [23] because the fringing fields are produced by asymmetrical H-shaped parasitic elements designed on each side of the centrally fed patch antenna element in order to produce maximum resonances in order to enhance the antenna bandwidth. ε_r is also modified with the superstrate layer with ε_r 10.2 and this also modifies the fringing fields and thus the center frequency.

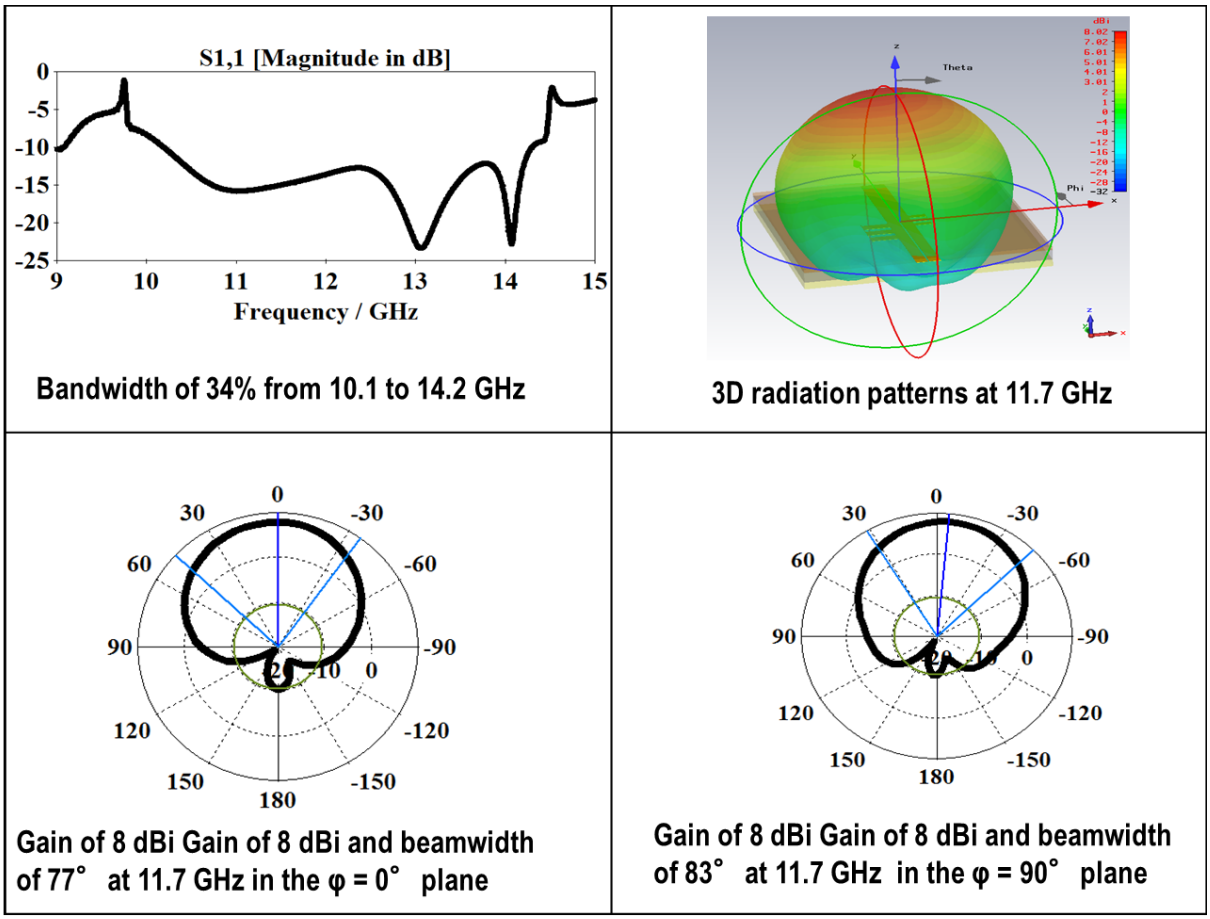

Figure 24 The S_{11} (dB) vs. frequency/ GHz and gain for the optimized antenna element showing a bandwidth of 34%.

7.5 Superstrate Effect of the H-shaped Patch Antenna

Next, the effect of the superstrate layer 1 on dielectric substrate Rogers 6010 of ε_r 10.2 is examined. Figure 25 shows the gain in dBi versus frequency in GHz of the antenna element when the superstrate layer 1 is included (with superstrate) or removed (no superstrate). The plot shows the gain obtained in the $\varphi = 0°$ plane and the $\varphi = 90°$ plane, with and without the superstrate layer, that is, when the top layer 1 is present or absent. As seen in the plot from Figure 25, the effect of the superstrate is significant with a much higher gain over the frequency range from 9 to 15 GHz for both the $\varphi = 0°$ plane and the $\varphi = 90°$ plane. The superstrate acts as a cover layer over the H-shaped patch. The loading of a high permittivity superstrate layer on a patch antenna increases both its gain and its bandwidth as explained by Huang [54].

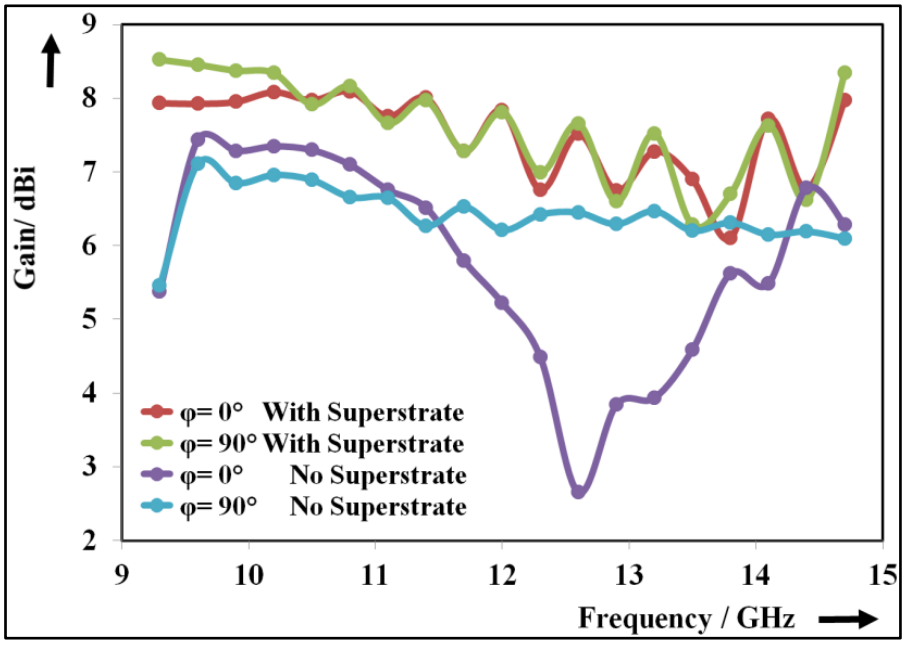

Figure 25 The gain in dBi of the antenna element with and without superstrate

7.6 Chapter Conclusion

This chapter is concluded on a positive note that a simple patch antenna has been optimized using CST Microwave studio 2015 in order to design a high gain and high bandwidth patch antenna element covering the frequency band from 10.1 GHz to 14.2 GHz. The four-layer design, with the dimensions of 25.6 mm by 25.6 mm by 2.56 mm, comprises of a superstrate layer of ε_r 10.2 on top of a metal layer centrally fed with coplanar lines. The metal layer comprises of six parasitic H-shaped elements on top of strategically placed slots in the substrate layer of ε_r 2.2 underneath. The final layer is the ground layer. The design has a 34% bandwidth between 10.1 GHz to 14.2 GHz and high gain of 8 dBi in both $\varphi = 0°$ and $\varphi = 90°$ and with a beamwidth of 77° in the $\varphi = 0°$ plane and 83° in the $\varphi = 90°$ plane in the far-field.

The H-shaped patch antenna seems ideal as it satisfies the 3 B's: beamwidth, bandwidth and beam gain. However, the main disadvantage of the H-shaped patch antenna is its size. It is indeed a perfect antenna element and will work well in a large array that is spaced properly to avoid mutual coupling. The H-spaced patch antenna, unlike a simple patch antenna element, is terminated with coupled lines where there is a better chance of reducing mutual coupling in a tighter array configuration where the antenna element's spacing is small. However in order to avoid grating lobes when it is integrated in an array, it must not have a size more than $\lambda/2$ in order to avoid grating lobes in the far-field. The size of the H-spaced antenna is already

more than λ/2 or 12.8 mm such that it is impossible to avoid grating lobes even if the H-spaced antenna elements are arranged side by side next to each other.

This means that the H-spaced antenna element is an excellent improvement of a patch antenna where a lot of bandwidth enhancement methods have been applied. Even its feedline of $S^{+}S^{-}$ is excellent and is indeed better than a simple microstripline single-ended transmission line in order to experience minimal mutual coupling in an array configuration. Unfortunately, having a size larger than λ/2 or 12.8 mm means the inevitable presence of grating lobes in an array and thus, one cannot keep exploring the H-shaped patch antenna and must re-examine the choice of the antenna element to make sure everything is respected: all the 3 B's, that is, the beamwidth, bandwidth and beam gain, along with the size constraint of a width not more than λ/2 to prevent grating lobes as well as a feedline that will allow a minimized mutual coupling in an array. Other antenna elements must be investigated as detailed in the next chapter.

8. THE BUTTERFLY ANTENNA

8.1 Back to the Roots

Although the patch antenna is simpler, it simply cannot satisfy the thesis requirements described in the conclusion of the previous chapter, and in a quest to examine alternative antenna elements, it is necessary to go back to the Father of the patch antenna element, that is, the butterfly or the bow-tie antenna. The detailed reason why this step is taken is further clearer as one proceeds in this section and in the upcoming chapters. The quick answer is the requirement of *frequency independent antennas* and more specifically the *slotted butterfly antenna element with CPW feedline*, the gem of antenna elements, which allows us to satisfy the width requirement of $\lambda/2$ in order to avoid grating lobes and minimize mutual coupling as well as to fulfil the 3 B's of beamwidth, bandwidth and beam gain defined in Chapter 2.

8.2 Old is Gold

The rectangular patch antenna is modified to the butterfly shape which has a larger bandwidth. This can immediately be seen in Figure 26, where the bandwidth is greater than 2 GHz covering the desired frequency range of 10.7 GHz to 12.7 GHz for satellite TV broadcasts. However the impedance of the butterfly antenna is very high at 188Ω. We can

resort to the butterfly slot version where the impedance here is 50Ω. 50Ω is desired to match to the characteristic impedance used by CST or an actual network analyzer.

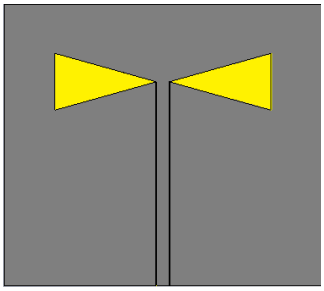

a) Butterfly Antenna Element from CST

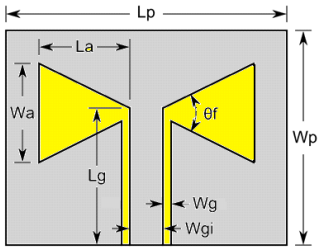

(b) Top view with dimensions

(c) Side view

Lp : 32.6 mm	Lg : 20.9 mm
Wp : 28.8 mm	Wgo : 1.55mm
La : 10.4 mm	Wgi : 1.34 mm
Wa : 5.80 mm	H : 0.508 mm
θf: 30°	εr: 2.2

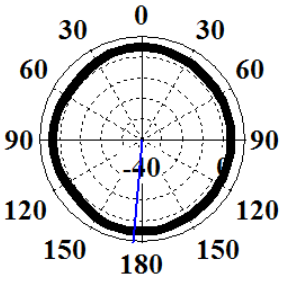

(d) Directivity = 4.8 dBi in φ = 0° plane at 11.7 GHz

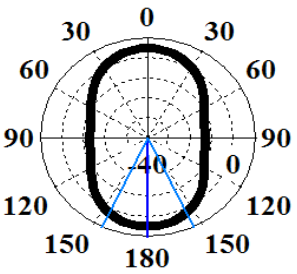

(e) Directivity = 4.8 dBi in φ = 90° plane at 11.7 GHz

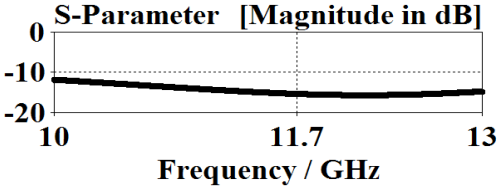

(f) S11 (dB) vs freq. (GHz) with BW > 2 GHz

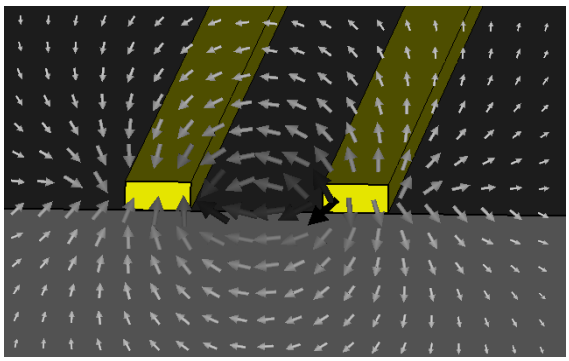

(g) E-field (voltage) plot at the differential port

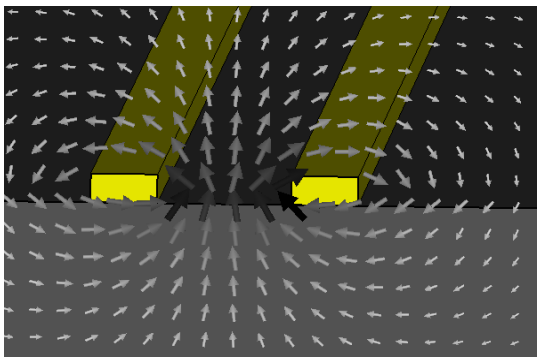

(h) H-field (current) plot at the differential port

Figure 26 The butterfly antenna element

(metal layer = yellow, substrate layer = grey)

8.3 The Gem of Antenna Elements: The Slotted Butterfly Antenna

The slotted butterfly antenna is hereby introduced. It is presented with an optimized bandwidth, a 50Ω impedance and a large beamwidth. The slotted butterfly antenna also known as the slotted bow-tie antenna is the slotted version of the butterfly antenna. As shown in Figure 27, the bandwidth is greater than 2 GHz and the directivity is 4.8 dBi in the φ = 0° plane and 4.7 dBi in the φ = 90° plane. Its electric and magnetic fields at its CPW feedline are also shown. Since this is a butterfly slotted version, the CPW port is fed as S^- S^+ S^- where S^- represents the mask or return path, while S^+ represents the signal path. This genius idea of using the slotted butterfly is enhanced by the fact that it uses the shape of the butterfly antenna and thus preserves the large bandwidth offered by a butterfly shape. Moreover, this antenna is ended with CPW feedline which means it is ended by $S^-S^+S^-$ signals as shown in Figure 27 where the metal layer is in yellow colour and the substrate layer is shown in grey colour. This means that the S^+ signal is already shielded from the next feedline form the next antenna element in an array configuration by one S^- on each side and this is an ideal configuration to avoid mutual coupling in an array. Also, the slotted version means more metal layer is exposed, encouraging more metal layer available for radiation.

The first effort to enhance the bandwidth of an antenna through a butterfly shape was performed by Brown and Woodward in 1952 where the input impedance and radiation were analyzed [21]. The coplanar waveguide slotted antenna printed on multilayer dielectric substrates was numerically analyzed by Laheurte using a full-wave integral equation technique and the method of moments [55]. The patch antenna is usually terminated by a simple microstripline. The other popular termination used here is the CPW. The CPW was first proposed as an MIC transmission line by C.P. Wen [56]. The CPW has the advantages of low dispersion, no need for via holes, which introduce undesirable parasitic inductances, ease of attaching both shunt and series circuit elements, and simple realizations of short-circuited ends such as the slotted butterfly antennas [57]. The planar slotted butterfly antenna [58] is thus preferred due to their superior characteristics on gain, bandwidth and especially size.

The slotted butterfly antenna is ended by a 50Ω CPW. The slot version of the butterfly antenna offers a larger metal surface area as compared to the non-slow version and more metal surface translates to more radiating surface and more radiation in the far-field. The coplanar waveguide is excited in the odd mode of the coupled slot line. This is also called the CPW mode. In this mode, the equivalent magnetic currents on the CPW slots radiate almost

out of phase, contributing negligibly to the cross-polar component of the radiating patterns and to mutual coupling as explained by Singh who reviewed mutual coupling in phased arrays [6]. This feature of the CPW feed is useful in the design of an antenna array, since the mutual coupling between adjacent lines is minimized.

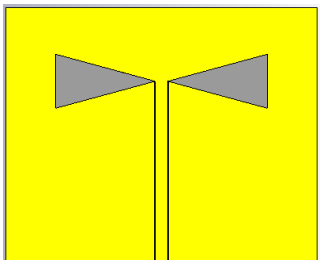

a) Slotted Butterfly Antenna Element from CST

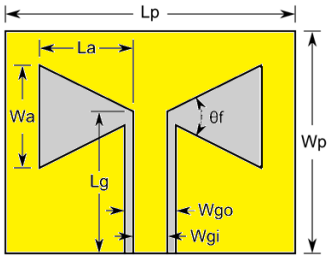

(b) Top view

(c) Side view

Lp : 32.6 mm	Lg : 20.9 mm
Wp : 28.8 mm	Wgo : 1.55 mm
La : 10.4 mm	Wgi : 1.34 mm
Wa : 5.80 mm	H : 0.508 mm
θf: 30°	εr: 2.2

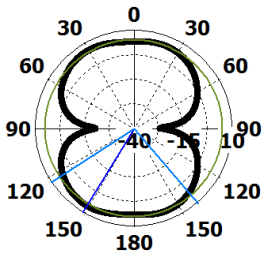

(d) Directivity = 4.8 dBi in φ = 0° plane at 11.7 GHz

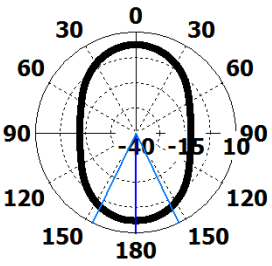

(e) Directivity = 4.7 dBi in φ = 90° plane at 11.7 GHz

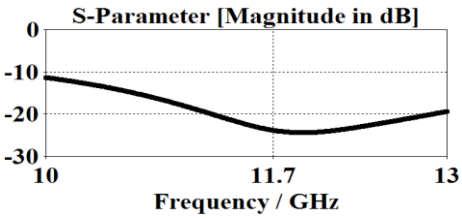

(f) S11 (dB) vs freq. (GHz) with BW > 2 GHz

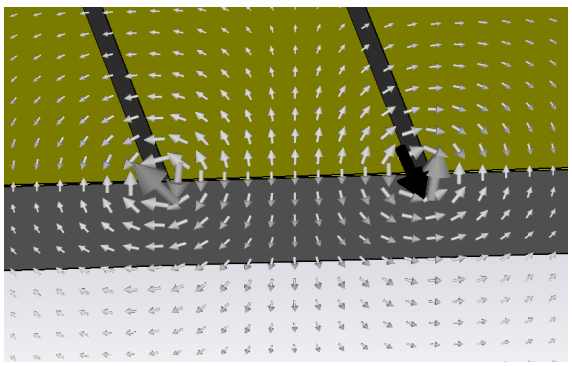

(g) E-field (voltage) plot at the $S^{-}S^{+}S^{-}$ (CPW) port

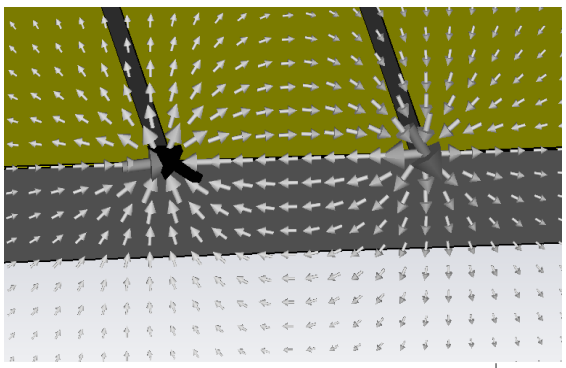

(h) H-field (current) plot at the $S^{-}S^{+}S^{-}$ (CPW) port

Figure 27 The slotted butterfly antenna element

(metal layer = yellow, substrate layer = grey)

As an effort to use bandwidth enhancement methods learnt in the previous chapters, the stacking of metals was tried. And the same principle of stacking is applied to the slotted butterfly antenna as shown in Figure 28 where a superstrate layer is added on top of the slotted butterfly antenna. Stacking means an extra substrate layer is added and more metals are added on each side of the butterfly antenna. Adding metals means the sharp ends of the butterfly antenna are covered and it also helps towards more impedance matching which introduces more substrates in the stacked version. Thus, the impedance is maintained at 50Ω while the bandwidth is greater than 2 GHz. When four rectangular metals are added at the corners of the slotted butterfly antenna, extra radiating surfaces are created without disturbing the impedance match and the broad bandwidth. The directivity is then increased to 7.2 dBi in the $\varphi = 0°$ plane and it is 4.2 dBi in the $\varphi = 90°$ plane.

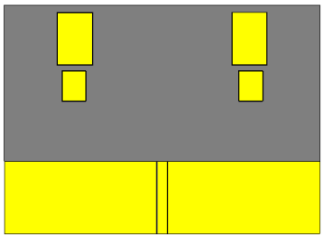

(a) Stacked slotted butterfly with a superstrate and four metal rectangles on top of the corners of the slotted butterfly

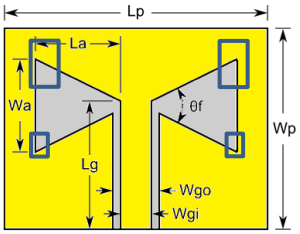

(b) Top view

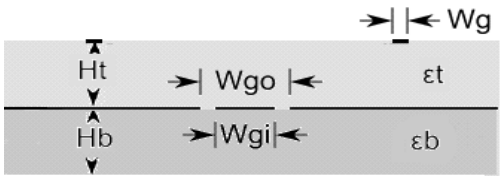

Lp : 35.7 mm
Wp : 24.0 mm
La : 9.45 mm
Wa : 5.03 mm
θf: 30°
Lg : 18.1 mm
Wgo : 1.30 mm
Wgi : 1.12 mm

Wg : 2.70 mm
Hb: 0.423 mm
Ht: 0.595 mm
εt = εb = 2.2
Top rectangular metals: 4.00 mm by 5.56 mm
Bottom rectangular metals: 2.70 mm by 3.26 mm

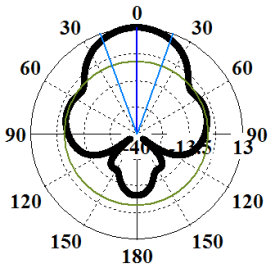

(d) Directivity = 7.2 dBi in φ = 0° plane at 11.7 GHz

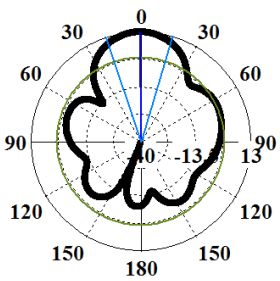

(e) Directivity = 4.2 dBi in φ = 90° plane at 11.7 GHz

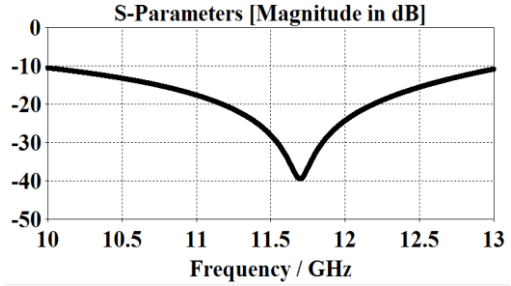

(f) S11 (dB) vs frequency (GHz) BW > 2 GHz

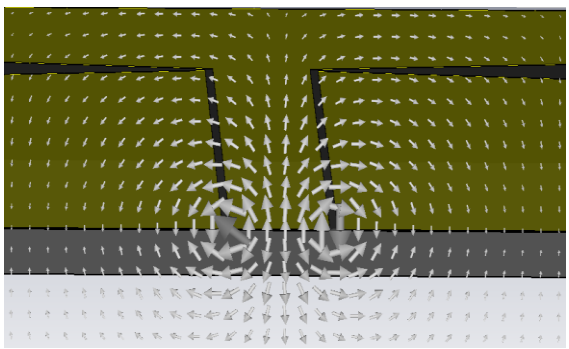

(g) E-field (voltage) plot at the $S^- S^+ S^-$ (CPW) port

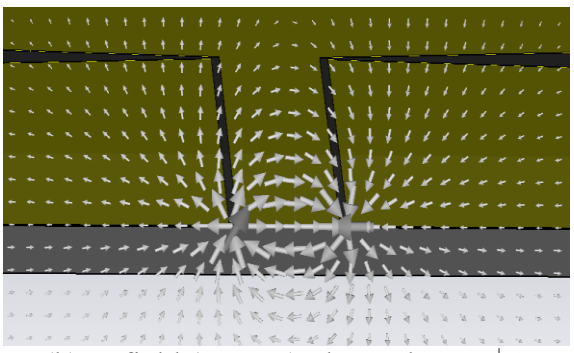

(h) H-field (current) plot at the $S^- S^+ S^-$ (CPW) port

Figure 28 The stacked slotted bow–tie antenna element with a superstrate and four metal rectangles placed on top of the corners of the slotted butterfly

(metal layer = yellow, substrate layer = grey)

With optimizations using CST Microwave Studio 2013, the slotted butterfly antenna is designed in a stacked version with four small extra radiating surfaces at its four corners in order to provide a large bandwidth in both polarization planes while being terminated with 50Ω CPW at the center frequency of 11.7 GHz. These results have been published in the journal and conference shown in [59], [60].

8.4 Chapter Conclusion

One can summarize that the slotted bow–tie or the slotted butterfly is an excellent antenna element which may satisfy the thesis specifications in an array configuration. An extra step to improve its bandwidth by trying some stacked bandwidth enhancement methods has been tried.

In Chapter 2, it is explained how mutual coupling increases when the antenna elements are spaced closed together, while it is also explained how an antenna spacing of λ/2 is ideal to avoid grating lobes. With the use of the slotted butterfly antenna with CPW feedline, an antenna spacing of λ/2 can fortunately be used.

However, the particular antenna examined is larger than λ/2.

Fortunately, the slotted butterfly antenna comes from the butterfly antenna element and the latter is part of the family from the frequency independent antennas i.e. it can be resized to fit the size of λ/2 maximum spacing, as desired to avoid grating lobes.

9. FREQUENCY INDEPENDENT ANTENNAS

9.1 The Butterfly Antenna is a Frequency Independent Antenna.

The butterfly or bow-tie antenna, as seen in the previous chapters, is a planar version of the finite biconical antenna which can be printed onto a substrate. The antenna is lightweight, has a small profile and a low manufacture cost. It was popular in the 1930s and 1940s and became the basis for the earliest television receiver antenna [61]. The introduction of the microstrip patch antenna in 1973 pushed it aside in the antenna ranking, but, it became popular again in 2002 when the US Federal Communications Commission (FCC) authorized the unlicensed use of the frequency band from 3.1 GHz to 10.6 GHz in USA. In Europe, the regulation restricts the band from 6-9 GHz [62]. Several papers have been written to cover this frequency band particularly that written by Yazdandoost and Kohno who proposed and patented a butterfly antenna exhibiting a low VSWR of 2.5-2.8 from 3.1 to 10.6 GHz [63]. The butterfly antenna for wideband frequencies is a symmetrical structure where the currents are principally concentrated at its edges. The antenna dipole-like radiation is omnidirectional in the plane perpendicular to the antenna. Studies have been carried out in order to evaluate the influence of the flare angle on the radiation patterns and antenna bandwidth. Brown and Woodward examined the flare angles of the biconical antenna in conical and triangular forms with straight and round ends and concluded that straight-end with a flare angle of 60° was the best choice to maintain a low VSWR over a wide frequency range [21]. DuHamel working on

frequency independent antennas showed that when the aperture angle of the butterfly antenna is 90°, the geometry is self-complementary and therefore well matched to stability [64]. In fact, the term frequency independent is reserved for antennas that have no theoretical limitation on the bandwidth of operation. Frequency independent antennas had their beginning in research conducted in the late 1950s at the University of Illinois. The exact definition of a frequency independent antenna is stated as an antenna with a bandwidth of about 10:1 or more [65]. The biggest constraint towards a frequency independent antenna is that most structures have geometry specified by angles rather than length and thus reflection is caused by the inevitable point of truncation. The principle of scaling indicates that frequency and length are invariably interconnected and Rumsey in 1950s set out to eliminate length as much as possible in the description of antenna geometry [66]. When a butterfly antenna is specified solely by the angle between the two triangles of the butterfly metal pieces, and the antenna feed is made invisible to the structure, with a feed starting at the center of the butterfly structure, the antenna becomes indefinitely low in both direction such as wavelength is no longer a variable in the antenna design and the antenna would theoretically have an infinite bandwidth. When it works for one frequency point, it must work for all frequencies as the antenna is exactly the same at all wavelengths. Haupt explained that an antenna whose geometry is described completely by angles, such as an infinite biconical antenna or its planar butterfly version, would make an ideal broadband radiator since its operation is theoretically completely independent of frequency [67]. Wiesbeck, Adamiuk and Sturm described that most wideband antennas have a balanced topology, that is, they require a balanced feeding structure to properly excite the fundamental radiating mode. Thus, they need differential feeding currents which are equal in magnitude and 180° differential phase to radiate the fundamental mode. The two wires transmission lines or the broadside coupled stripline are examples of balanced symmetrical structures [68]. Rumsey has also noted that wideband antennas follow the Mushiake principle that was published by Mushiake from Tohoku University in 1949 and they have an impedance of 189Ω [69]. The Mushiake principle states that the impedance of any planar antenna whose shape is the same as the shape of its complement is independent of frequency and equal to 60πΩ [70].

In theory, the frequency independent antenna must have a near-field and a far-field pattern that is independent of frequency. It must also be able to avoid low frequency limit and have a very small feed region to remove the high frequency limit [71], [72]. This is further reinforced in the patent from DuHamel [73] that explains that a planar antenna that originates from the

biconical antenna such as the butterfly antenna is theoretically an independent antenna. He explains how the end effects of the butterfly antenna, responsible for limiting the radiation pattern, are constant. In our butterfly antenna simulations, the feedline was simulated as a loss free feedline which adds no loss tangent. Here, the feed is maintained at 189Ω right in the middle of the butterfly structure and the 189Ω is maintained till its end at the port. As it is lossless, it is invisible to the butterfly antenna structure.

Thus, our butterfly antenna combines all these ideas from the cited authors. It is a simple design of a metal layer on top of a substrate layer fed with coplanar striplines on the metal layer. The butterfly antenna is designed to be symmetrical with a flare angle of 90° and it is fed at its midpoint by a coplanar stripline which is maintained at 189Ω or 60πΩ.

The butterfly is compared under four case scenarios with the flare angle changed from 90° to 60° and the butterfly end changed from straight to round end. The E-fields, H-fields, impedance plot, S-parameters, VSWR, and radiation patterns are given in order to appreciate the broadband feature of the four butterfly antennas.

9.2 The Design of the Butterfly Antenna

The design of the proposed butterfly antenna is very simple and as a first start it follows the equations for rectangular patches [74]. Equations 20 to 24 from [75], [76] calculate the resonant frequency, *fr*, of the butterfly antenna, where the values are given in Figure 29 and Figure 30.

$$f_r = \frac{c}{4\sqrt{\varepsilon_{effective}}L}\left(\frac{1.152}{R_t}\right) \quad \text{Eq. 20}$$

$$R_t = \frac{L(W_a + 2\Delta L)(d + 2\Delta L)}{(W_a + 2\Delta L)(2L_a + W_{gi} + 2\Delta L)} \quad \text{Eq. 21}$$

$$\Delta L = H\frac{0.412(\varepsilon_{effective} + 0.3)(\frac{W_x}{H} + 0.262)}{(\varepsilon_{effective} - 0.258)(\frac{W_x}{H} + 0813)} \quad \text{Eq. 22}$$

$$\varepsilon_{effective} = \left(\frac{\varepsilon_r + 1}{2}\right) + \left(\frac{\varepsilon_r - 1}{2}\right)\left(1 + \frac{12H}{W_x}\right)^{-\frac{1}{2}} \quad \text{Eq. 23}$$

$$W_x = \left(\frac{W_a + d}{2}\right) \quad \text{Eq. 24}$$

Table 4 shows the four butterfly cases being investigated.

Antenna Name	**Flare angle**	**Butterfly Shape**
Straight - 60	60°	Straight End
Straight - 90	90°	Straight End
Round - 60	60°	Round End
Round - 90	90°	Round End

Table 4 The antenna naming convention

Figure 29 and Figure 30 give the detailed design geometry of the Straight-60 and the Round–60 antennas. The Straight-90 follows the same geometry as the Straight-90 except with the change of the flare angle from 60° to 90°. The same applies to the Round-90 antenna which follows the same design as the Round-60 except for the change of the flare angle from 60° to 90°. As seen, the spacing between the coplanar stripline is very small at 0.121 mm. The four butterfly antennas are fed symmetrically in the center of the design and the coupled feedline is designed to maintain the desired 189Ω impedance.

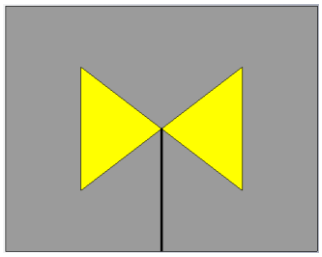

(a) Straight-60

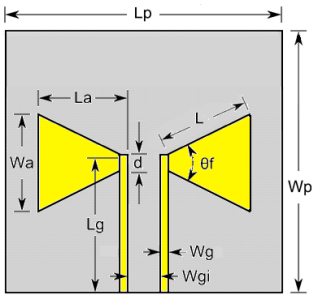

(b) Top view

(c) Side view

Lp : 55.5mm	d : 0.2mm
Wp : 43.8 mm	Lg : 22.0mm
La : 14.3mm	Wg : 0.061mm
Wa : 22.0 mm	Wgi : 0.121mm
L : 17.9 mm	H : 0. 250 mm
θf: 60°	εr: 2.2

Figure 29 The butterfly with a flare angle of 60° and straight ends (antenna straight-60).

Straight-90 is exactly the same, except the flare angle is changed from 60° to 90°

(metal layer = yellow, substrate layer = grey)

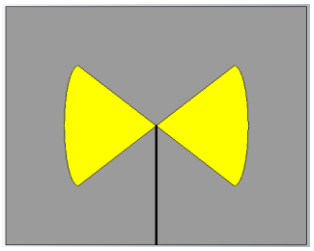

(a) Round-60

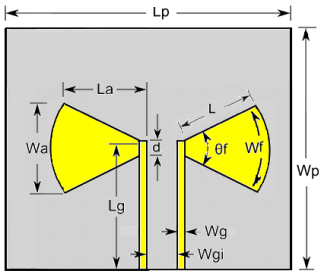

(b) Top view

(c) Side view

Lp : 55.5 mm	Lg : 22.0 mm
Wp : 43.8mm	Wg : 0.061mm
La : 14.3 mm	Wgi : 0.121mm
Wa : 22.0 mm	Wf: 23.5mm
L: 17.9mm	H : 0.250 mm
θf: 60°	εr: 2.2
	d: 0.2mm

Figure 30 The butterfly with a flare angle of 60° and round ends (antenna round-60).

Round-90 is exactly the same, except the flare angle from 60° to 90°

(metal layer = yellow, substrate layer = grey)

9.3 The Results of the Frequency Independent Antennas

The four antennas were simulated from 5 to 60 GHz using CST Microwave Studio 2013. The S-parameters and VSWR are shown in Figure 31 and Figure 32. The S-parameters and VSWR show that the antennas are broadband from 5 to 60 GHz. The Straight-90 and the Round-90 antenna showed the best results starting from 5 to 60 GHz, while the other antennas operate more as from 10 GHz onwards. The full symmetrical feature of the antennas with the flare angle of 90° enables the radiating waves to extend down to the start frequency of 5 GHz. The results from Figure 31 show that the periodicity of 7.7 GHz could probably extend the bandwidth to higher frequencies but further analysis would obviously be required. Note that here the VSWR is low and this does not translate automatically into radiation. A low VSWR means that power is being delivered to the antenna and not reflected [77]. In the studied case as the dielectric substrate is simulated as a lossless case and the metal is simulated as a PEC, then it is accurate to conclude that most of the energy is radiated making our butterfly antenna a good radiator.

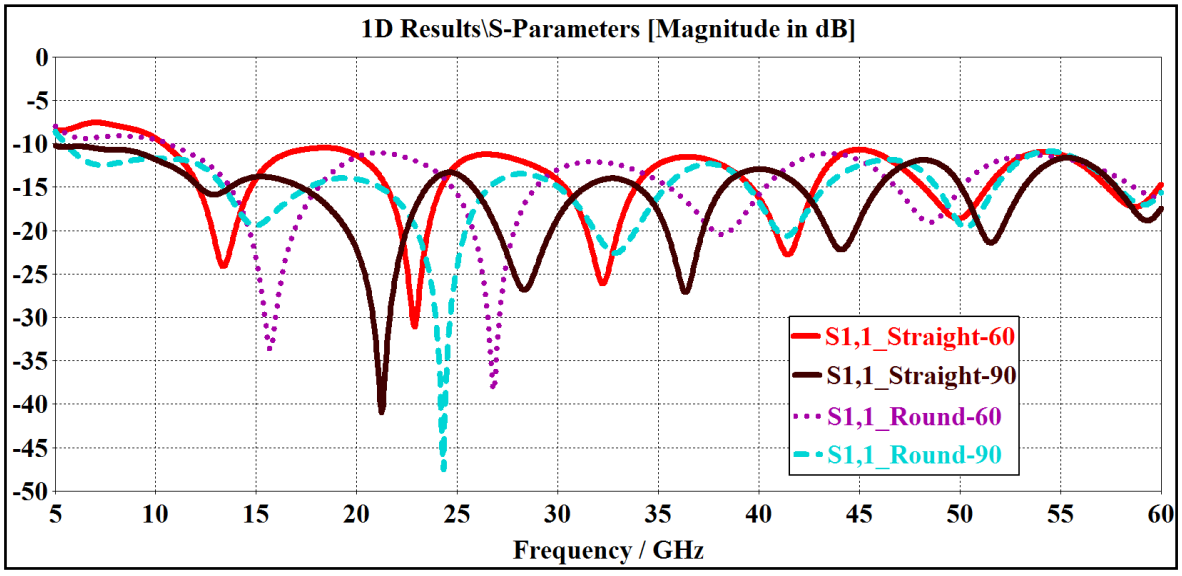

Figure 31 The S_{11} (dB) of the four butterfly antennas from 5 to 60 GHz

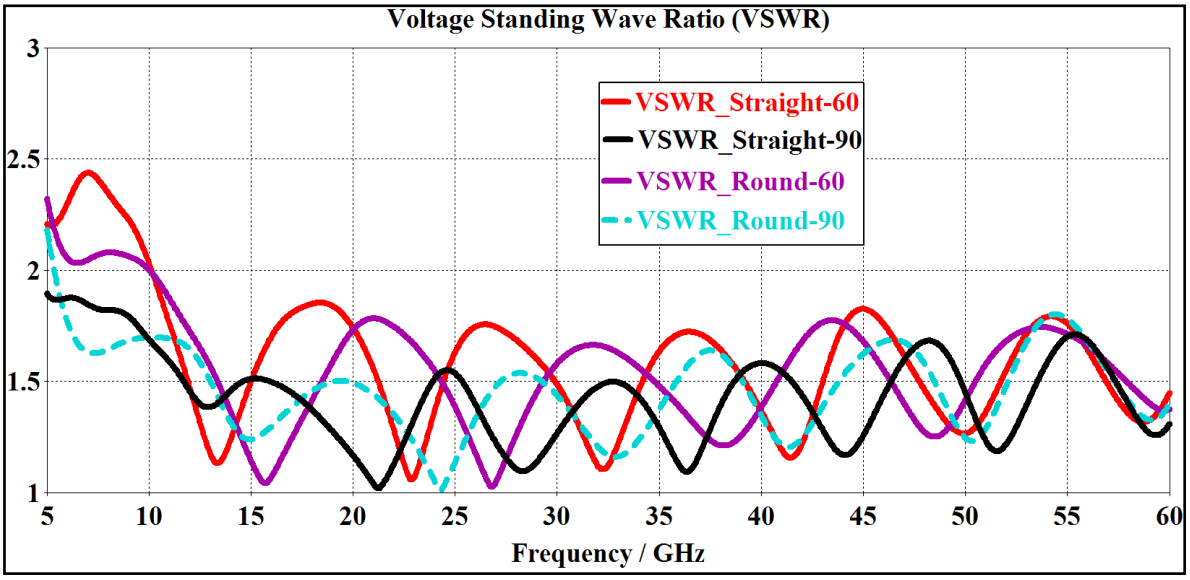

Figure 32 The VSWR of the four butterfly antennas from 5 to 60 GHz

The resonant frequency for the butterfly antenna is calculated using Equations 20-23. These equations were derived for microstrip patch type butterfly antennas and are used as an initial design for coplanar butterfly antennas. The butterfly antenna is by default a broadband antenna element and when it is designed and optimized as a frequency independent antenna over a wide range of frequencies, the butterfly antenna will have periodic resonance frequencies. Thus, when the design is finely tuned and optimized, the resonant frequency will shift as explained by Durgun, Balanis, Birtcher and Allee [78]. The antenna has a resonant frequency of 7.7 GHz and in fact, between 10 to 60 GHz where the VSWR is less than 2, the butterfly antennas are seen to resonant periodically at multiples of 7.7 GHz exhibiting the broadband feature of frequency independent antennas.

The impedance plot of the butterfly antenna is shown in Figure 33.

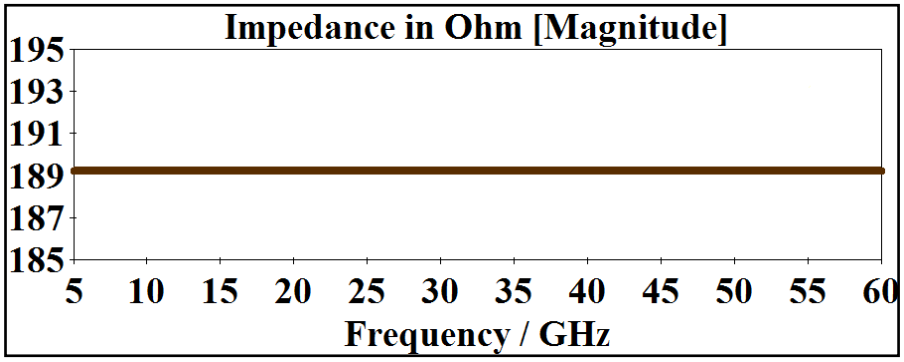

Figure 33 The impedance of 189Ω of the antenna from 5 to 60 GHz

The impedance is shown to be constant at 189Ω. This impedance is shown by all four butterfly antennas across all the frequency range from 5 to 60 GHz. Such a property of impedance of 189Ω reinforces the ultra-broadband property of our butterfly antennas. The E-fields and the H-fields at the port of the ultra-broadband butterfly antenna are shown in Figure 34. The signal at the port is S^+S^- for a coplanar port where S^+ is the signal and S^- is the mask or return path.

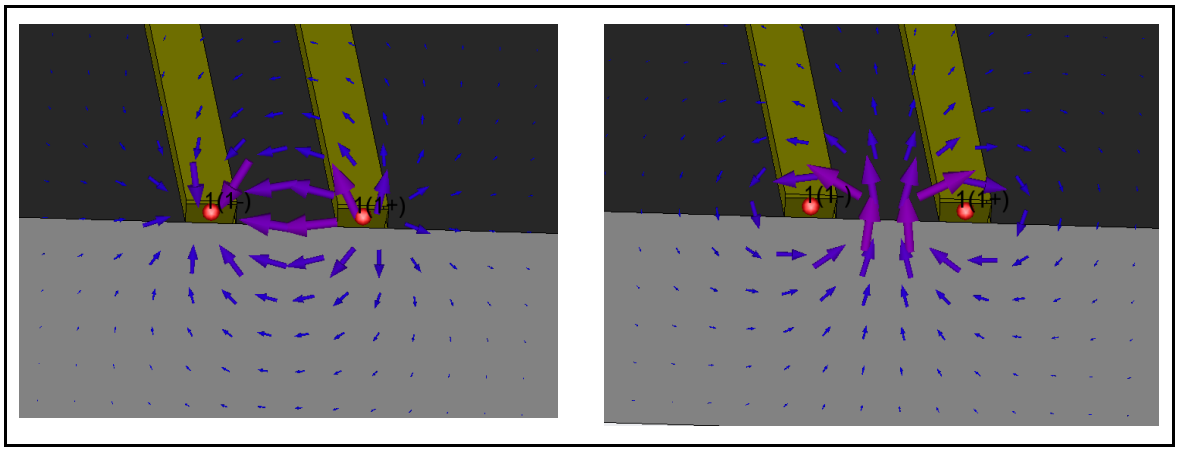

Figure 34 The E-fields (left) and the H-fields (right) at the port of the antenna

The radiation patterns were examined in the far-field and the directivity in the azimuth plane ($\varphi = 0°$ plane) and elevation plane ($\varphi = 90°$ plane) are shown in Figure 35 and Figure 36 respectively.

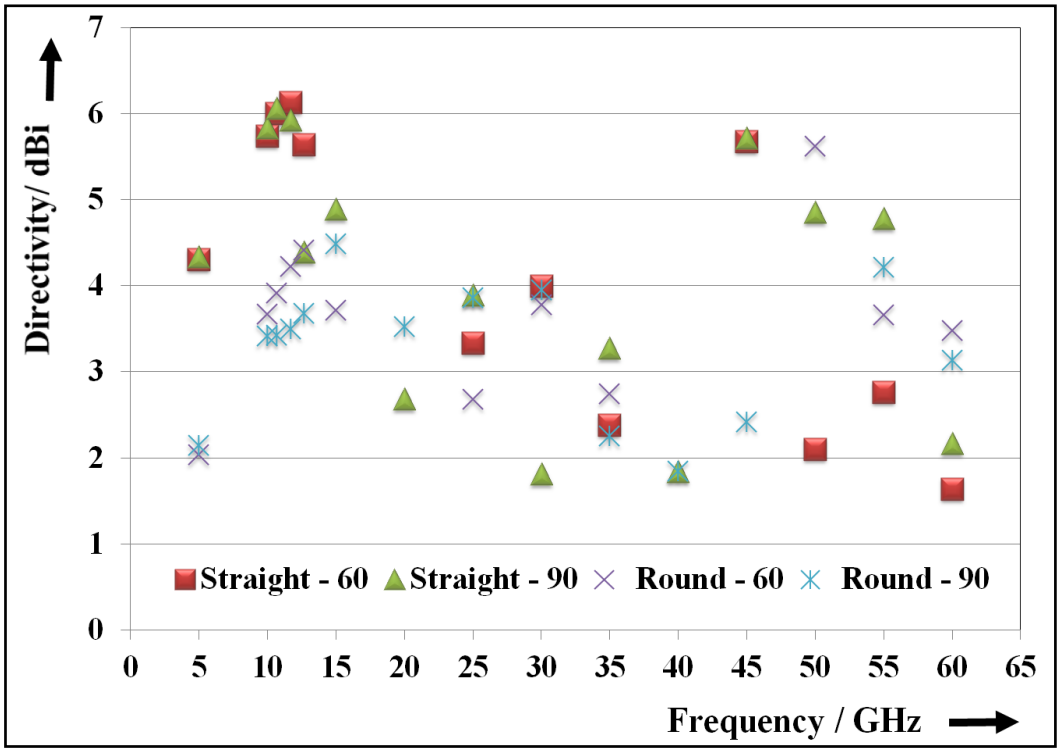

Figure 35 The directivity plots in the φ= 0° plane (azimuth)

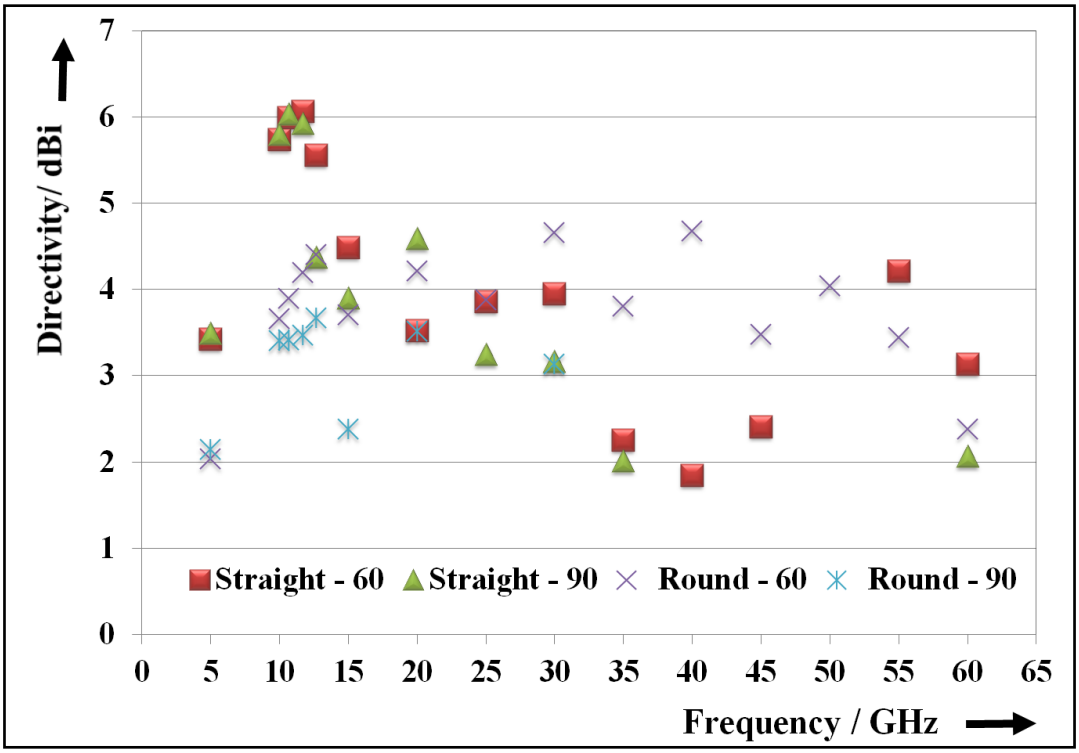

Figure 36 The directivity plots in the φ= 90° plane (elevation)

The straight-end antennas performed better than the round-end antennas. The straight-end antennas have a highest directivity of 6 dBi while the round–end antennas have a maximum directivity of 4.5 dBi in the far-field. The 3D far-field patterns of the four butterfly antennas at 11.7 GHz are shown in Figure 37.

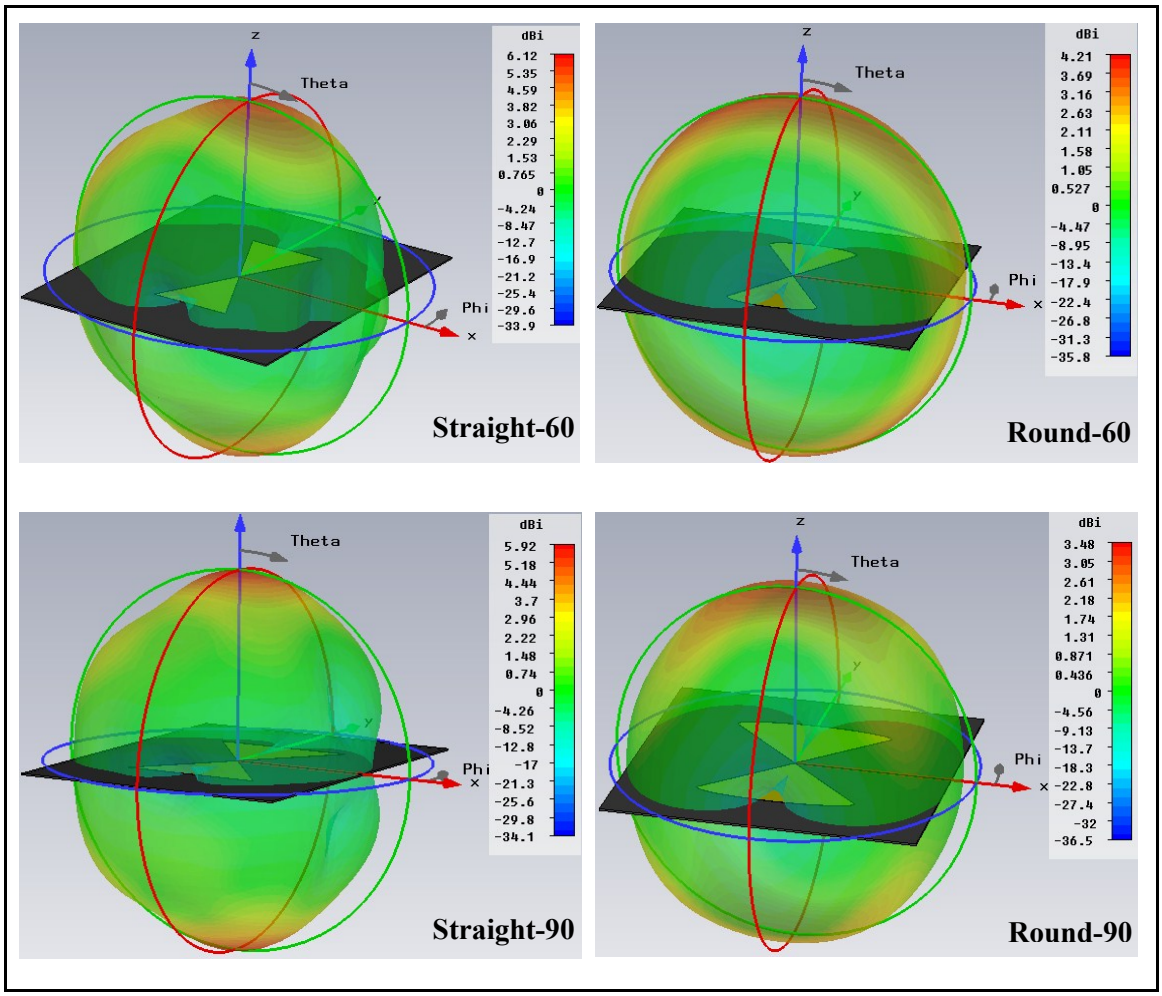

Figure 37 The 3D radiation patterns of the four butterfly antennas at 11.7 GHz

Again, the straight-end antennas performed better than the round-end antennas. Here, in both cases, an antenna with a flare angle of 60° antenna gave a slightly higher gain than an antenna with a flare angle of 90°.

Thus, although S-parameters and VSWR results show that the Straight-90 antenna performs the best among the four butterfly antennas, the directivity of the Straight-60 antenna was marginally better than that of the Straight-90 antenna.

9.4 Chapter Conclusion

We can conclude this chapter by saying that we have successfully designed and analyzed an ultra-wideband butterfly antenna covering the frequency range from 5 to 60 GHz. From 5 to 60 GHz, the VSWR < 2 for the straight-end butterfly antenna with a flare angle of 90°. The antenna has a maximum directivity of 6 dBi in the far-field. The antenna is simply built with just a metal layer on top of a substrate. It is compared with three other butterfly antennas where the flare angle was changed from 90° to 60°, and the butterfly end was changed from straight-end to round-end. All four butterfly antennas are fed with coupled stripline with an impedance of 60π or 189Ω. They all exhibit a VSWR <2.5 from 5 to 60 GHz. These results are novel and have been successfully published in a journal and a conference paper [79]-[80].

An examination of the frequency independent antennas shows that to satisfy our width spacing requirement of not more than λ/2, the butterfly or the bow-tie antenna must be modified to fit under a smaller dimension as described in the next chapter, where the butterfly antenna is resized to fit the width of less than λ/2.

First, this butterfly antenna must be converted into its slotted version which has the preferred feedline of CPW, ensuring again that the λ/2 spacing is respected. This fixes the width of the slotted butterfly antenna. Then, its length must be resized. The length of the slotted butterfly antenna is determined by the length of the longest phase shifter required to move the main lobe by 45°.

In the next chapters, a quick history of the antenna array is given along with an examination of the feed of the antenna array. This is important in order to understand the path to follow when the slotted butterfly is resized to fit in an array configuration.

10. THE ANTENNA ARRAY

10.1 The Antenna Array

The antenna array is the array factor multiplied by the element pattern.

The element pattern of an antenna element is a vector while the array factor is a scalar.

The element pattern has a polarization. The array then assumes the same polarization as the element pattern. Usually, and in the case studied here, the array polarization is the same as the element polarization because all the antenna elements are oriented in the same direction.

However, it should be mentioned that this is not a fixed rule, as one can position the elements such as the array antenna is made to have a different polarization from the antenna element. Huang has investigated that case on a 2 x 2 array of a rectangular patch antenna. Each patch is rotated 90° as shown in Figure 38 [81]. The rectangular patch antennas are linearly polarized while the array here demonstrates circular polarization because of the way they are fed and positioned.

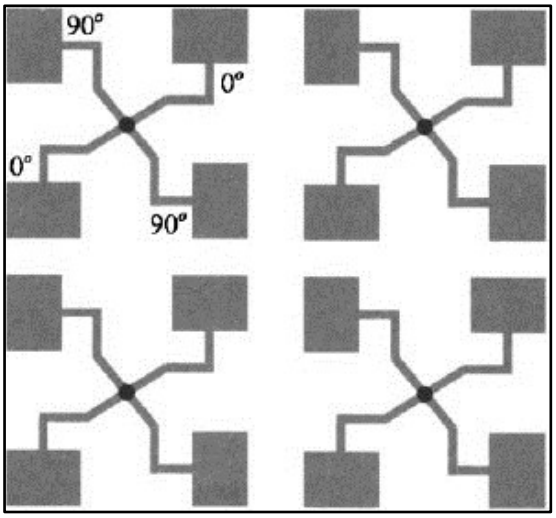

Figure 38 An array with circular polarization from linearly polarized rectangular patches [81].

Of course when the peak of all the antenna elements point in all the same direction and it is not submitted to any rotation, the array factor in the direction of the element is enhanced as well as the main lobe and one can obtain a higher gain with a smaller beamwidth or opening angle.

One antenna element will usually have a wide beamwidth and the direction of its main lobe cannot be changed without the help of a phase shifter. Thus, in the absence of a phase shifter, the antenna array is built with antenna elements all pointing in the same direction and the main lobes are enhanced while the sidelobes are degraded. Then, the opening angle or beamwidth is slowly reduced as the array is built up and the main lobe is enhanced.
Solutions have been developed by authors to modify the element weight or spacing to play with the side lobes and change them [82]. In the specifications, the elements must all be identical and thus the weight or size or the antenna spacing must be kept identical in order to enable a smooth uniform phase shifting when the phase shifters are added on the feedlines.

An antenna array is attractive as it is a system that is reliable or trustworthy as if one antenna element fails, the remaining antenna elements keep the antenna array still in operation. Its main disadvantage is that the upfront cost to set it up is higher, to account for the engineering research behind, but, as it is trustworthy, an array can have a long lifetime.

10.2 The History of the Antenna Array

The German Karl Ferdinand Braun invented the phased array antenna in 1905 as described in his Nobel Prize lectures in pages 239-240 [83]. He was also the first one to build the first Cathode-Ray Tube (CRT) in 1897 and the cathode ray tube oscilloscope, still referred to the Braun-Tube in Germanic countries [84].

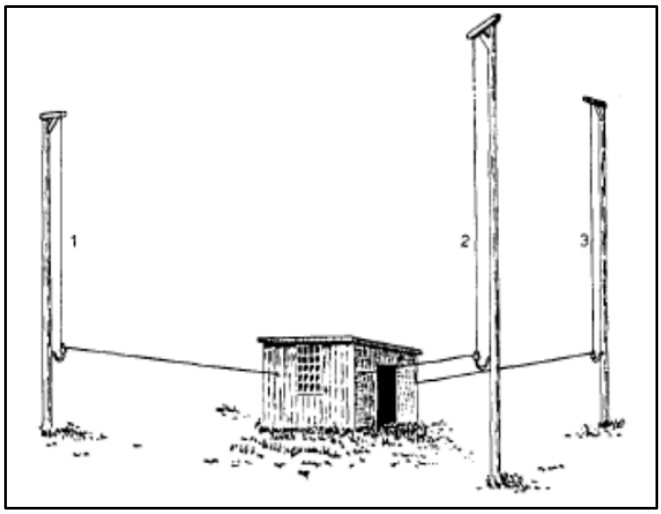

Figure 39 The first switchable phased array with a three element system [83]

Braun further went on to pioneer the early warning radar during World War 2 by building the phased array Fu 41/41 Mammut [85]. The Mammut phased array was a fixed array where the main lobe was moved electronically by 100° and it was able to detect targets coming at an altitude up to 8000 m and a range of 300 km.

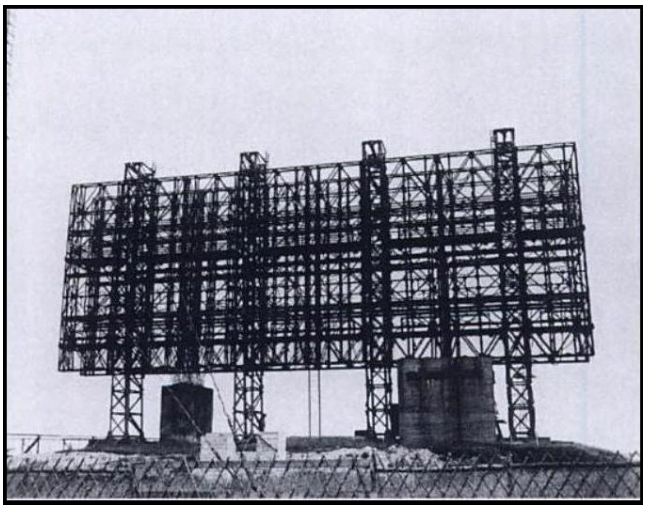

Figure 40 The early warning Mammut Radar [85]

Figure 41 shows the World's largest phased array antenna in Alaska/Canada:- 3 panels of 30x30m with 12288 antenna elements.

Figure 41 The World largest phased array antenna in Alaska/Canada [86]

The bandwidth of a phased array antenna is influenced by many variables. When the antenna element spacing is too high, grating lobes can decrease the bandwidth at the highest frequency of interest.

In order to have a broadband array, the antenna element must first cover the frequency of interest. To achieve a planar antenna, the butterfly or the bow-tie antenna is ideal. It is in fact the two dimensional or planar version of the biconical antenna.

10.3 The Antenna World: A Matter of Size

The size of the antenna element matters. Big antenna will collect lots of electromagnetic waves just like a big coffee mug will collect lots of rain. This is why in the case of a parabolic antenna, the larger the parabolic antenna, the more gain it has.

When the same result as a large coffee mug is needed, a lot of smaller coffee mugs can be used instead of one large coffee mug. When the outputs of the smaller coffee mugs are combined the antenna works as an array. On a small scale, one can think of it as: three separate one-shot expresso coffee is equivalent to a triple large expresso coffee shot.

In the antenna world, the largest single aperture is the Arecibo Observatory. Built from the 1960s to 2011, the telescope spaces the frequency from 300 MHz to 10 GHz with the possibility of processing up to 800 MHz of bandwidth [87].

The Arecibo radio telescope shown in Figure 42 is located in Puerto Rico. It is the largest single aperture antenna in the World with a dish of 305m diameter and 50.9m depth covering 80 937 m^2 (20 acres). Since heat is an issue, the receivers are immersed in a bath of liquid helium to maintain a very low temperature.

Figure 42 The world largest single aperture antenna [87]

10.4 The Origins of Phase Shifters in an Array

Friis and Feldman originated the concept of moving the main lobe with the help of a phase shift in the signal [88]. They started by presenting the idea behind a two element array with phase shifters. At that time, the army wanted to be able to rapidly scan a region without moving the antenna and this is why the parabolic antenna was not efficient and was replaced by the phased array antenna. Let's have a quick look at the parabolic antenna and its features before proceeding with the phase shifters on phased array antenna.

10.5 The Parabolic Antenna

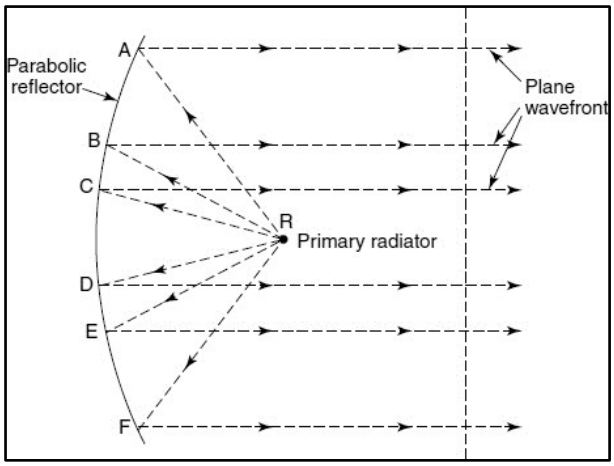

Figure 43 The radiation from a parabolic antenna [89]

Figure 43 shows the radiation from a parabolic antenna that is used as a reflector antenna. Here the parabola has its primary radiator at its focal point R. The waves are spherical by nature and they are converted into planar waves when the signals are reflected on the points A to F on the parabolic surface [89].

Equation 25 gives the effective area of the parabolic antenna while Equation 26 expresses the gain that can be obtained by the parabolic antenna. In Equation 25, *D* is the diameter of the parabolic antenna. The gain equation here assumes that the parabolic antenna is 100% efficient which is not the case in reality.

$$\text{Area}_{\text{effective}} = \pi\left(\frac{D}{2}\right)^2 \quad \text{Eq. 25}$$

$$\text{Gain} = \frac{4\pi}{\lambda_0^2}\,\text{Area}_{\text{effective}} \quad \text{Eq. 26}$$

As the phase array antenna with dielectric phase shifter is supposed to replace the parabolic antenna, it has to achieve the same performance as the parabolic antenna as required for satellite broadcast , i.e. a gain of approximately 30 dB and a beamwidth of 3°.

In the case of an antenna array, the beamwidth and the beam gain depend essentially on the number of elements, N. When the elements are spaced by λ/2 in order to avoid grating lobes, the antenna elements, N, the beamwidth, θ, and the Gain, G, are linked by a simple relation as shown in Equation 27 and 28 where η is the antenna efficiency [90].

$$N^2 \approx \frac{10\,000}{\theta^2_{\text{beamwidth}}} \quad \text{Eq. 27}$$

$$G \approx \eta\pi N^2 \quad \text{Eq. 28}$$

Thus, in the studied case, as the beamwidth is 3°, the number of elements is 32 when the spacing is λ/2. The maximum gain that can be possible when N=32 elements is $\pi * 32^2$ or 3217 or 35 dB assuming a 100% efficiency. This means that it is possible to obtain the gain of approximately 30 dBi as desired, in order to obtain the same performance as the parabolic antenna.

10.6 Chapter Conclusion

In this chapter, the antenna array has been described, followed by a short history lesson. The parabolic antenna has also been presented and it is seen that the size and performance of the array must match that of the parabolic antenna. In the next chapter it is investigated how the antenna elements are connected together through the feed network. Unfortunately the feed network is a necessary evil that is required to connect the antenna elements together and as it is an added feature, it only adds loss and decreases the bandwidth and gain and must thus be

very carefully designed in order to ensure that the 3 B's, that is the bandwidth, beamwidth and beam gain, are still satisfied in the final design that includes the feed network.

11. ARRAY FEED

11.1 The Antenna Feed

There are different ways in which an array can be fed. The serial feed is the easiest feed that comes to mind. As the patch antenna is the simplest antenna that can be designed, it can be used as the easiest reference for each feedline configuration. The patch antenna is shown in the literature in an array configuration with a serial feed [91]. This is depicted in Figure 44 where four patch antenna elements are serially fed and joined together by a feed network to make an 8x4 array. The configuration is repeated with the slotted stacked butterfly antenna as shown in Figure 45 (The slotted stacked antenna element is shown in Figure 28). The S-parameters plot of the 8x12 array made with slotted stacked butterfly antenna is shown in Figure 46. After optimizations, the bandwidth is satisfied from 10.7 GHz to 12.7 GHz. This is a very compact design with 96 antenna elements, each of size 3.57cm by 2.4cm. However, there is not much space for the phase shifters, and as it is designed for a center frequency of 11.7 GHz, the phase shifter will only operate linearly for that one center frequency and not for the other frequency range in the bandwidth from 10.7 GHz to 12.7 GHz. This means that the serial fed array is perfect for only one frequency and not for the whole bandwidth and thus cannot be used to have a linear smooth uniform main lobe change in direction with the dielectric phase shifters for a broad frequency range. Thus, it will not be further investigated in this work.

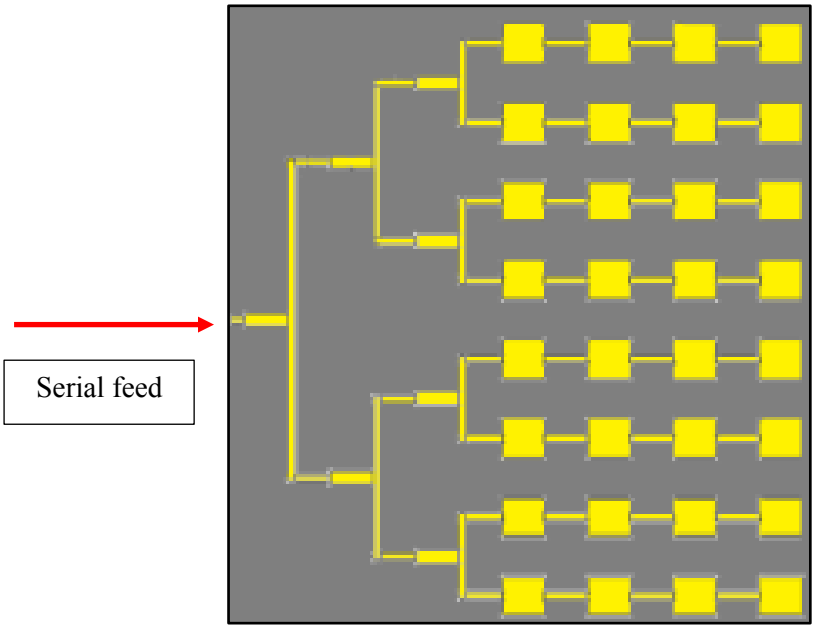

Figure 44 The serial fed with the patch antenna [91]

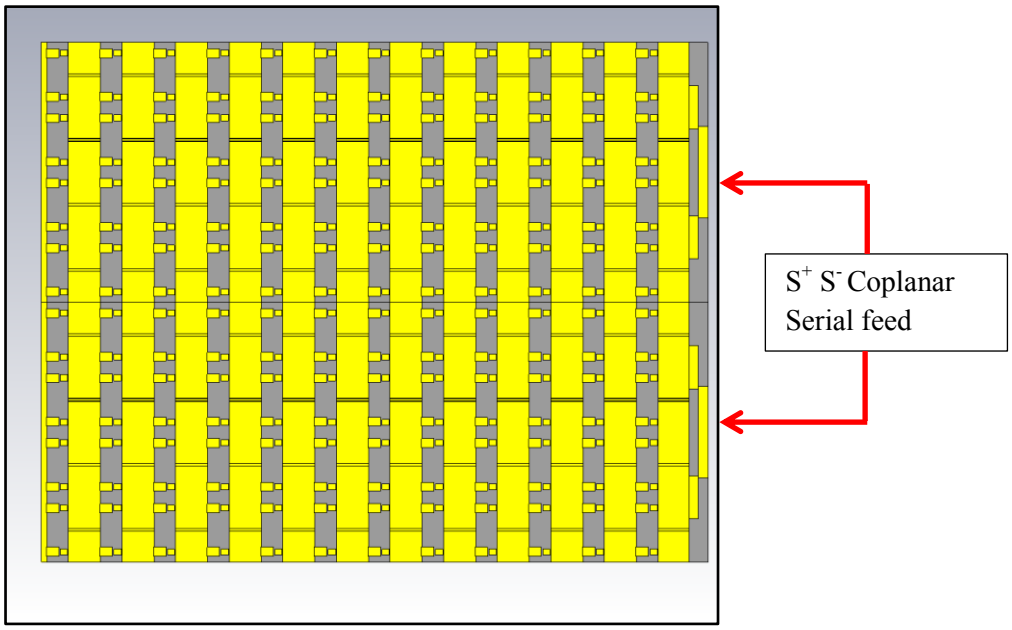

Figure 45 The serial feed with the slotted stacked butterfly antenna

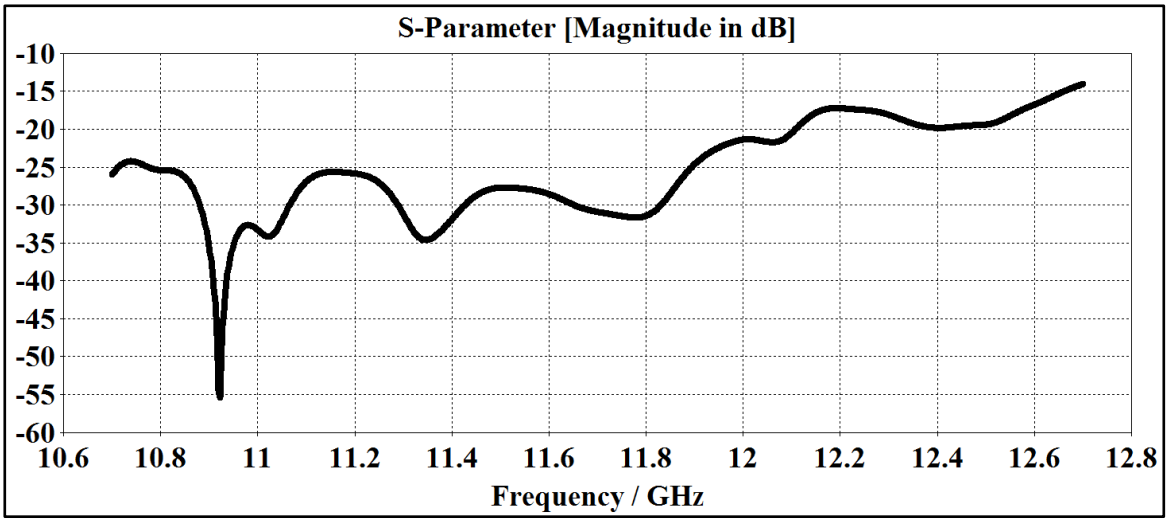

Figure 46 The S_{11} (dB) versus frequency/GHz for serial feed

A second feedline configuration can be the patch antenna fed in the middle as shown in Figure 47, where the metal layer is in yellow and the substate layer is in grey. As seen in Figure 48, the bandwidth is not satisfied both because patch antennas elements are used and how difficult it is to optimize the center fed array.

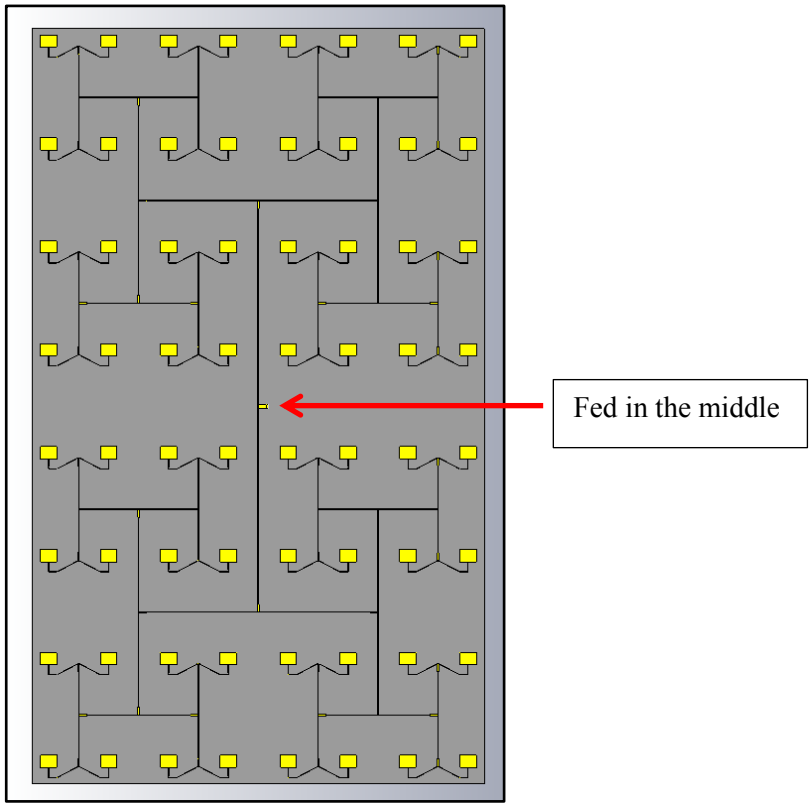

Figure 47 The patch array fed in the middle

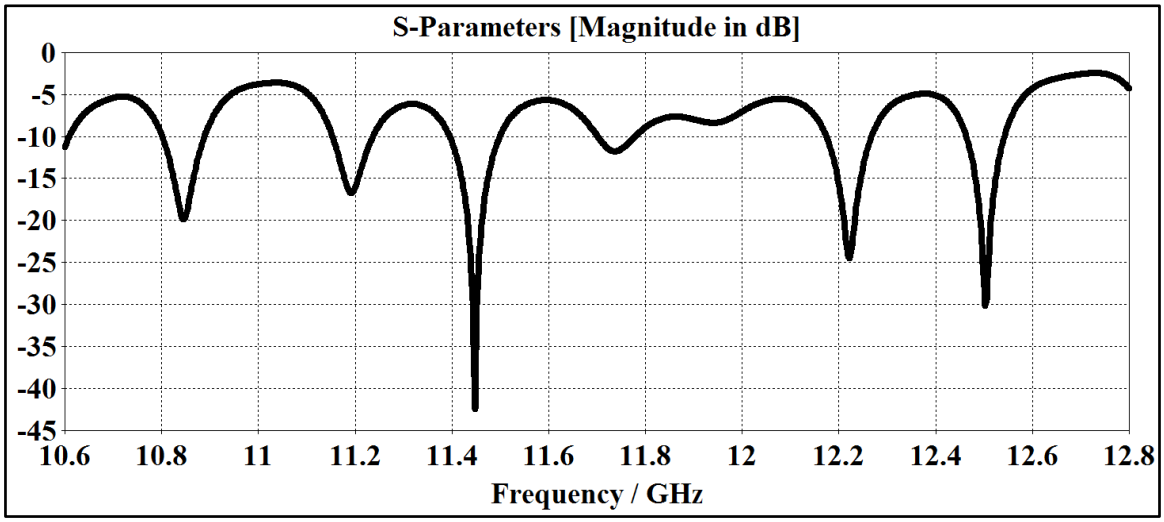

Figure 48 The S_{11} (dB) versus frequency /GHz for mid fed patch array

The same design is repeated with the butterfly antenna element from Figure 26 from Chapter 8 and it is fed in the middle similarly to the patch antenna, as seen in Figure 49 where the metal layer is in yellow and the substate layer is in grey. The regular butterfly antenna is used here because it is easier to merge in the middle as a first trial for a mid-array feed. The S-parameters plot in Figure 50 shows that the bandwidth specification is not fulfilled. In fact, there is no space for the phase shifters to operate on the N^{th} element with this configuration fed in the middle. It is extremely difficult to minimize loss when the antenna elements and feed network are located on the same layer. In this design we have 8 x 8 antenna elements and it is very hard to strongly optimize 64 antenna elements along with its feedline because the CST software has the number of mesh cells limited to 50 million [92]. 50 million mesh cells seem like a lot but to put in perspective, about 2 million mesh cells are required per antenna element for a strong optimization so in fact only about 16 antenna elements maximum can be simulated when 2 million cells are used per antenna element. 32 elements can be simulated with a medium optimization setting or a medium mesh cell settling of 1 million mesh cells per antenna element, or, 64 elements with a fair optimization setting or with a fair optimisation setting of 500, 000 mesh cells per antenna element. Some mesh cells must of course be kept for the meshing of the feed network. Moreover, these optimizations already consume a lot of computational time even when used with a GPU card and the hardware acceleration option, as described in the CST software description in chapter 4. Per experience, to optimize a 2 million meshed antenna element using the GPU card, one need between 1 to 2 hours of CST simulation, so for 50 million mesh cells one would need about 50 hours per simulation. Each

optimisation step requires one full simulation run and each design requires several full optimizations of each design variable. Therefore, as you proceed through the PhD manuscript, please take a brief moment to appreciate the total simulation time required in this work.

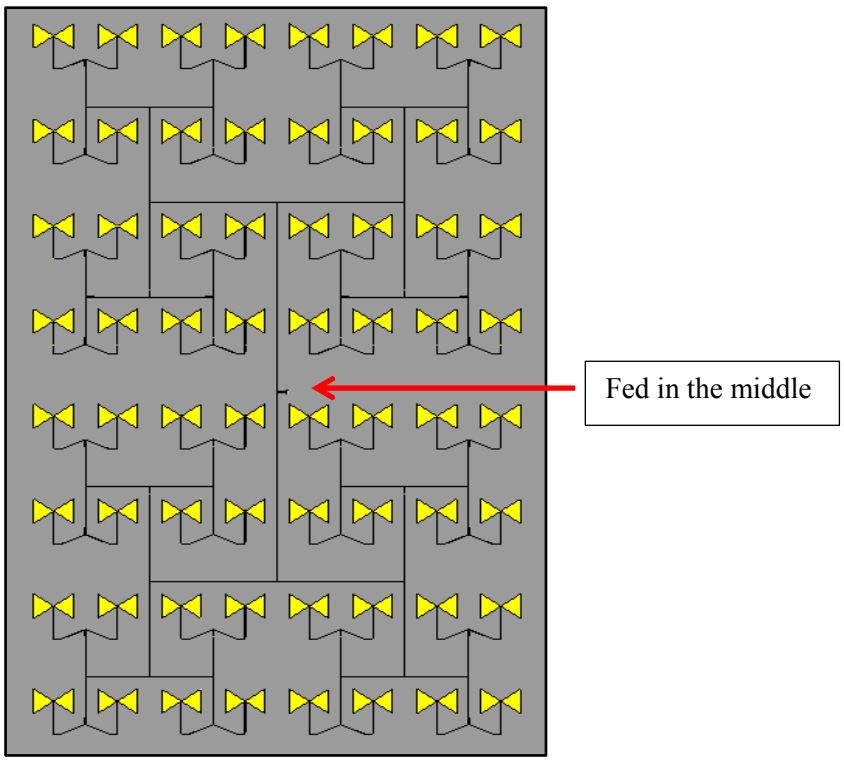

Figure 49 The butterfly antenna fed in the middle

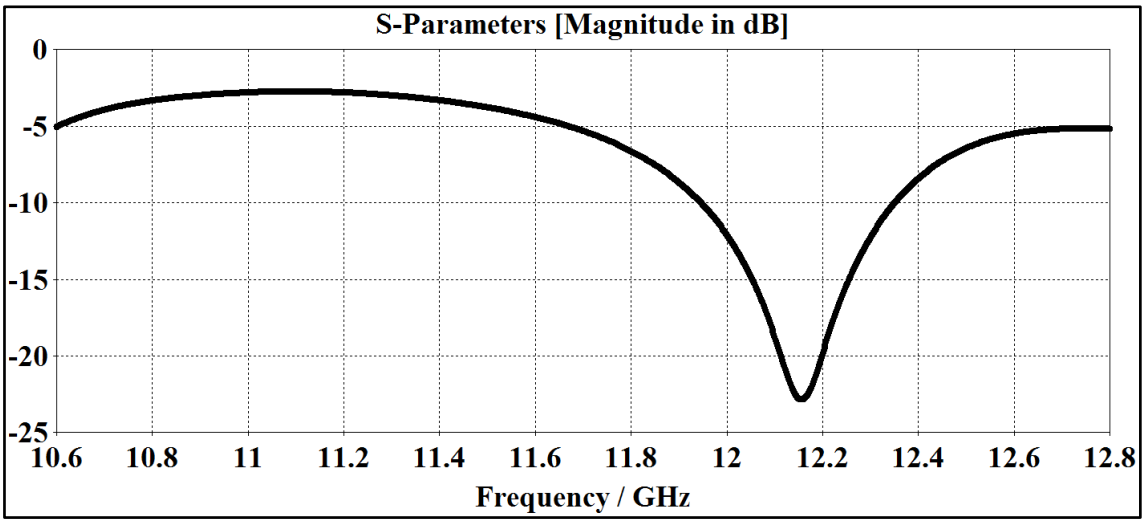

Figure 50 The S_{11} (dB) versus frequency /GHz for the mid fed butterfly array

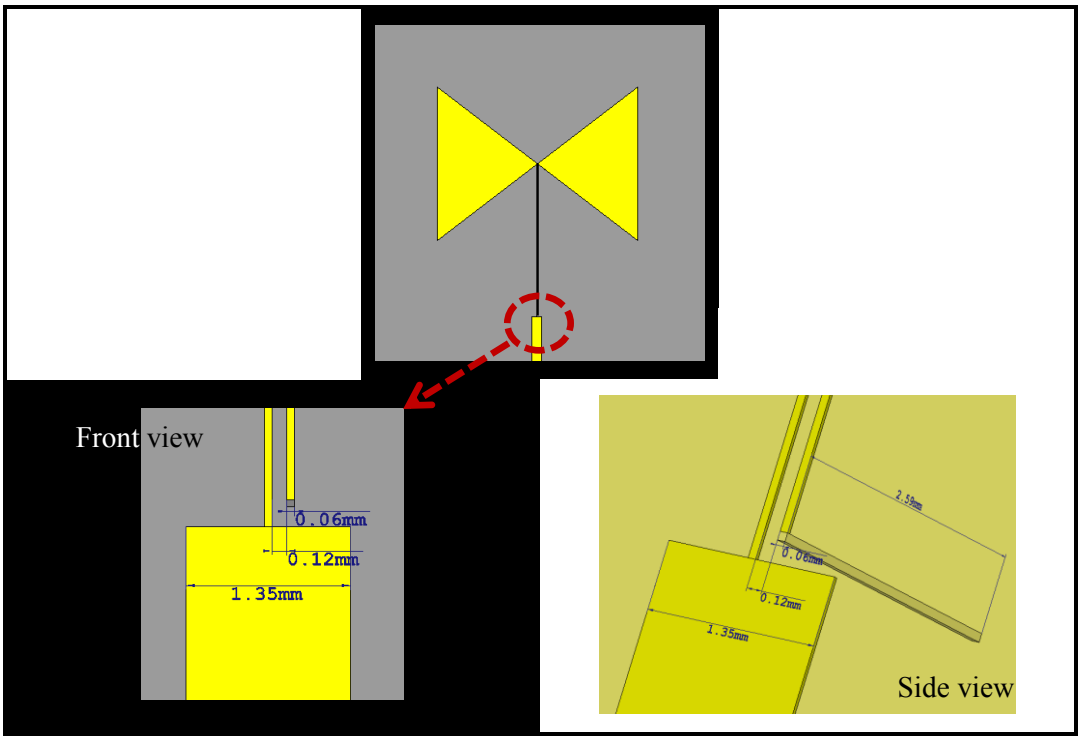

Figure 51 The butterfly antenna with the zoomed-in views

When linking the butterfly antenna elements from Figure 26 to the feed network, a via is required to transit from the S^- on the top layer, where the metal layer is in yellow and the substate layer is in grey, to the ground layer underneath the substrate layer as shown in Figure 51. Here only one via is needed because only one S^- must transit from the top layer through the substrate to the bottom ground layer in the feed network side. For the slotted butterfly element described in Figure 25, as there are two S^- signals on the top layers, two vias would be needed to transit to the ground layer when linking the antenna element to the feed network. This is described in more details in the array section in Chapter 13.

One observation that must be made here is that the metal is designed to be a perfect electric conductor (PEC) throughout the project because it takes less time, requires less meshing and makes the project much faster, but here we have resimulated the same antenna element from Figure 51 with the consideration that the metal as normal or copper to reflect the reality at best and this is all to show that there is barely any difference between the use of the PEC metal and Copper case, such that for this work, it is acceptable to simulate the metals as PEC to save time and progress faster throughout the thesis. These results are shown in Figure 52 and Figure 53.

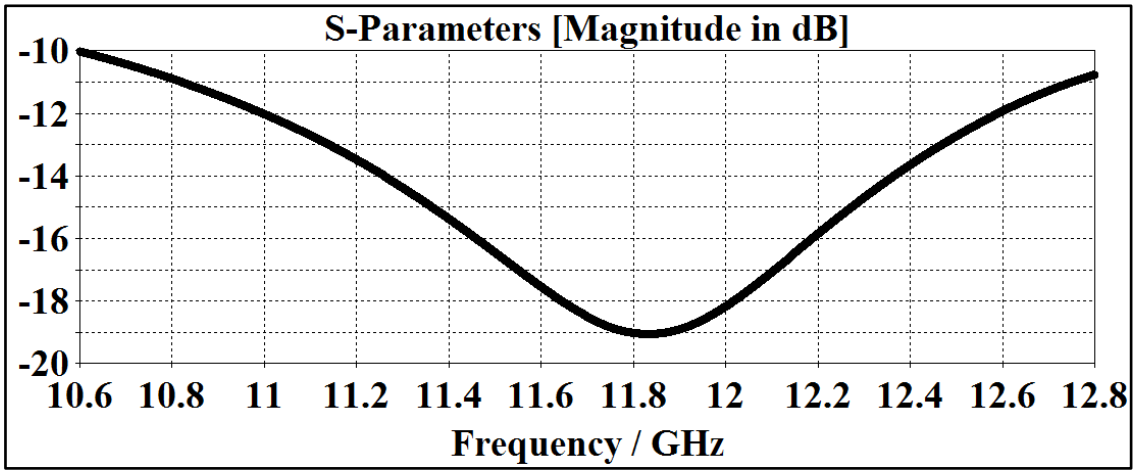

Figure 52 The S_{11} (dB) versus frequency/GHz with PEC metal

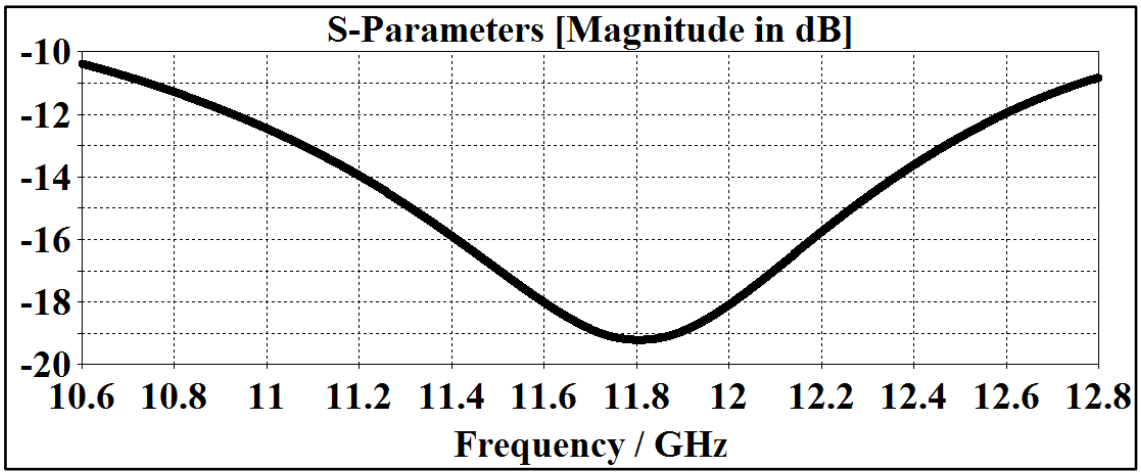

Figure 53 The S_{11} (dB) versus frequency/GHz with Copper metal

11.2 Chapter Conclusion

Several conclusions can be reached at this level.

1. Only a slotted butterfly antenna with a CPW feedline and a maximum width of λ/2 can be used as an antenna element.
2. The feedline must also be carefully designed. A serial feed isn't allowing the thesis to be satisfied and neither is the mid fed. The bandwidth is not reached. It is also seen that the length of the feedline is limited. It is impossible to make a center feed and design with a center feed and obtain the gain and allow for place for the phase shifter.

A different feed network must be used to permit the large phase shifter feedline length while allowing the beamwidth of 3° in an array that covers the wide bandwidth requested by the thesis. The exact length of the phase shifter needed to move the N^{th} antenna element in the array is examined in the upcoming chapter.

12. THE DIELECTRIC PHASE SHIFTERS

12.1 The Dielectric Phase Shifters

The dielectric phase shifters in this project are designed to work by changing the phase velocity and thus the angle or direction of the main lobe of the antenna array.

In order to design the phase shifters, a calculation must be made on the change in dielectric constants with and without the phase shifters. Also, on an array version, the phase shifters must be evaluated up the N^{th} element of the array. In our design, the phase shifters are built on ε_r 10.2 and are placed on top of a substrate of ε_r 2.2. The change in the phase velocity with the addition of the phase shifter can be used to calculate the change in the main lobe direction for antenna element 2. Since one is working with a change of phase velocity, antenna element 1 would not need a phase shifter. Thus, the phase shifters are added from antenna element 2 up to the N^{th} antenna element. Then the phase shifter's length must be evaluated for the N^{th} where the phase shifter for the N^{th} antenna element = phase length multiplied by $(N-1)^{th}$ so, for example, in the studied case as calculated by Equation 32, the length of the phase shifter needed to change the direction of the main lobe by 45° is 6.03 cm and thus for the 32th element, the length of the phase shifter needed = 31 * 6.03cm = 18.69 cm. This length of phase shifters on the N^{th} or 32^{nd} element is placed on top of the feedline of the antenna element in the array so all this length must be accounted for when the antenna element is

built. It is necessary for the feedline design to be included with the antenna element, as a feed network would add loss and this will reduce the bandwidth.

In summary, it is not possible to simply design an antenna element and replicate it N^{th} time as needed and to just add the feed network with the designed length and expect to have the desired results of bandwidth, beamwidth and beam gain. This step has been tried in a rinse and repeat cycle but it has not been possible to maintain a large bandwidth when the feed network is designed separately from the butterfly antenna. This is because in a large array, the feed network has a large presence as it is required to link the entire antenna elements up to the N^{th} one together and its loss effect is certainly not negligible. Thus, the only way to maintain the large bandwidth was to design the antenna element with the long feedline and move the phase directly on top of the feedline of the antenna element. Consequently, one has to directly consider the length of feedline needed with the antenna element itself.

With the restriction of a maximum width of $\lambda/2$ or 1.28 cm when λ is 2.56 cm for the mid frequency of 11.7 GHz, and a length of 18.69 cm minimum, one can understand that an antenna element of 1.28 cm by 18.69 cm minimum is needed, as described further on in this chapter.

First, one needs to take advantage of the frequency independent properties of the butterfly antenna described in Chapter 9 to design a scaled version of the slotted butterfly antenna.

One question that might arrive here is: how small can one go? How small can the frequency-independent antenna be scaled down to?

Grzegorz Adamiuk, Xuyang Li and Werner Wiesbeck explained in [93] that an antenna is far below resonance when it has a dimension less than $\lambda/10$. Thus, we cannot go lower than $\lambda/10$.

The dielectric phase shifters are responsible to direct the main lobe in the desired direction as shown in Figure 54.

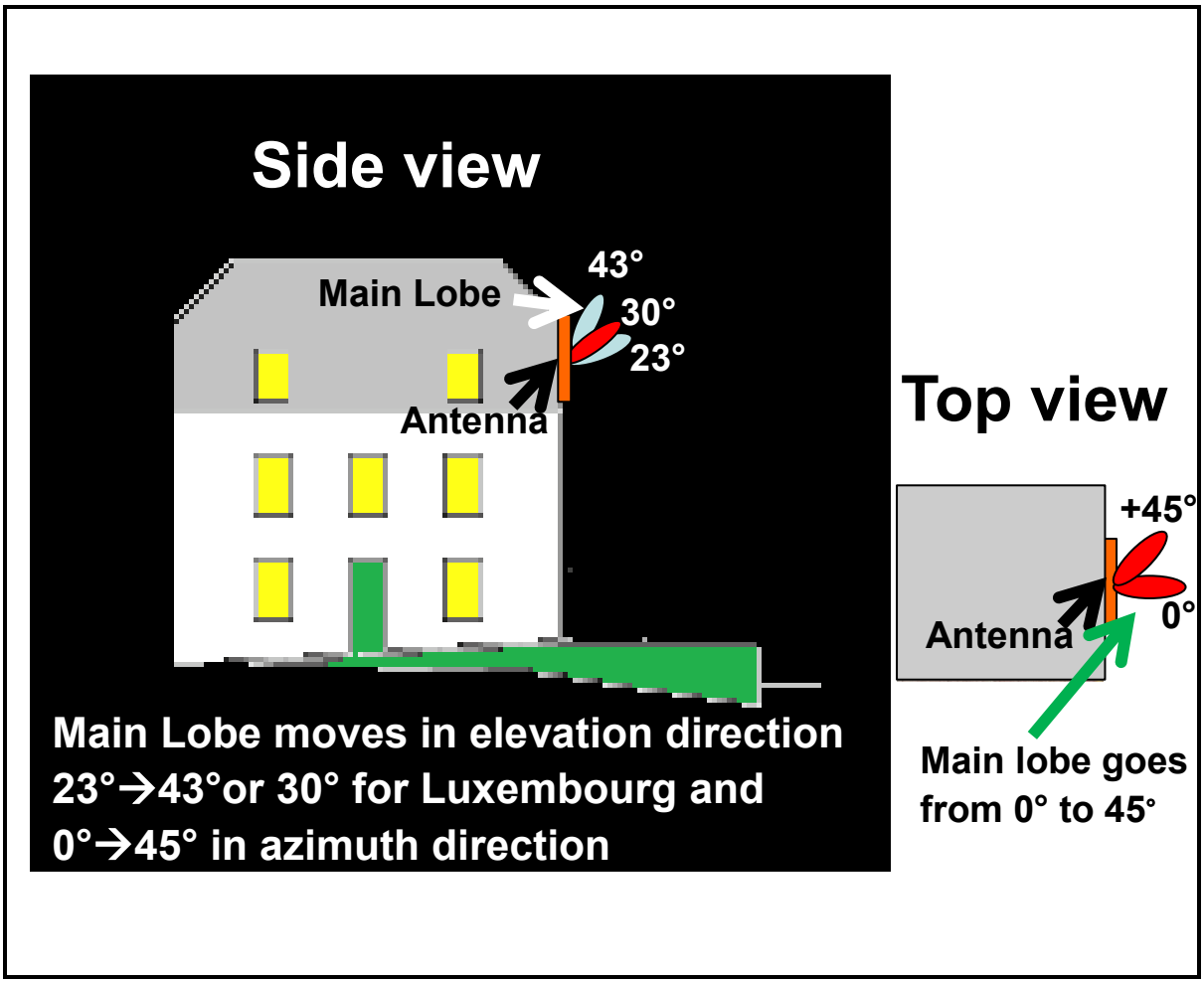

Figure 54 The main lobe movement in the azimuth and the elevation planes

12.2 Design of the Dielectric Phase Shifters

The dielectric phase shifters must be designed so that they can move the main lobe by an angle up to 45°. The phase shifter movement (in degrees) needed to shift the array by 45° is 127.27° as shown in Equation 29 [94] . This means to move the array by 45°, the phase shifter must allow a change of phase angle of 127.27°.

$$\text{Angle needed} = \frac{360^0}{\lambda} * \frac{\lambda}{2} * \sin 45^0 = 127.27^0 \quad \text{Eq. 29}$$

Next the lengths of phase shifters required for both a single ended and a dual feedline case are calculated. This will depend on the group delay of the transmission line. When the phase

delay is linear, the group delay is the same as the time delay which is just a different way of describing the phase delay of the transmission line. The phase delay is described in degrees or in radians, while the time delay is described in units of time.

12.3 The Group Delay

The dielectric phase shifters have been designed on the simplest transmission line: the single-ended transmission line which is just a strip of metal on top of a dielectric. Here the dielectric is Rogers RT5880 of ε_r 2.2, the same that is used all the time for the patch or butterfly or any antenna element in this thesis. The leftmost design in Figure 55 depicts the singe-ended transmission line without phase shifter while the rightmost design from the same Figure reveals the same design with the phase shifter on top. The phase shifters are, as always, built with Rogers RT6010 with ε_r 10.2. A zoomed-in with the dimensions of the singe-ended transmission line design is shown in the middle. Here, the width of the transmission line is set to $\lambda/2$ or to 1.28 cm. The length is set to 27.79 cm as explained further along this thesis. For the moment, the length value is irrelevant as the group delay is always calculated per unit length.

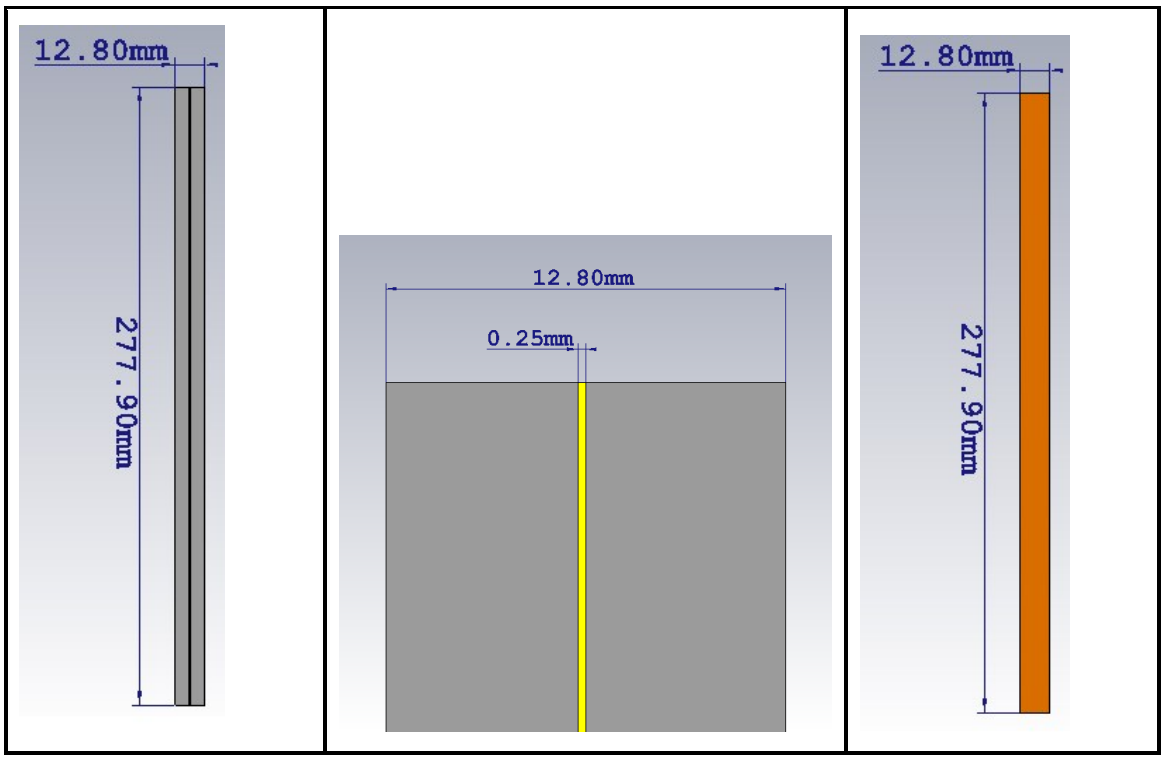

Single-ended transmission line	Zoomed-in of the single-ended transmission Line	Transmission line with dielectric phase shifters on top

Figure 55 The single-ended phase shifter

The group delay extracted for the single-ended transmission with and without the phase delay is shown in Figure 56. The graph is plotted to cover the frequency range from 10.7 to 12.7 GHz and at the center frequency of 11.7 GHz, the group delay for a total length of 27.79 cm is 1.2347 ns and it is 2.1086 ns in the presence of the phase shifter with ε_r 10.2 . This makes sense as when the phase shifter is present, since it has a higher dielectric constant, the signal moves slower and the group delay is larger because the effective permittivity is increased by the phase shifter. This can help to explain how a substrate with a high dielectric constant has a high group delay. The dielectric constant is the ratio of the permittivity of a substrate to the permittivity of free space. It defines how a substrate concentrates the electric flux and the higher is the electric flux, the higher is the dielectric constant and the higher is the group delay value.

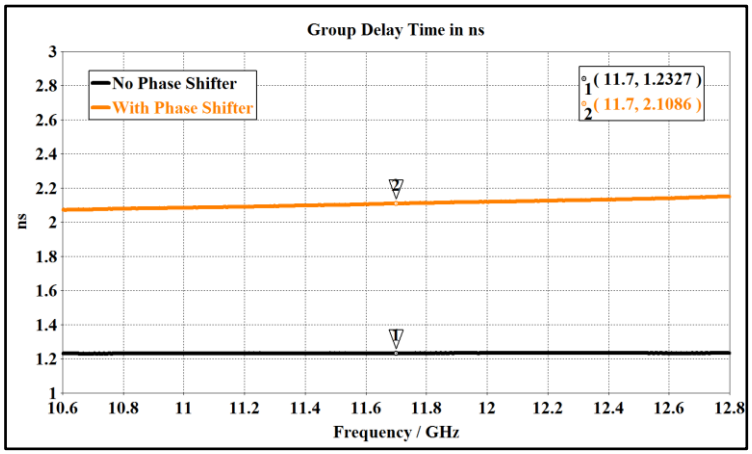

Figure 56 The group delay for the single-ended transmission line

The change of group delay (or the time delay in the studied case since the group delay is linear) with respect to the feedline length is given in Equation 30.

$$\frac{\Delta t}{\text{length}} = \frac{\text{Group Delay}_{\text{withPhase Shifter}} - \text{Group Delay}_{\text{without Phase Shifter}}}{\text{length of feedline}} \quad \text{Eq. 30}$$

The same procedure is repeated for the dual feedline in the slotted version. The slotted butterfly antenna feedline without the antenna element is designed and the group delay is evaluated just as for the simplest case of the singe ended transmission line. This is shown in Figure 57 where again the dielectric of the substrate is Rogers RT5880 of ε_r 2.2. The leftmost design in Figure 57 depicts the dual transmission without phase shifter while the rightmost design from the same figure reveals the same design with the phase shifter on top. The phase shifters are as always built with Rogers RT6010 with ε_r 10.2. A zoomed-in with the dimensions of the dual transmission line design is shown in the middle. As seen, the width of the transmission line is set to $\lambda/2$ or to 1.28 cm. The length is set to 27.79 cm, as explained further along this work. For the moment, the length value is irrelevant as the group delay is always calculated per unit length.

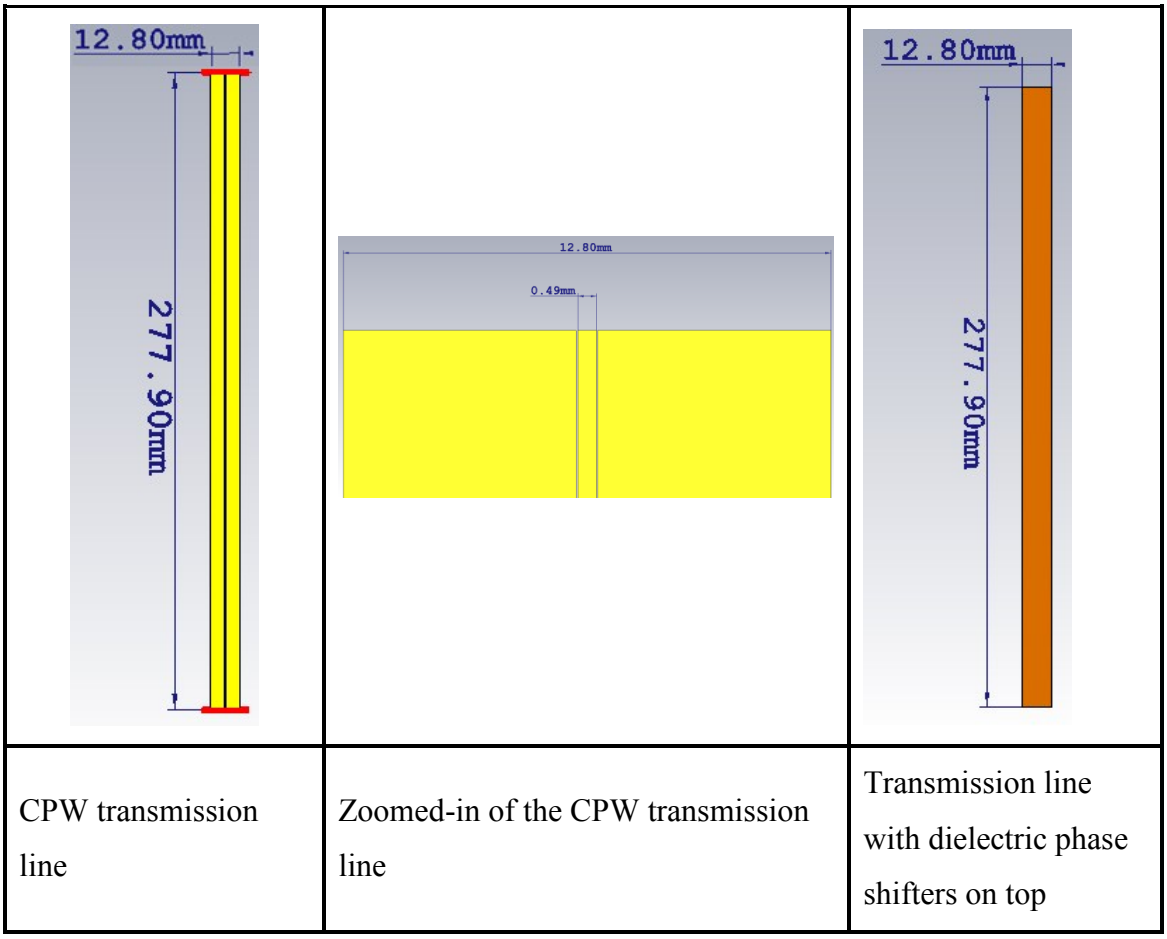

CPW transmission line	Zoomed-in of the CPW transmission line	Transmission line with dielectric phase shifters on top

Figure 57 The CPW phase shifter

The group delay extracted for the CPW transmission line, with and without the phase shifter, is shown in Figure 58. At the center frequency of 11.7 GHz, the group delay for a total length of 27.79 cm is 1.07 ns and it is 2.46 ns in the presence of the phase shifter with ε_r 10.2.

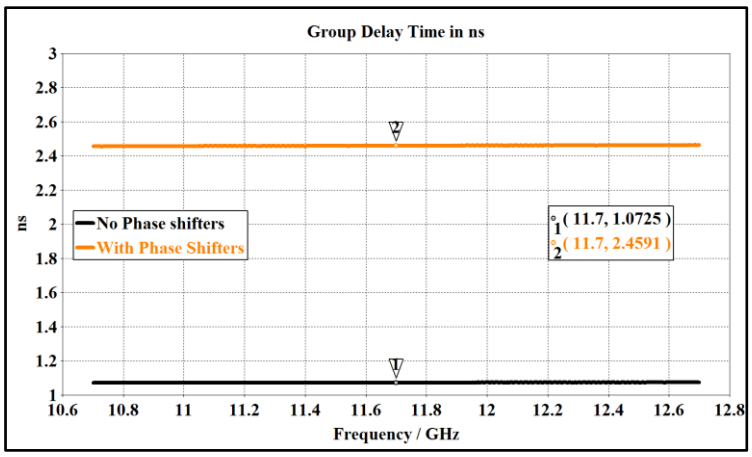

Figure 58 The group delay of the CPW transmission line

Already when the single-ended case is compared with the CPW case, one can see that the difference in the group delay is larger for the CPW line which means that a shorter phase shifter would be required for the CPW line as compared to the single-ended case such that less real estate would be required for the same phase shifter design when the CPW is used. This is very interesting, as while the length different is not as high for 1 phase shifter, when this is multiplied for the N^{th} antenna element, the required phase shifter length quickly accelerates to a much higher value So it makes sense to use a CPW in order to save real estate which means less feedline length is required for the design of the phase antenna array with dielectric phase shifters, so less materials are required, resulting in a smaller and cheaper design.

The group delay from Figure 58 for the CPW transmission line is calculated from Equation 30 and is given in Equation 31 as 5 ps per mm.

$$\text{Time delay} = 5\,\frac{\text{ps}}{\text{mm}} \quad \text{Eq. 31}$$

When the total phase shifter length is calculated for the N^{th} element, it can be seen from Equation 32 that 18.69 cm would be required for the 32^{nd} antenna element in the array.

$$\text{Angle for element 2} = \frac{\Delta t}{\text{length}} * 360^0 * 11.7 * 10^9 = 21.1^0 \text{ per mm}$$

If 21.1^0 is needed for 1 mm,

then for 127.27^0 , 6.03 mm is needed,

then for the 32nd element, 186.9 mm is needed Eq. 32

12.3 Dielectric Phase Shifters Measurement Boards

	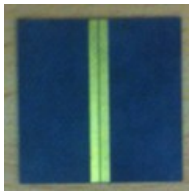	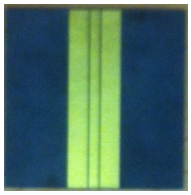	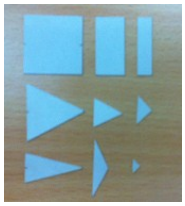
SE microstrip	S^+S^- coplanar lines	GSG microstrip line	Phase shifters

Figure 59 The built and measured boards with dimensions 2.5 cm by 2.5cm and phase shifters (*rightmost*)

The dielectric phase shifters have been built and measured using the Rohde Schwarz 40 GHz Vector Network Analyzer in the university laboratory with the help of Thomas Kopf, as shown in his Master Thesis [95]. Both triangular and rectangular phase shifters were built. Initially, triangular phase shifters would have been used in this project but the triangular phase shifters require very large number of mesh cells to mesh the ends of the sharp ends of the phase shifters and require a long computational time when using CST. Although the sharp ends of the triangular phase shifters were rounded off to counteract the high mesh requirements, the CST meshings were still very high. It became difficult and too lengthy to simulate large arrays, and thus the phase shifters were converted to rectangular structures.

12.4 The Scaled Slotted Butterfly Antenna Element.

The slotted butterfly antenna was scaled to reflect the specified size i.e. the length of 1.28 cm and a length of 27.79 cm. This is an optimized length using CST. The minimum length of the phase shifter needed to move the main lobe by 45° is 18.69 cm and the extra feedline length is useful to add antireflection coatings. From the signal integrity side, when a high dielectric substrate of ε_r 10.2 is placed on top of a dielectric substrate with a low dielectric constant of ε_r 2.2 , there is a large change in dielectric values form 2.2 to 10.2 and this invites a large mismatch for the propagation signal. Thus antireflection coatings will help to minimize this large discrepancy caused by the large change in dielectric constants. This is described in more details in Section 12.5.

First let's show in Figure 60 the scaled slotted butterfly antenna with the dimension of 1.28 cm by 27.79 cm along with the S_{11} results in Figure 61 and the 3D far-field radiation patterns with a gain of 6.22 dB shown at 11.7 GHz in Figure 62. The detailed far-field results are shown in Figure 63 and Figure 64 for the gain in the φ = 0° plane and the φ= 90° plane respectively. Figure 63 is a bit spottier because the slotted butterfly shape is very small and the resolution is very small for such a scaled slotted butterfly antenna of 1.28 cm.

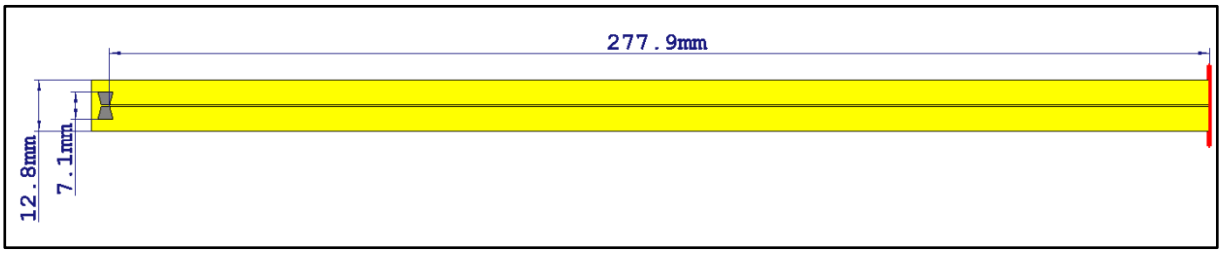

Figure 60 The resized and optimized slotted butterfly antenna element

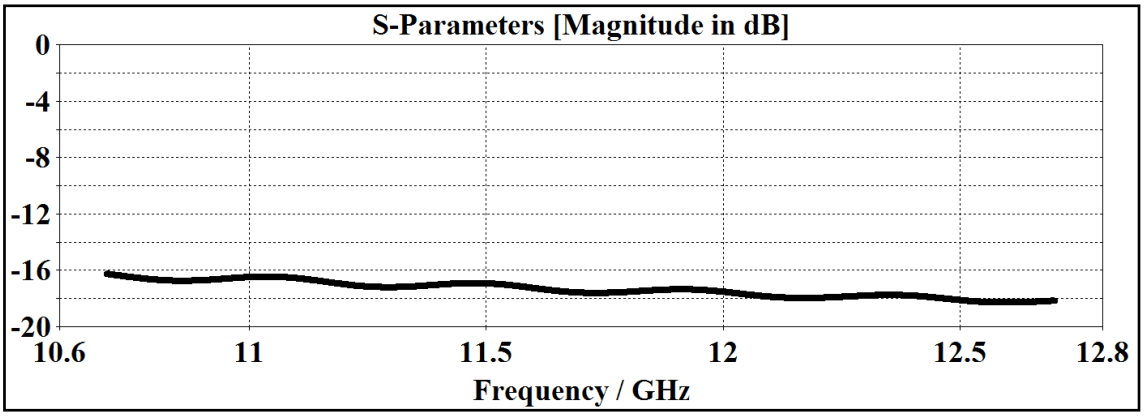

Figure 61 shows the S_{11} (dB) for the optimized slotted butterfly antenna element

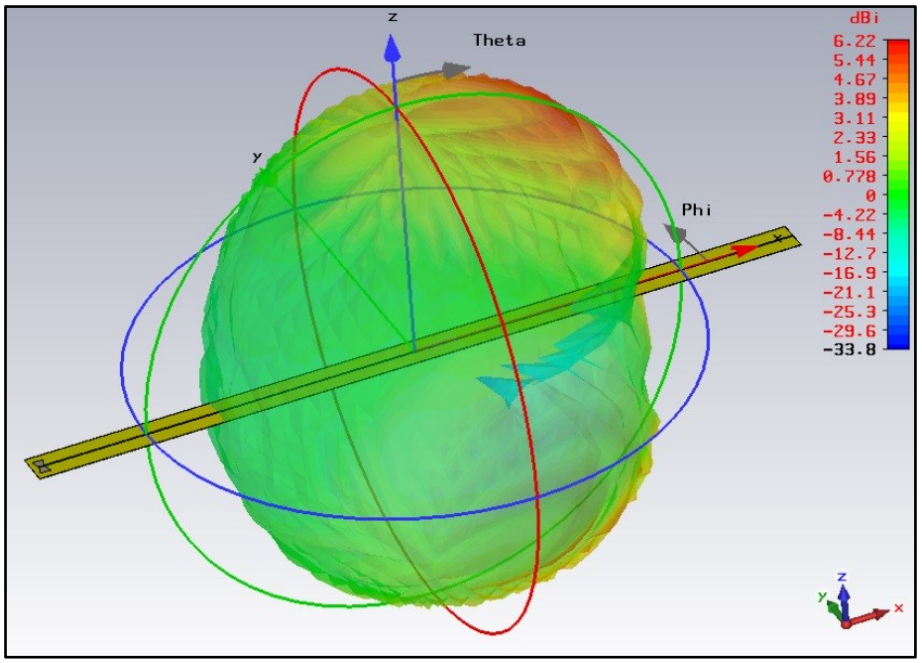

Figure 62 The 3D far-field patterns of the optimized slotted butterfly antenna element

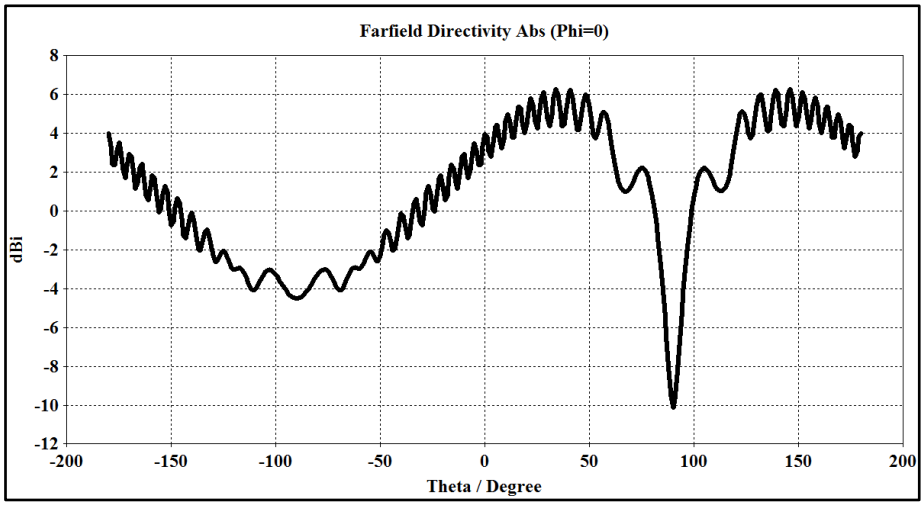

Figure 63 The directivity in the φ = 0° plane (azimuth) at 11.7 GHz

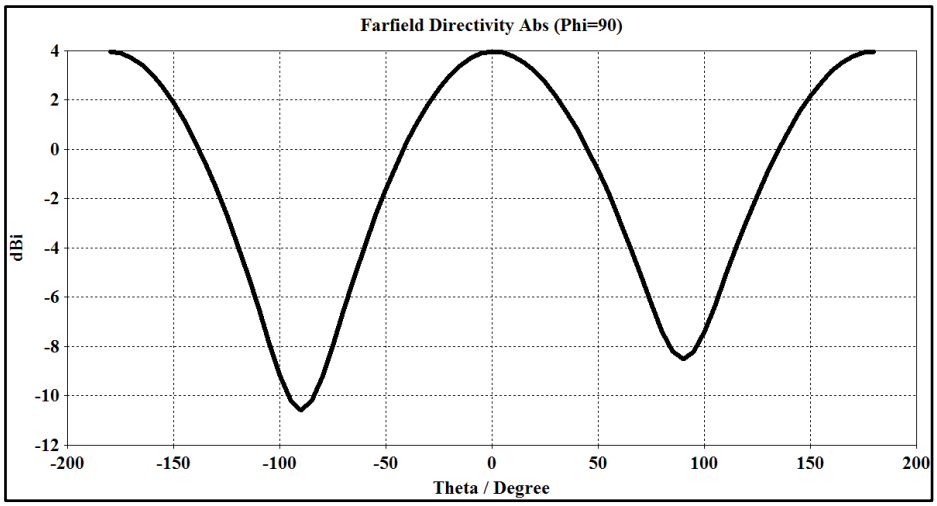

Figure 64 The directivity in the φ = 90° plane (elevation) at 11.7 GHz

12.5 The Antireflection Coating of the Phase Shifters

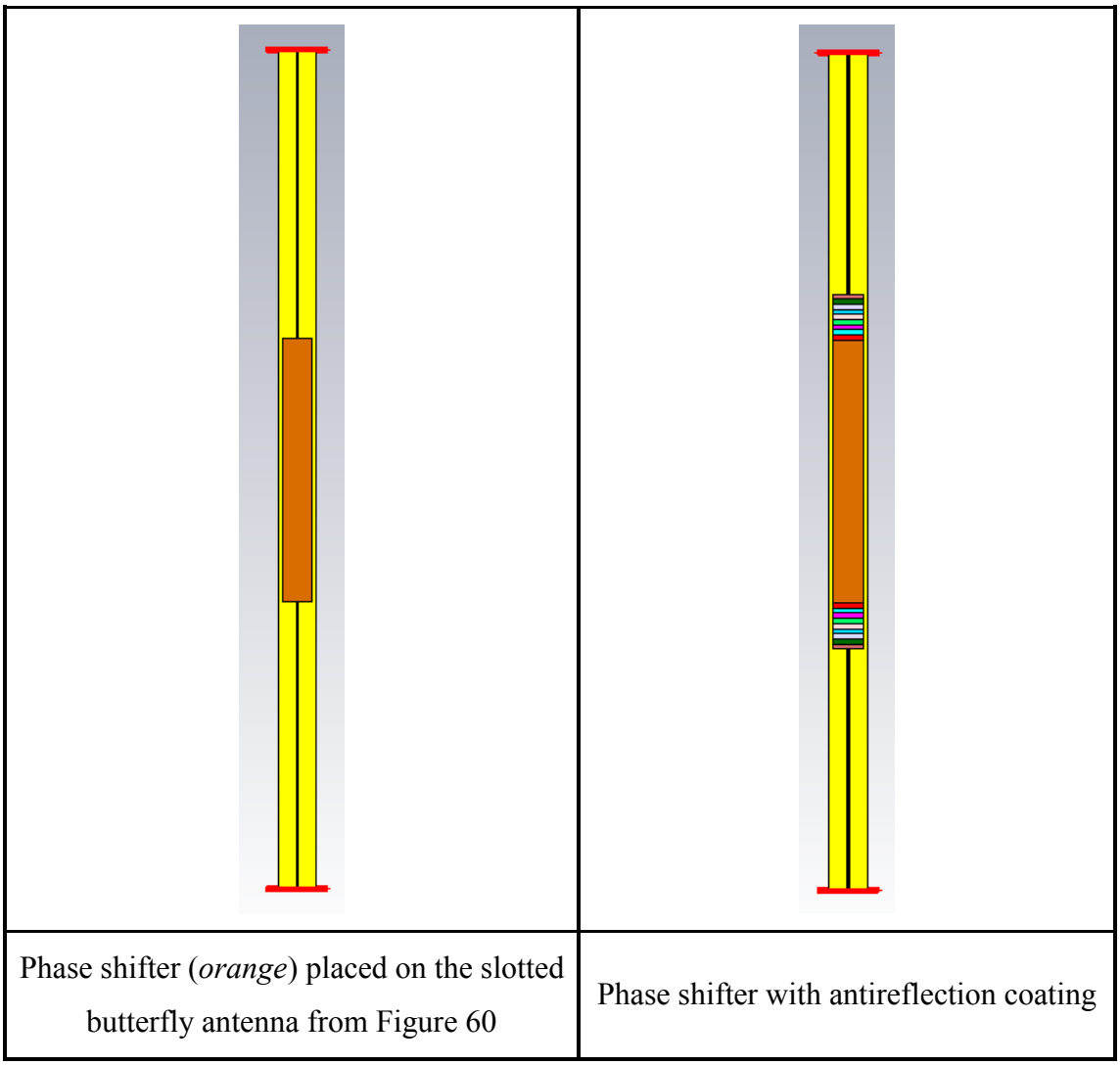

Phase shifter (*orange*) placed on the slotted butterfly antenna from Figure 60	Phase shifter with antireflection coating

Figure 65 The design of the antireflection coating on the CPW with phase shifter.

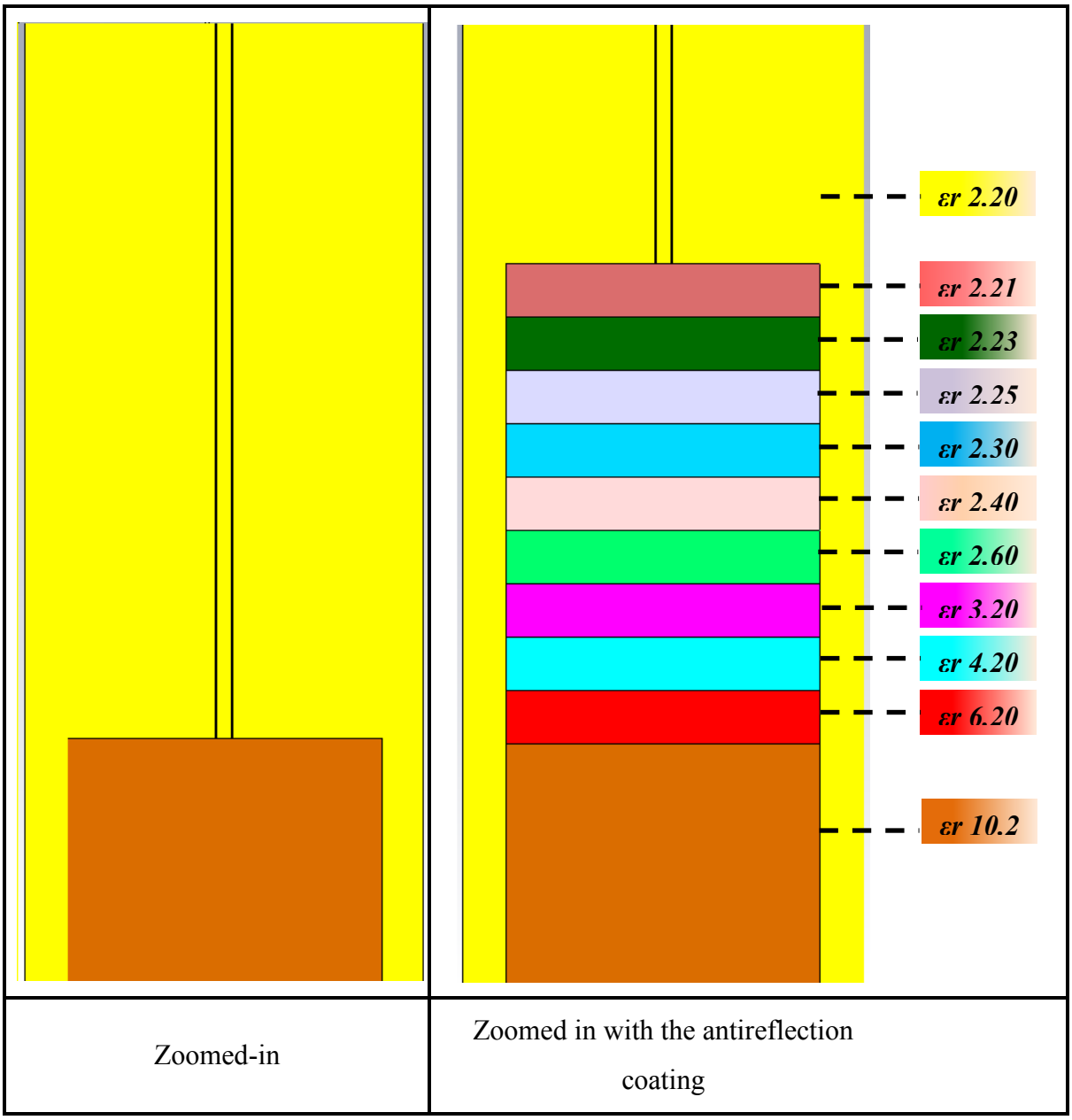

Figure 66 The zoom-in transmission line from Figure 65

Figure 65 shows the design of the antireflection coating with Figure 66 showing a zoomed-in. The antireflection coating is simply made with several substrates with the ε_r values each time averaged out between the high ε_r and the low ε_r in order to obtain an intermediate ε_r that will gradually minimized the S_{11}.

For example the substrate of the transmission line has an ε_r of 2.2 while that of the phase shifter is made with ε_r 10.2. Obviously this is a very sharp change in dielectric constant and this will results in a very large loss as shown in Figure 67 where the S_{11} is very lossy and it is more than -10 dB. With the help of many substrates, where each substrate is an average of the

intermediate dielectric values, the difference between each ε_r is gradually minimized such as ε_r 6.2, ε_r 4.2, ε_r 3.2 up to ε_r 2.21 are added and the simulation results with the addition of the antireflection coating can clearly be seen in Figure 67 where the S_{11} is less -10 dB.

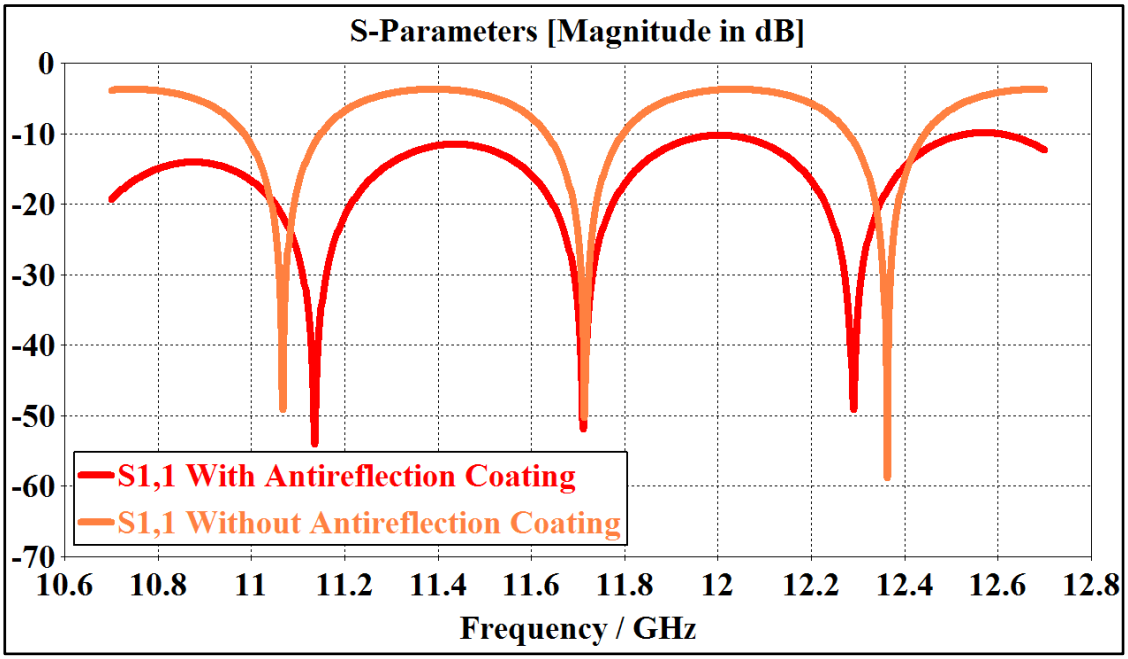

Figure 67 The S_{11} (dB) versus frequency/GHz, with and without the antireflection coating, for the transmission line that includes the phase shifter

The antenna element has successfully been designed with the desired width and length. The effect of the change in ε_r on S_{11} has been addressed by using antireflection coatings.

Now the array can be designed with the antenna elements and the S_{11} along with the change in direction of the main lobe can be examined with and without the presence of phase shifters in the next chapter.

13. PHASED ARRAY ANTENNA WITH DIELECTRIC PHASE SHIFTERS

13.1 The Phased Array Antenna with Dielectric Phase Shifters

The phased array antenna can now be designed with the antenna element from Figure 60 described in the previous chapter. First, for a beamwidth of 3°, 32 x 32 antenna elements are needed. Since the antenna has a width of 1.28 cm which corresponds to λ/2 and the maximum spacing between antenna elements is λ/2, the antenna elements are all positioned next to each other as shown in Figure 68. The dimension of the array of 32 x 1 elements is seen to be 40.96 cm by 28.25 cm.

When the feed network is added as shown in Figure 69, the length of the array of 32 x 1 elements is unchanged and it is still 40.96 cm and the width increases to 32.57 cm. A zoomed-in of the feed network connection from the end of the antenna element is shown in Figure 70. The CPW transition is shown along with the via transitioning to the bottom ground layer. This follows the via described in Figure 51 but here one is working with CPW where the signals are $S^-S^+S^-$ so two S^- from the top layer transition to the bottom layer via two vias, instead of just one but using the same idea from the unslotted version of the butterfly antenna element

from Figure 51. Figure 69 also shows the phase shifters element on top of the 31 of the 32 elements.

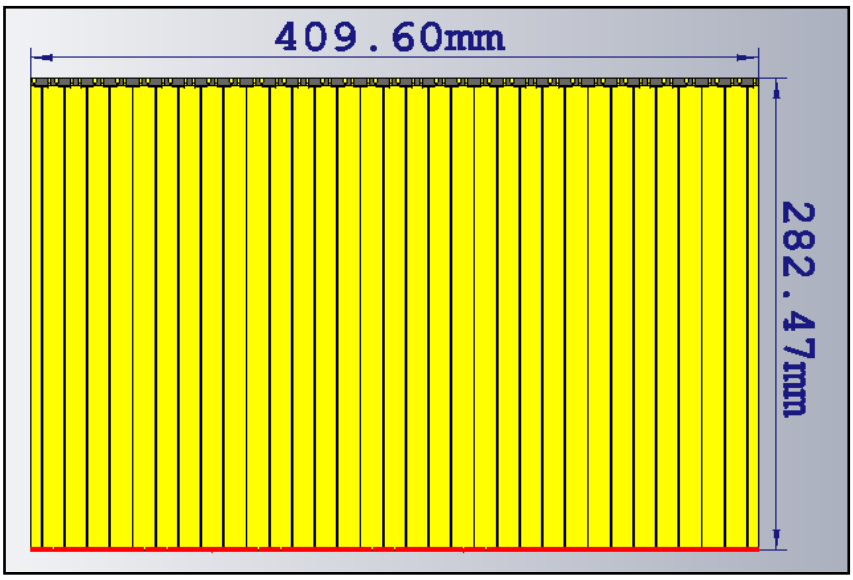

Figure 68 The 32 antenna elements added next to each other

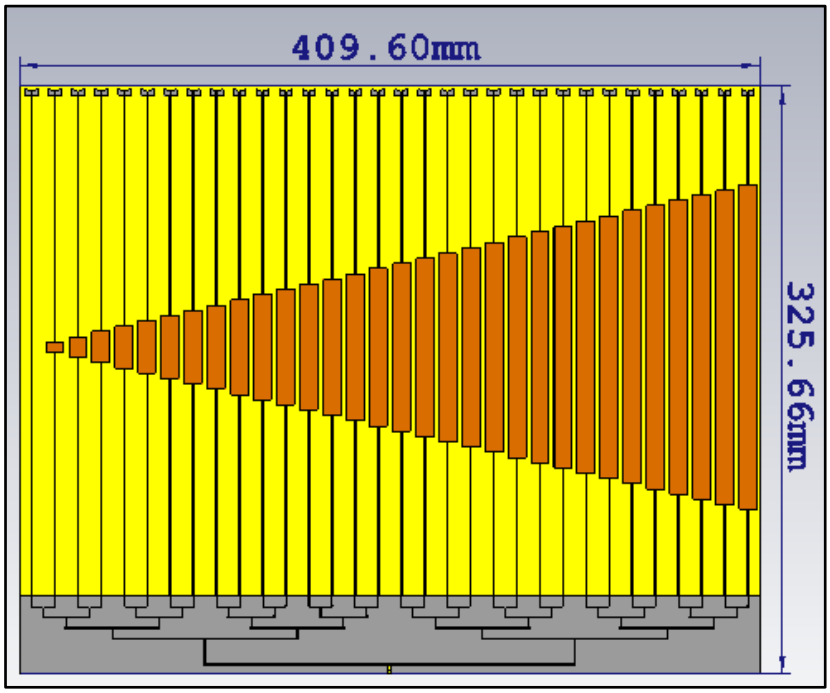

Figure 69 The 32 x 1 array with the feed network

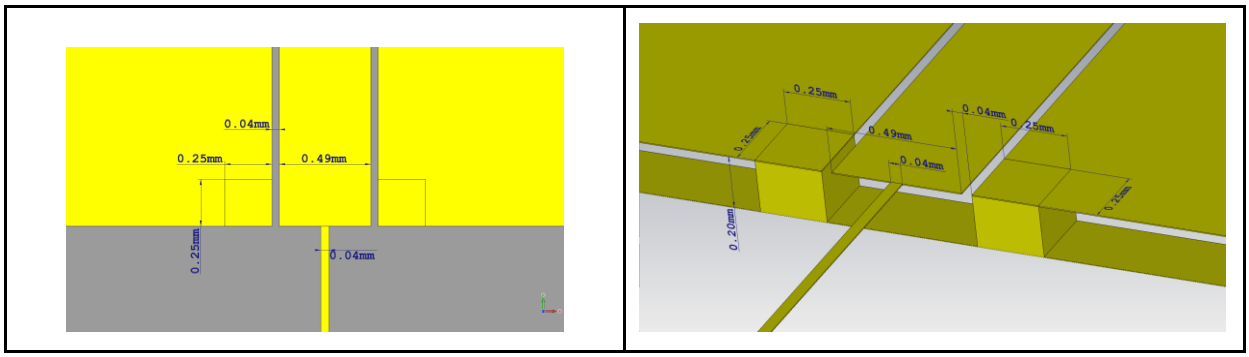

Figure 70 A zoomed-in of the feed network connection with the 2 vias transitions.

The 4 layers of the design from Figure 69 are shown in Figure 71 where layer 1 is the phase shifter layer. Layer 2 shows the 32 elements. The metal layer is yellow which the substrate layer is grey in colour. The butterfly structure is taken into advantage. In the slotted version of the butterfly antenna element, maximum metal layers are exposed, resulting in maximum radiation. Layer 3 represents the substrate layer 2.2 on Rogers RT5880 with ε_r 2.2. Layer 4 represents the ground layer. The two vias transit from the top two S- through the substrate to end on the ground layer.

The 4 Layers	
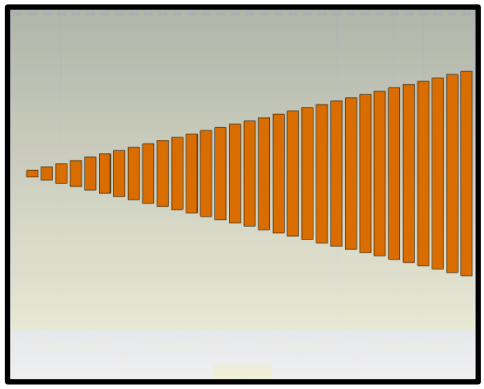	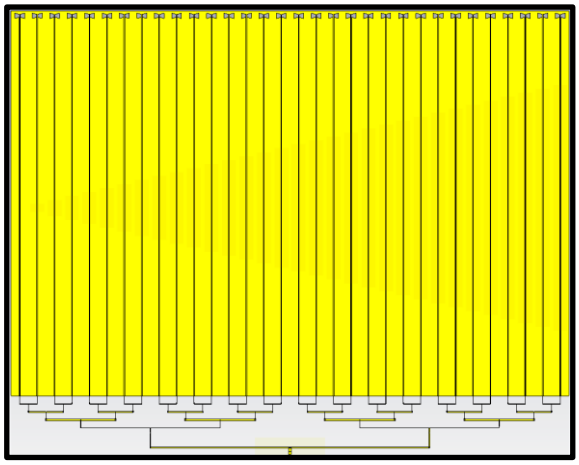
Layer 1	Layer 2

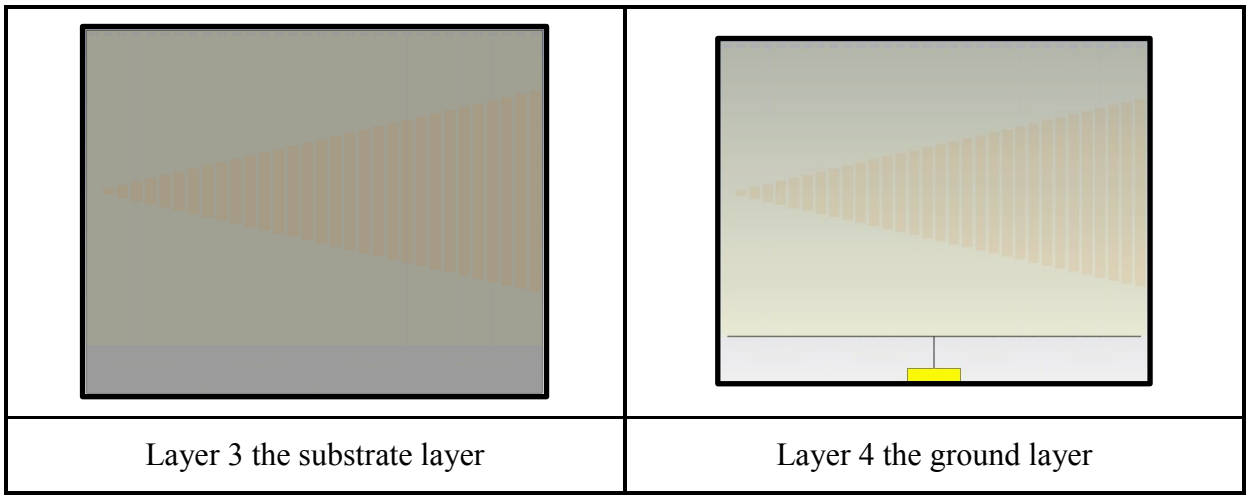

Layer 3 the substrate layer	Layer 4 the ground layer

Figure 71 The 4 layers of the 32 x 1 array with the feed network

The final S-parameters of the 32 x 1 elements with and without phase shifters are shown in Figure 72 and Figure 73 respectively.

They are highly optimized and meshed results, which required long computational time even with the use of the GPU. This is because a large array requires many mesh cells. The mesh cells information were more detailed in Chapter 11 but each array run time here required up to 50 million cells in the transient domain solver and required a computational time of at least 50 hours. Of course these arrays are optimized as much a possible so a long time is used in order to obtain the S-parameter results from Figure 72 and 73.

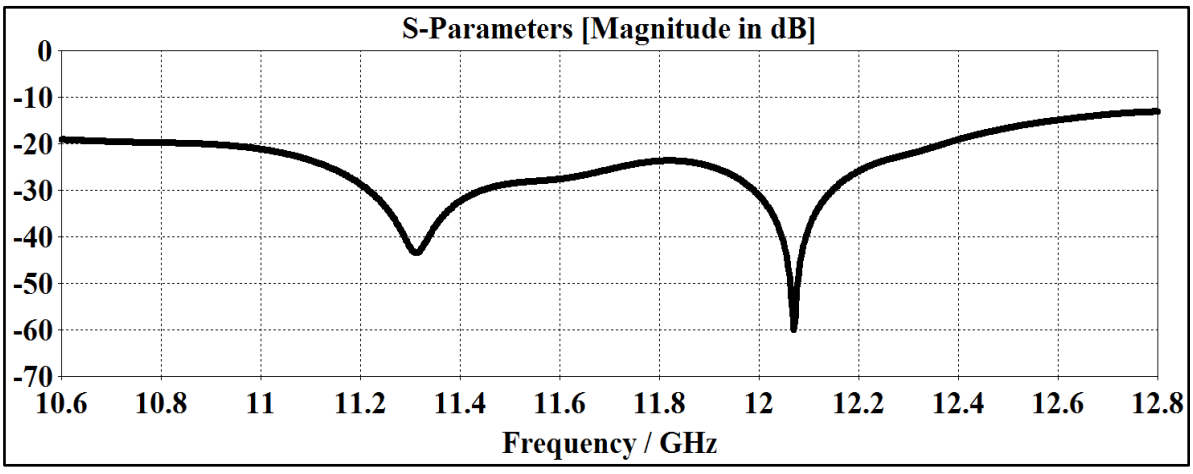

Figure 72 The S_{11} (dB) of 32 x 1 array without phase shifters

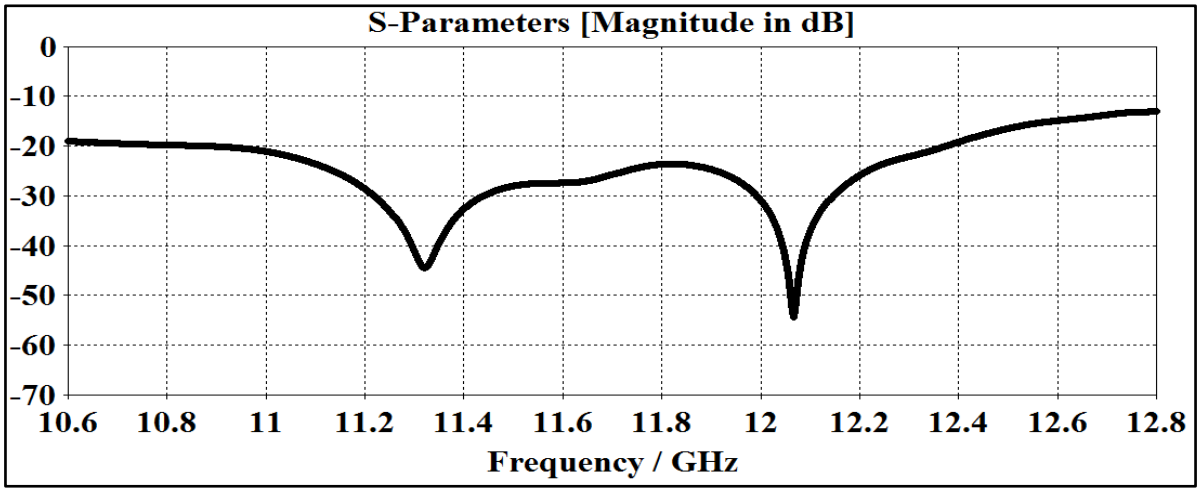

Figure 73 The S_{11} (dB) of 32 x 1 array with phase shifters

When Figure 72 and Figure 73 are compared, they have the same profile. This is normal as the phase shifters have more effects on the phase change to change the direction of the main lobe in the far-field but one can see form both plots that the bandwidth has been satisfied in both cases. The loss from the phase shifters are not seen here because one is not positioning the port right at the end of the phase shifter where a discontinuity is immediately seen. Instead, the port is placed at the end of the feed network so the loss effects of the phase shifters are not as noticeable even if they are present and antireflection coatings must be used. The ground is very carefully designed to only be underneath the end of the feed network, as shown in layer 4 from Figure 71, which considerably helped to keep the uniformity in the antenna elements and not to add loss.

In order to obtain a 32 x 32 array, the 32 x 1 array are stacked 32 times, λ/2 away from each other in the y direction as shown in Figure 74. To appreciate its profile along the z-direction, a zoomed-in of the 32 x 32 array is also shown in Figure 74. The distance between each stacked 1 x 32 elements is 2 mm resulting in a total size of 6.37 cm in the z-direction. This is quite a small distance between each 32 x 1 array. The ideal distance would be between λ/2 to 0.55λ as described in the literature [96]. In the literature, the FPS-85 is made with 72 x 72 elements and the arrays are spaced 0.55λ away. Two separate antennas arrays are made to phase shift in the horizontal and vertical plane separately. These must be investigated in future work as described in Chapter 14.

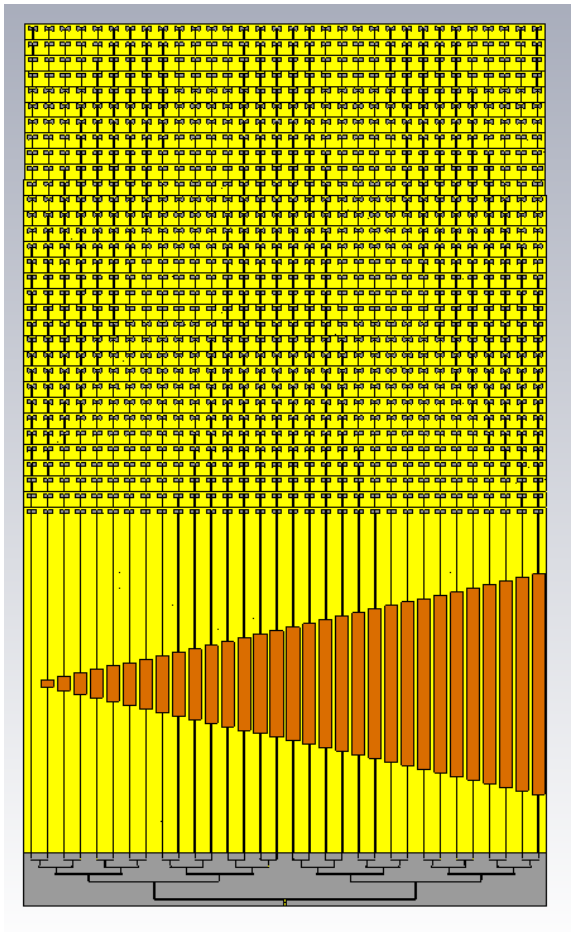

Front view of the 32 x 32 elements

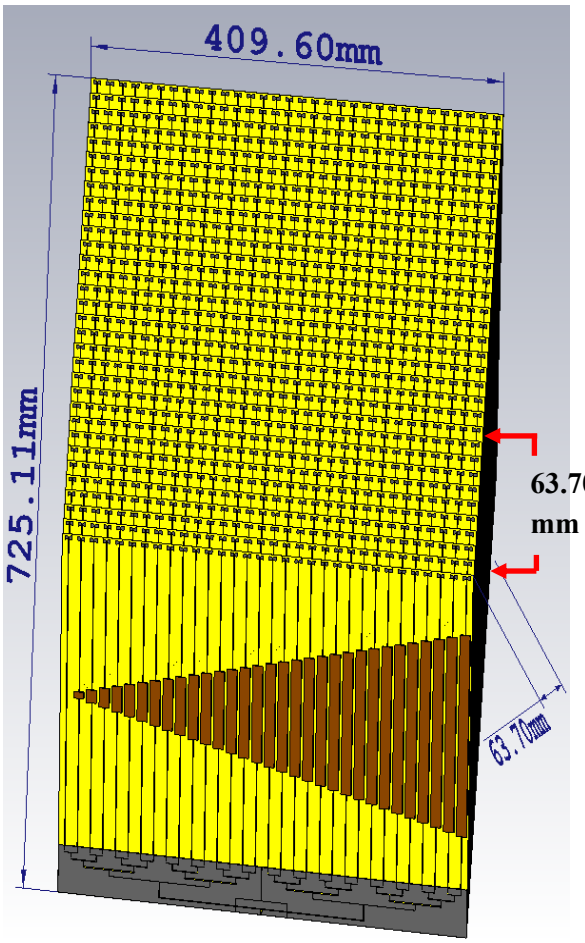

Slight side view of the 32 x 32 elements

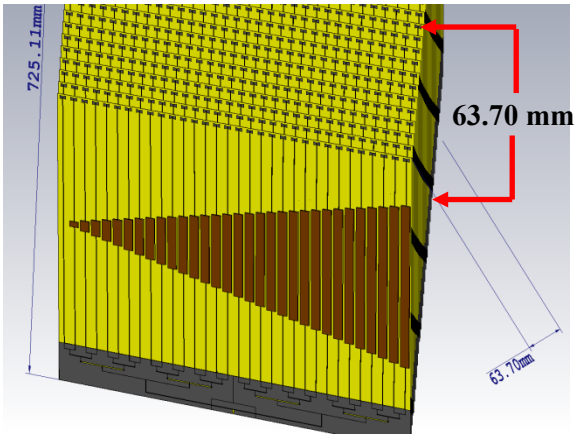

a zoomed in of the 32 x 32 elements with a thickness of 63.70 mm

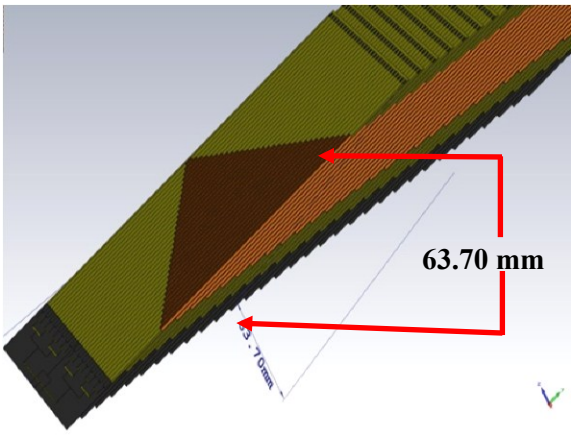

Zoomed-in to show the 32 x 32 array in the z-direction with thickness of 63.70 mm

Figure 74 The 32 x 1 array stacked 32 times on top of each other to form a 32 x 32 array

Now that the designs have been examined and the S-parameter plots of the arrays have been analyzed, one can move on to the far-field to examine how the main lobe changes direction with the addition of the phase shifters.

First, the far-field results of the 32 x 1 elements are examined. Here in the φ= 90° plane with no phase shifter present, the main lobe is at 0°, as shown by the peak at 0°, in the plot from Figure 75. The beamwidth is seen to be 3° while the directivity of the 32 x 1 array is 16.9 dBi.

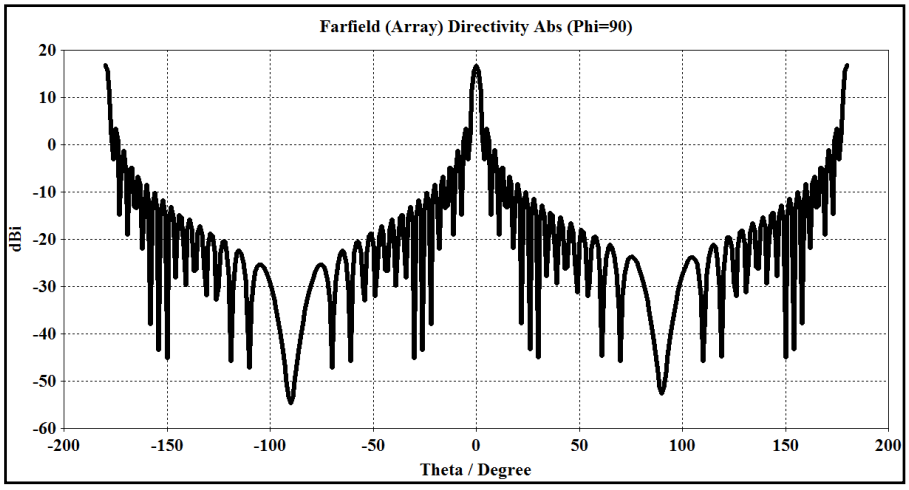

Figure 75 The far-field at 11.7 GHz in the φ= 90° plane without phase shifters

The phase shifters are added and the results are shown for the frequency of 11.7 GHz when

a) the main lobe direction is oriented to 45°
b) the main lobe direction is oriented to 22.5°
c) the main lobe direction is oriented to 11.25°
d) the main lobe direction is oriented to 5.625°

The results from Figure 76 shows that for a) the main lobe does go to 45°, while for b) the main lobe moves to 21°, while for c) the main lobe moves to 10° and for the last d) case the main lobe moves to 5°. This is certainly a very good result when the main lobe with a beamwidth of 3° moves within ±3° to the desired value.

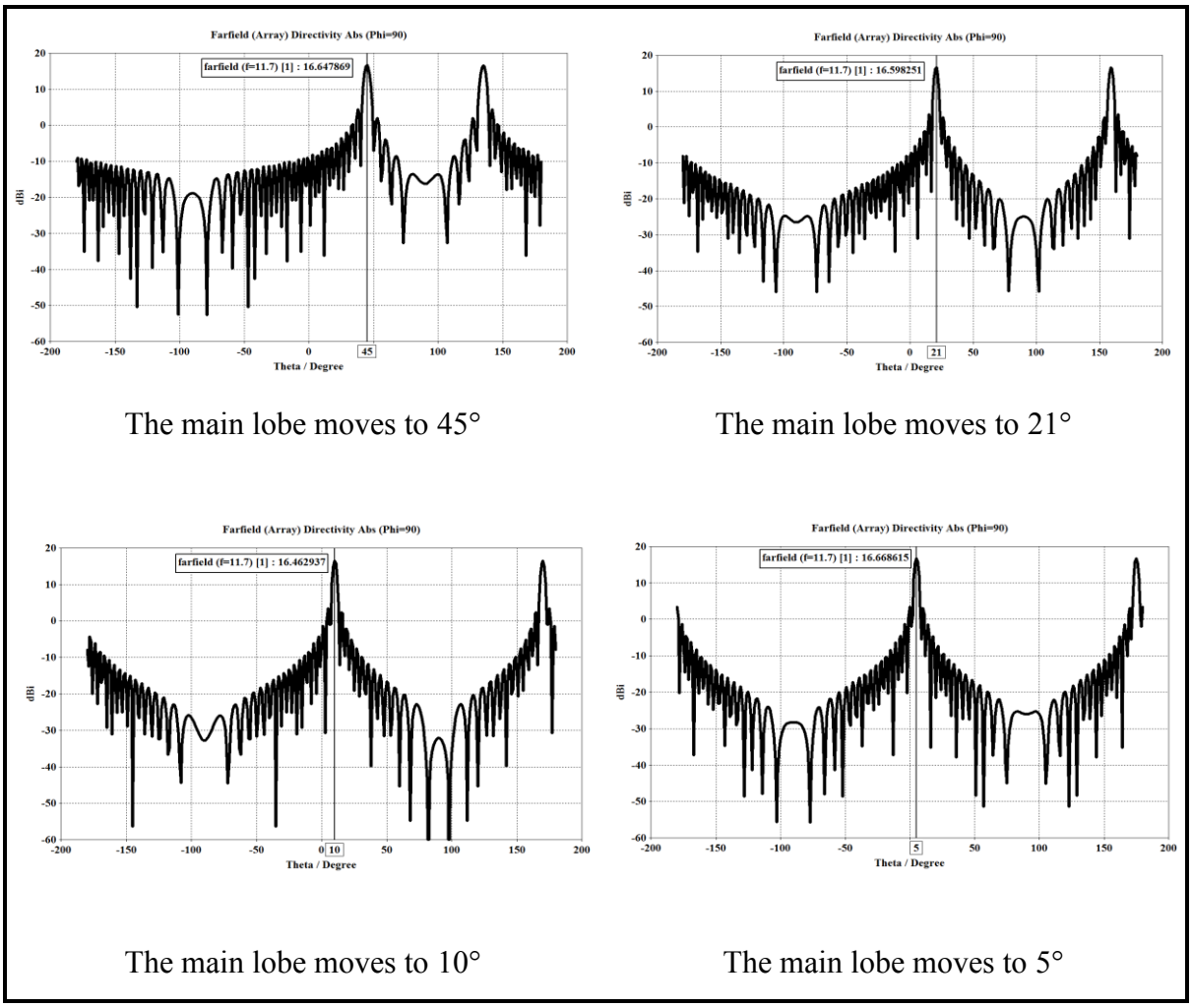

Figure 76 The far-field at 11.7 GHz of 32 x 1 array with phase shifters

The detailed results for the whole frequency range from 10.7 GHz to 12.7 GHz are plotted in Figure 77 to show how the main lobe changes direction as it is oriented to 45°, 22.5°, 11.25° and 5.625°. The plot shows a good result with the main lobe staying within 3° to the desired value so that a true main lobe direction change can be obtained. However for the 45° , the end cases shows a deviation certainly more than 3° and up to 10% showing that the end frequencies might not work properly for European countries situated with elevation angles close to 45° for such frequencies as 10.7 GHz to 11 GHz and from 12.5 GHz to 12.7 GHz.

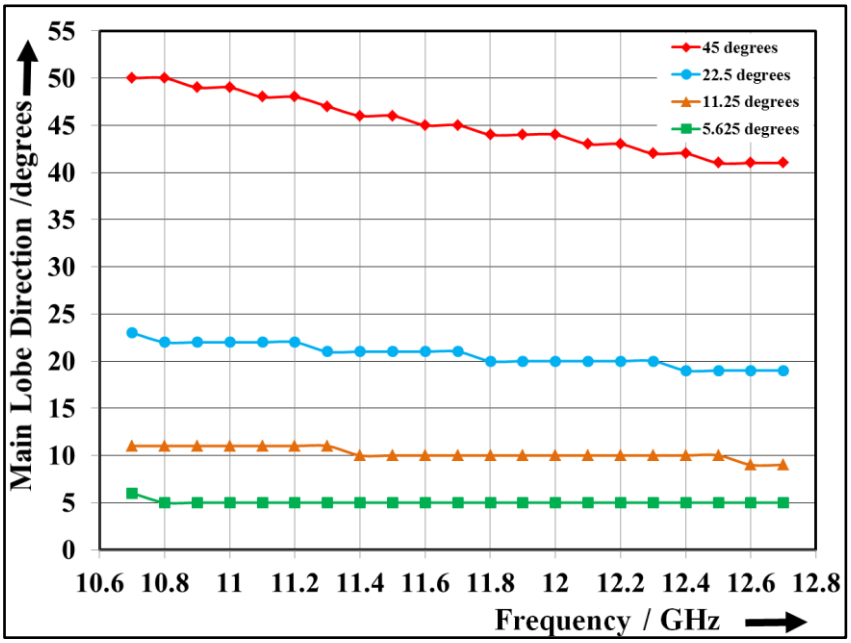

Figure 77 The 32 x 1 array plot in the φ= 90° plane with phase shifters

The analysis is repeated when the 32 x 32 antenna is made into an array as shown from Figure 78. Here, one first shows the plot in Figure 78 of the 32 x 32 antenna array with λ/2 spacing but without phase shifters. The leftmost plot shows the far-field plot in the φ= 0° plane while the rightmost plot shows the far-field in the φ= 90° plane. For the leftmost plot, at a frequency of 11.7 GHz, the beamwidth is 3.1° and the magnitude of the directivity is 33 dBi while for the rightmost plot the beamwidth is 3.2° with the magnitude of the directivity to be 33 dBi.

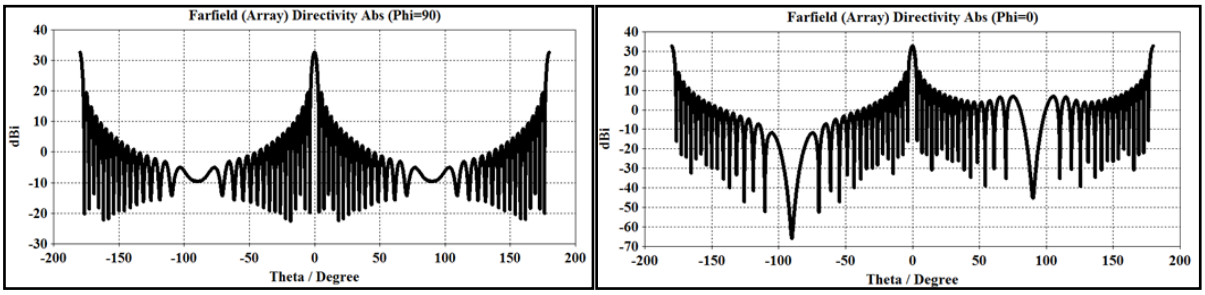

Figure 78 The 32 x 32 antenna array at 11.7 GHz without phase shifters

The phase shifters are added and the results are shown for the frequency of 11.7 GHz when

a) the main lobe direction is oriented to 45°

b) the main lobe direction is oriented to 22.5°

c) the main lobe direction is oriented to 11.25°

d) the main lobe direction is oriented to 5.625°

The results from Figure 79 shows that for a) the main lobe does go to 45°, while for b) the main lobe moves to 21° while for c) the main lobe moves to 10° and for the last d) case the main lobe moves to 5°. This is certainly a very good result when the main lobe with a beamwidth of 3° moves within ±3° to the desired value. One must note that the results are similar to that of the 32 x 1 array from Figure 76.

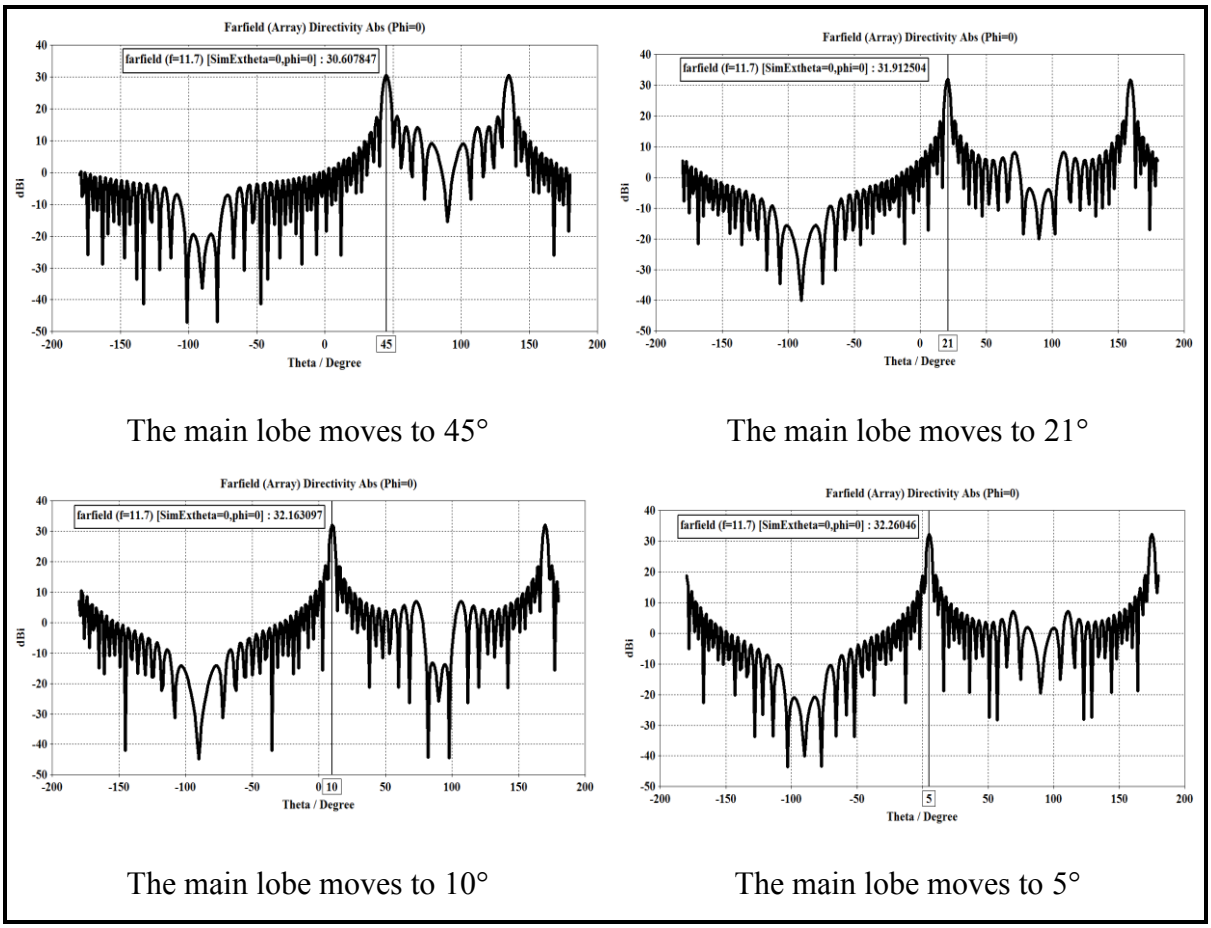

Figure 79 The far-field at 11.7 GHz of 32 x 32 array with phase shifters

The detailed results for the whole frequency range from 10.7 GHz to 12.7 GHz for the 32 x 32 array are plotted in Figure 80 to show how the main lobe changes direction as it is oriented to 45°, 22.5°, 11.25° and 5.625°. The plot from Figure 80 shows a good result with the main lobe staying within 3° to the desired value so that a true main lobe direction change can be

obtained. However, for the 45°, the end cases show a deviation certainly more than 3° and the errors are certainly more than 10% especially for 10.7 GHz at 45°. The errors here for that specific frequency of 10.7 GHz is more in the range of 13% showing that the end frequencies might not work properly for European countries situated with elevation angles close to 45°, especially for such frequencies from 10.7 GHz to 11 GHz and from 12.5 GHz to 12.7 GHz. For the other main lobe directions, the whole range of frequency will work fine with a deviation of not more than 3° for 22.5° or 11.25° or 5.625°.

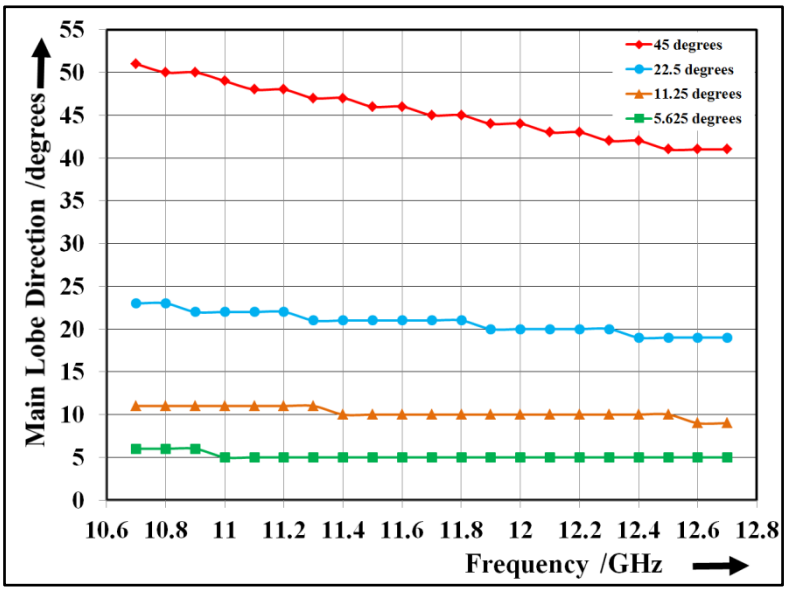

Figure 80 The 32 x 32 array plot in the φ= 0° plane with phase shifters

Table 5 shows the list of countries in Europe for which the phased array antenna with dielectric phase shifters is intended to be used. The table is plotted in descending order of the elevation angles and we can see that most countries apart from Malta and Cyprus are less than 45° [97]. The antenna will, of course, work for Malta and Cyprus. However with the errors seen at the extremities of the 45° plot From Figure 80, the end frequencies might not work properly as a deviation up to 10% can be seen from 10.6 GHz to 10.9 GHz and from 12.5 GHz to 12.7 GHz.

European Countries	Elevation Angle°
Malta	48°
Cyprus	46.5°
Greece	44.6°
Albania	42.4°
Macedonia	41.9°
Turkey	41.9°
Italy	41.1°
Vatican City (Holy See)	41.1°
Kosovo	40.8°
Montenegro	40.7°
Bulgaria	40.3°
Serbia	39.2°
San Marino	38.9°
Bosnia and Herzegovina	38.7°
Monaco	38.2°
Croatia	37.9°
Andorra	37.7°
Spain	37.6°
Romania	36.9°
Armenia	36.5°
Portugal	36.3°
Hungary	35.7°
Georgia	35.3°
Austria	35.2°
Azerbaijan	35.2°
Switzerland	35.1°
Liechtenstein	34.9°
Moldova	34.8°
France	34.3°
Slovakia	34.1°
Ukraine	33.2°
Czech Republic	32.8°
Luxembourg	31.5°
Germany	30.8°

Poland	30.6°
Belgium	30.5°
Netherlands	29.0°
Belarus	28.1°
Lithuania	26.9°
Denmark	25.8°
Latvia	25.1°
Ireland	24°
United Kingdom	23.7°
Estonia	23.2°
Sweden	21.8°
Norway	20.8°
Finland	19.7°
Kazakhstan	18.5°
Iceland	10.9°

Table 5 The European countries along with their Elevation Angle [97]

13.2 Chapter Conclusion

This chapter can be concluded by saying that the phased array antenna has been successfully designed to work from one antenna element built up into an array configuration. It is able to show that the main lobe has a beamwidth of 3°. When the dielectric phase shifters are placed on top of the antenna element feedline, the main lobe is seen to successfully move up to 45° in the azimuth or the horizontal plane. As done by [96], it can be rotated by 90° to cover the phase shift in the elevation or the vertical plane. The bandwidth, beamwidth and beam gain have been satisfied. So we can conclude that the desired results of the thesis have successfully been accomplished.

14. FUTURE WORK

For future work, the phased array antenna with dielectric phase shifters can be manufactured and tested in order to verify its theoretical and simulation results. This has not been achieved in this thesis. The individual phase shifters have already been built along with the single ended, coplanar and CPW transmission lines and have showed excellent results.

The phase shifters work perfectly in a 1x 32 elements array and these have been stacked 32 times to achieve a 32 x 32 antenna array. The research work can be deepened by designing phase shifters between each 32 x 1 array.

Furthermore, the antireflection coatings can be investigated in order to minimize the effective permittivity that exists when a substrate of low ε_r is used along with a phase shifter of high ε_r value.

In this thesis, Rogers have been used as dielectric substrates. Other dielectric constants with higher ε_r can be investigated to see if the use of larger ε_r causes an even higher change of phase velocity requiring less real estate to change the direction of the main lobe by up to 45°. This can surely result in an array with antenna elements having more compact feedlines.

15. CONCLUSION

A phased array antenna with dielectric phase shifters has been designed and demonstrated in this PhD thesis. A slotted version of the butterfly antenna element was chosen to build the array. It has numerous benefits and perfectly fits the description of the required antenna element to work in an antenna array with dielectric phase shifters.

The array with slotted butterfly antenna elements has the first advantage of allowing the most metal with maximum exposed radiation while benefiting from the second advantage of having a large bandwidth due to its slotted butterfly antenna shape. It has the third advantage of using CPW feedline, ideal to minimize mutual coupling among antenna elements in an array configuration. Furthermore, the CPW feedline, with and without phase shifters, has a larger group delay difference as compared to the single-ended transmission line case such that less real estate is needed for the design of the phased array antenna using dielectric phase shifters, resulting in a smaller and cheaper design. The fifth advantage of such a slotted antenna element with CPW feedline, is that, as it comes from a frequency independent butterfly antenna element, it has been easily resized to satisfy the maximum antenna element spacing of $\lambda/2$ in order to avoid grating lobes in the far-field. It has thus the further plus of being able to work for any frequency range in case the phased array antenna with dielectric phase shifters would be used with a different bandwidth or frequency range.

The phased array has been built with the phase shifters, made with Rogers RT6010 of ε_r 10.2, placed on top of the CPW feedline of an antenna element, built on Rogers RT5880 of ε_r 2.2, in order to take advantage of the large change of dielectric constant causing a large shift in the

phase velocty of the signal as it transitions from ε_r 2.2 to ε_r 10.2. This phase change enables the main lobe to move up to 45°. An array of 32 x 32 elements was built in order to satisfy the 3° beamwidth and a gain of 30 dBi requirements across the whole bandwidth from 10.7 GHz to 12.7 GHz.

It is a very exciting time ahead for 'A Phased Array Antenna with dielectric Phase Shifters' as this work has proved to be very positive and has opened the doors to further analysis towards a potential candidate for the replacement of the parabolic antenna. One can surely predict that, in not such a distance future, the parabolic antenna would be an antiquity, and we or our kids would be watching satellite TV using a phased array antenna with dielectric phase shifters.

16. BIBLIOGRAPHY

[1] A. Ludwig, “The definition of cross polarization, “Antennas and Propagation, IEEE Transactions, Vol. 21, 1997

[2] R. Garg, P. Bhartia I. Bahl and A. Ittipiboon, “Microstrip Antenna Design Handbook,” Artech House, 1991

[3] K.P.Kumar, K.S.Rao, V.M.Rao, K. Uma, A Somasekhar and C.M. Mohan, “The effect of dielectric permittivity on radiation characteristics of co-axially feed rectangular patch antenna: Design& Analysis,” IJARCCE, Vol.2 Issue2, Fe, 2013, pp. 1254-1258

[4] http://www.rogerscorp.com/acs/products/32/RT-duroid-5880-Laminates.aspx

[5] http://www.rogerscorp.com/acs/products/36/rt-duroid-6006-6010-Laminates.aspx

[6] H.Singh, H. L. Sneha, and R. M. Jha, “Mutual Coupling in Phased Arrays: A Review,” International Journal of Antennas and Propagation, vol. 2013, 2013.

[7] http://nl.mathworks.com/help/antenna/ug/mutual-coupling.html

[8] Grating Lobes, www. Antenna-theory.com

[9] S. Orfanidis, “Electromagnetic Waves and Antennas”, Rutgers University, 1999

[10] I. Stewart, In Pursuit of the unknown, 17 Equations that changed the world, First Trade Publishing, 2013.

[11] "Einstein the greatest". BBC News (BBC). 29 November 1999. Retrieved 2 April 2010

[12] Maxwell, James Clerk, “A Treatise on electricity and Magnetism, “Clarendon Press Series, Macmillan & co. 1873,

[13] Lodge, Oliver; "On the Theory of Lightning Conductors" The London, Edinburgh, and Dublin Philosophical Magazine, Series 5, vol. 26, August, 1888, pp.217-230.

[14] Lodge, Oliver, "On the work of Hertz and his successors," the Electrician, fourth edition, London 1894

[15] Lodge, (1898), "Improvements in Syntonized Telegraphy without Line Wires, "British Patent Office, No. 609154, August 1898

[16] Dolbear, "Mode of electrical communication, "US patent No. 350 299, 1886

[17] M.Kulling and R.Rudnicki, "Making Contact!: Marconi Goes Wireless, "Tundra Books, September, 2013

[18] Braun , Ferdinand " Improvements relating to the transmission of electric telegraph signals without connecting wires, US750429A, 1899

[19] Sungook Hong, "From Marconi's Black-Box to the Audion (Transformations: Studies in the History of Science and Technology) Publisher: The MIT Press (January 22, 2010).

[20] Stutzmann W,-L, Thiele G.A., "Antenna Theory and Design," 2nd ed., Wiley, New York, 1997.

[21] G.H. Brown and O.M. Woodward, "Experimentally determined radiation characteristics of conical and triangular antennas", RCA Rev., December 1952, pp. 425-452

[22] J.M Laheurte, "Compact Antennas for Wireless Communications and Terminals: Theory and Design," John Wiley & Sons, 2011

[23] X. Ding and A.F. Jacob, "Novel broadband slot antenna with low cross-polarization," Annual Report, Institut für Hochfrequentztechnik, TU Braunschweig, 1995

[24] http://www.ieee.org

[25] G. Deschamps and W. Sichak, "Microstrip Microwave Antennas," Proceedings of Third Symposium on USAF Antenna Research and Development Program, October 18–22, 1953

[26] R. E. Munson, “Single slot cavity antennas assembly”, U.S. patent No. 3713 162, January 23, 1973.

[27] D. R. Jackson and N. G. Alexopoulos, Simple approximate formulas for input resistance, bandwidth, and efficiency of a resonant rectangular patch, IEEE Trans. Antennas Propagat., Vol. 39, No. 3, 1991, pp. 407–410.

[28] http://www.cst.com

[29] http://www.antennamagus.com

[30] K. R. Carver and J. W. Mink, “Microstrip antenna technology,” IEEE Trans. Antennas Propagat., vol. AP-29, pp. 2-24, Jan. 1981

[31] V.P. Patil, “Enhancement of Bandwidth of Rectangular Patch Antenna using two square slots Techniques”, International journal of Engineering, & Emerging Technology, Oct.2012.

[32] M.A. Matin and A. I. Sayeed, “A Design Rule for Inset-fed Rectangular Microstrip Patch Antenna,” WSEAS Trans. on Communications, Jan 2010, pp63-72

[33] H. Legay and L. Shafai, “New Stacked Microstrip Antenna with Large Bandwidth and High Gain,” IEE Proc. Microwave, Antennas Propagat, Pt. H, vol. 141, no. 3 (June 1994), pp. 199–204.

[34] R. C. Compton and R. C. McPhedran, Z. Popovic, G. M. Rebeiz, P. P. Tong, D. B. Rutledge, "Bow-tie antennas on a dielectric half-space: theory and experiment," IEEE Transactions on Antennas Propagat, vol. 35, pp. 622–631, June 1987

[35] J.Dong, A.Wang, P.Wang and Y.Hou, “A novel stacked wideband microstrip patch antenna with U-shaped parasitic elements,” Antennas, Propagation and EM Theory, 2008, pp185 - 188

[36] J.R. James and P.S. Hall, “Handbook of Microstrip Antennas” (IEE Electromagnetic Waves Series- 28), 1989

[37] E.A. Soliman, S. Brebels, P. Delmotte, G.A.E Vandenbosch and E. Beyne, “Bow-tie slot antenna fed by CPW,” Electronics Letters, Vol. 35, 1999, pp. 514- 515

[38] E. Nishiyama and M. Aikawa, “Wide-band and high-gain microstrip antenna with thick

parasitic patch substrate, “Antennas and Propagation Society International Symposium, 2004, pp 273- 276

[39] A.A. Roy, J.M.Mom and G.A. Igwue, “Enhancing the bandwidth of a microstrip patch antenna using slots shaped patch, “American Journal of Engineering Research, 2013, pp. 23-30.

[40] J.S. Row and Y.Y Liou, “Broadband short-circuit triangular patch antenna, “IEEE Trans. On Antennas Propagat, Vol.54, July 2006, pp.2137-2141

[41] **A.Moonshiram** and M.Marso, “High gain patch antenna for broadband applications from 10.1 to 14.2 GHz,” International Journal on Networking and Communication, vol.4, October 2015

[42] **A.Moonshiram** and M.Marso, “High Gain Patch Antenna for Broadband Applications from 10.1 to 14.2 GHz,” International Conference on Communication Information Technology and Robotics, August 2015

[43] V. Palanisamy and R .Garg,”Rectangular ring and H-shaped microstrip antennas - alternatives to rectangular patch antenna,” Electronic letters, 1985, pp. 874-876

[44] Thakur K, Kaushik, “ Compact design of H-shape fractal microstrip patch antenna using different DSG for wireless Applications, “ International Journal of Innovative Research in Science, Engineering and Technology, Oct 2014, pp. 17042-17051

[45] R.S. Kushwaha, D.K. Srivastava and J.P. Saint, “ A design of H-shaped slot loaded wideband microstrip patch antenna, “ International Journal of Electronics and Computer Science Engineering, 2013, pp. 533-537

[46] M.T. Islam, M.N. Shakib and N. Misran, “Broadband E-H shaped microstrip patch antenna for wireless systems, “ Progress in Electromagnetics Research, PIER 98, 2009 pp. 163-173

[47] B. Kumara Swamy, S. Anil Kumar, P.D. Vasanth Kumar, N. Yesu Mariyamma and K. Jagadeesh Babu, “A concave H-shaped patch antenna with improved bandwidth and isolation for MiMo systems, “International Journal of Energy, Information and Communications, “014, pp 27-34

[48] V. Tarange, T. Gite, P. Musale, V. Sanjay, Khobragade and V.R Anita, " A Broadband design of H-shaped microstrip antenna with capacitive feeding, "Emerging Trends in Networks and Computer Communications, 2011 pp 182-184

[49] S.S. Zhong, G. Liu and G. Qasim, "Closed Form Expression for Resonant Frequency of Rectangular Patch Antennas with multidielectric layers, " IEEE Trans. Antennas and Propagat., Vol. AP-42, 1994, pp 1360-1363

[50] N.Alexopoulos and D.Jackson, "Fundamental superstrate (cover) effects on printed circuit antennas, "IEEE Trans Antennas and Propagat, Aug 1984, pp. 807-816

[51] J.R. James, P.S. Hall and C.Wood, Microstrip Antenna: Theory and Design, Peter Peregrinus, London UK, 1981

[52] http://personal.ee.surrey.ac.uk/Personal/D.Jefferies/jefferies-stub.html

[53] R. Janaswamy and D.H.Shaubert, "Characteristics impedance of a wide slotline on low permittivity substrate, "IEEE Trans, MTTs, Vol. MTT.34, 1986, pp900-902

[54] C.Y.Huang, J.Y.Wu, C.F. Yang and K.L.Wong, "Gain-enhanced compact broadband microstrip antenna, "Electronic letters, IET, 1998, pp.138-139.

[55] J.M. Laheurte, L.P. B. Katehi and G.M. Rebeiz, "CPW-Fed Slot Antennas on Multilayer Dielectric Substrates," IEEE Trans. on Antennas Propagat, Vol.44, No. 8, August 1996, pp. 1102-1111

[56] C.P. Wen, "Coplanar Waveguide: A Surface Strip Transmission Line Suitable for Nonreciprocal Gyromagnetic Device Applications," IEEE MTTs Trans, Volume: 17, Issue: 12, 1969, pp. 1087-1090

[57] H. Liu, T. Horno and N.G. Alexpoulas, "Radiation of printed antennas with a coplanar waveguide feed," IEEE Trans., 1995, AP-43, pp. 1143-1 14

[58] K.M.Z. Shams and M. Ali, "CPW-Fed Inductively Coupled Modified Bow-Tie Slot Antenna, "Proc. IEEE Antennas Propagat. Symposium, Vol 3B, July 2005, pp. 365-368.

[59] **A. Moonshiram** and M.Marso, "A Novel Stacked Slotted Bow-Tie Antenna Element at 11.7 GHz," International Journal on Networking and Communication, vol.4, October 2015

[60] **A.Moonshiram** and M.Marso, "A Novel Stacked Slotted Bow-Tie Antenna Element at 11.7 GHz," International Conference on Communication Information Technology and Robotics, August 2015

[61] J. J. Carr, "Practical antenna handbook," McGraw-Hill, 2001

[62] Federal Communications Commissions, Revision of Part 15 of the commission's rules regarding ultra-wideband transmission system, First report and Order. ET Docket 98-153, FCC 02-48, 2002, pp.1-118

[63] Yazdandoost and Kohno, "Bow-tie antenna for UWB communication frequency, "IEEE Antennas and Propag. Society International Symposium, 2004 pp. 2520-2523

[64] R.H.DuHamel, "Logarithmically periodic antenna arrays, "WESCON/58, 1958, pp. 161-174

[65] B. Shanmugam, "Investigations and Performance of a Cavity backed Novel modified Balun free Archimedean Spiral Antenna and Planar Array Implementation," Thesis, San Diego State University, 2012

[66] P.E.Meyes, "Frequency-Independent antennas: Birth and Growth of an idea, "IEEE Antennas and Propagation Society Newsletter, Aug.1982, pp.5-8

[67] R.L.Haupt, "Antenna Arrays: A computational approach, "Wiley-IEEE Press, April 2000

[68] W.Wiesbeck, G.Adamiuk and C.Sturm, "Basic properties and design principles of UWB antennas, "Proc. IEEE, Vol.97, No 2, Feb.2009, pp. 372-385

[69] V.H. Ramsey, "Frequency independent antennas, "IRE 1958, pp.114-118

[70] Y. Mushiake, "Self-Complementary Antennas: Principle of Self-Complementary for constant impedance", Springer Verlag London, 1996

[71] J.L.Volakis, "Frequency Engineering Handbook," McGrawHill, Fourth Edition, 2007

[72] D.S.Filipovic and T.Cencich, "Frequency independent antennas, Chapter 13, McGrawHill, 2007

[73] R.H. Du Hamel, "Frequency Independent Antennas," US patent No. 2985879, May 23th, 1961.

[74] C.A.Balanis, "Antenna Theory, analysis and Design," Wiley, 2005.

[75] J.George et al, "New compact microstrip antenna, "Electron. Lett, Vol32, no 6, March 1996, pp. 508-509

[76] B.Garibello and S.Barbin, "A single element compact printed bowtie antenna enlarged bandwidth," Proc. SBMO/IEEE MTTS Int. Conf. on Microwave and Optoelectronics, Jul 1995, pp 354-358.

[77] Bow-tie antennas, www. antenna theory.com

[78] A.C. Durgun, C.A.Balanis, C.R.Birtcher and D.R.Allee, "Design, simulation, fabrication and testing of flexible bow-tie antennas, " IEEE Trans on Antennas and Propagat, Vol. 59, No 12, Dec 2011, pp 4425-4435

[79] **A.Moonshiram** and M.Marso, "Ultra-broadband Bow-tie antenna," International Journal on Networking and Communication, vol.4, October 2015

[80] **A.Moonshiram** and M.Marso, "Ultra-Broadband Bow-tie Antenna, International Conference on Communication Information Technology and Robotics, August 2015

[81] J.Huang, "A Technique for an array to generate circular polarization with linearly polarized elements," IEEE AP-S Transactions, Vol. 34, No. 9, September 1986, pp 1113-1124

[82] R. L. Haupt and D.W. Aten, "Low side lobe arrays via dipole rotation," IEEE AP-S Transactions, Vol. 57, No 5, May 2009, pp.1574-1577

[83] http://www.nobelprize.org/nobel_prizes/physics/laureates/1909/braun-lecture.pdf, page 239-240

[84] http://www.faculty.ccri.edu/panaccione/.../FamousGermanScientists.ppt

[85] J. E. Kaufmann, H. W. Kaufmann, "The Atlantic Wall: History and Guide, "Pen and Sword books Limited, 2012

[86] https://cedarweb.vsp.ucar.edu/workshop/tutorials/2004/heinselman04.pdf

[87] https://www.naic.edu/

[88] H.T Friss and C.B Feldman, " A Multiply Unit steerable antenna for short-wave reception, " Proceedings of the Institute of Radio Engineers, Vol. 25, No. 7, Juy 1937, pp 841-917

[89] D. C. Green, "Radio Systems Technology," Longman Scientific & Technical, Essex, United Kingdom, 1990

[90] V.Nair, T. Chow, E.Allen, S.Murarka, R.Thallon, K.Chang and I.Bahl, "RF and Microwave Circuit and Component Design for Wireless Systems," Wiley-Interscience, 2001

[91] http://esl.eng.ohio-state.edu/~csg/IE_Methods/IE-Patch-Result.htm

[92] updates.cst.com/downloads/GPU_Computing_Guide_2014.pdf

[93] G.Adamiuk, X.Li and W.Wiesbeck in Chapter 3 from W.Wiesbek, T.Zwick and J.Timmermann, "Ultra-wideband RF System Engineering," Cambridge University Press, 2013.

[94] http://www.radartutorial.eu/06.antennas/Phased%20Array%20Antenna.en.html

[95] T.Kopf, "Phased Array Antennas with Dielectric Phase Shifters," Master Thesis, Fachhochschule Kaiserslautern, 2014

[96] http://mostlymissiledefense.com/2012/04/12/the-fps-85-radar-april-12-2012/

[97] http://www.groundcontrol.com/Satellite_Look_Angle_Calculator.htm

17. PUBLICATIONS & PATENTS

17.1 Publications during PhD

21. Direct electro-optical pumping for hybrid nanocrystal/III-nitride based nano-LEDs". **Applied Physics Letters (Journal),** February 2016

20. High gain patch antenna for broadband applications from 10.1 to 14.2 GHz, **International Journal on Networking and Communication,** vol.4, October 2015

19. A Novel Stacked Slotted Bow-Tie Antenna Element at 11.7 GHz, **International Journal on Networking and Communication**, vol.4, October 2015

18. Ultra-broadband Bow-tie antenna, **International Journal on Networking and Communication**, vol.4, October 2015

17. Direct Electro-optical Pumping for Hybrid Nanocrystal/III-nitride based Nano-LEDs, **Nanoletters,** ACS Publications September 2015

16. High Gain Patch Antenna for Broadband Applications from 10.1 to 14.2 GHz, **International Conference on Communication Information Technology and Robotics**, August 2015

15. A Novel Stacked Slotted Bow-Tie Antenna Element at 11.7 GHz, **International Conference on Communication Information Technology and Robotics**, August 2015

14. Ultra-Broadband Bow-tie Antenna, **International Conference on Communication**

Information Technology and Robotics, August 2015

17.2 Publications from 2005 to 2007

13. Multi-GHz, Causal Transmission Line Modeling Methodology Using a 3D Hemispherical Surface Roughness Approach, **IEEE Microwave Theory and Techniques Transaction Journal**, December 2007

12. Electromagnetic Field Dynamics inside small conducting spheres**, Ansoft First Pass System Success Application Workshop**, October 2007

11. Dielectric modeling, characterization, and validation up to 40 GHz**, IEEE Signal Propagation on Interconnects**, May 2007

10. 67 GHz Measurements: Best Known Methods, **Intel High Frequency Measurement Conference**, November 2006

9. Surface Roughness Simulation Methodology for the Copper Interconnect, **Mediterranean Microwave Symposium**, September. 2006

8. Modeling Surface Roughness for 30 GB/s Chip-to-Chip Signals, **Intel Design and Test Technology Conference**, August 2006

7. SmoothLine - A Novel and Improved De-embedding Methodology, **Intel High Frequency Measurement Conference**, November 2005.

17.3 Publications from Bachelor Degree & Master Degree

6. Assessment of random and systematic errors in millimeter wave dielectric measurement using open resonator and Fourier Transform spectroscopy systems, **IEEE Transactions on Instrumentation and Measurement**, August 2004

5. Measurement of transmittance and permittivity of dielectric materials using dispersive Fourier transform spectrometer, **Microwave and Optical Technology Letters**, July 2003

4. Assessment of random and systematic errors in millimeter wave dielectric measurement, **IEEE Transactions on Microwave Theory and Techniques International Symposium**, June 2003

3. Comparison of Millimeter wave dielectric measurement using various techniques, **IEEE International Symposium on Antennas and Propagation**, June 2003

2. Assessment of random and systematic errors in millimeter wave dielectric measurements: open resonator system and Fourier transform spectroscopy**, IEEE Instrumentation and Measurement Technology Conference**, May 2003

1. Precise dielectric measurement of low loss materials at 60 GHz, **Conference on Precision Electromagnetic Measurements**, June 2002

17.4 Patents

1. Co-inventor of the patent, “Flexible waveguide cable with coupling antennas for digital signals”, US Patent no. 7474178, 2009

2. Co-inventor of the patent, “Ultra-High Data Rate Waveguide Cable”, US Patent no. 7301424, 2007